

For Reference

NOT TO BE TAKEN FROM THIS ROOM

Ex LIBRIS
UNIVERSITATIS
ALBERTAEANAE



A faint, sepia-toned background image of a classical building with four columns and a triangular pediment.

Digitized by the Internet Archive
in 2019 with funding from
University of Alberta Libraries

<https://archive.org/details/Jensen1981>

THE UNIVERSITY OF ALBERTA

RELEASE FORM

NAME OF AUTHOR Niels Jensen

TITLE OF THESIS Nyquist analysis and design of multivariable control
systems

DEGREE FOR WHICH THESIS WAS PRESENTED Doctor of Philosophy

YEAR THIS DEGREE GRANTED April 1981

Permission is hereby granted to THE UNIVERSITY OF ALBERTA LIBRARY to reproduce single copies of this thesis and to lend or sell such copies for private, scholarly or scientific research purposes only.

The author reserves other publication rights, and neither the thesis nor extensive extracts from it may be printed or otherwise reproduced without the author's written permission.

THE UNIVERSITY OF ALBERTA

Nyquist analysis and design of multivariable control systems

by



Niels Jensen

A THESIS

SUBMITTED TO THE FACULTY OF GRADUATE STUDIES AND RESEARCH

IN PARTIAL FULFILMENT OF THE REQUIREMENTS FOR THE DEGREE

OF Doctor of Philosophy

IN

Chemical Engineering

Department of Chemical Engineering

EDMONTON, ALBERTA

April 1981

THE UNIVERSITY OF ALBERTA
FACULTY OF GRADUATE STUDIES AND RESEARCH

The undersigned certify that they have read, and recommend to the Faculty of Graduate Studies and Research, for acceptance, a thesis entitled Nyquist analysis and design of multivariable control systems submitted by Niels Jensen in partial fulfilment of the requirements for the degree of Doctor of Philosophy in Chemical Engineering.

Abstract.

The nature of interaction in multivariable control systems is examined. The concept of matrix dominance is introduced as a weaker condition than diagonal dominance for the application of the multivariable Nyquist stability theorems. The Nyquist exact loci design technique, which uses the exact transfer function between the i^{th} input-output pair when the i^{th} loop is open and all other loops are closed, is developed and applied to the design of constant compensator/controllers for three chemical plant models.

Transmittances in a closed loop multivariable control system are shown to be either direct, parallel, interaction or disturbance transmittances. It is further shown, that interaction transmittances in an m -input, m -output multivariable system can be expressed as a sum of 1st, 2nd, up to $m-1^{\text{th}}$ order terms. A critical review of published interaction measures shows, that the relative gain array and similar indicators do not measure closed loop interaction. The direct Nyquist array, which is an integral part of a multivariable control system design technique, is shown to give information about both open and closed loop interactions.

The property of matrix dominance, based on the mathematical theory of M-matrices, is introduced together with simple numerical and graphical tests as a weaker condition than diagonal dominance for application of the multivariable Nyquist stability theorems. Row and column dominance are shown to be dual with respect to a diagonal similarity transformation, and an algorithm is presented for transferring dominance between rows or columns. This algorithm can be used to calculate minimal Gershgorin radii.

The exact transfer function $h_i(s)$ between the i^{th} input and the i^{th} output of a multivariable system when the i^{th} loop is open and all other loops are closed is derived. The Nyquist exact loci design technique, which uses polar plots of $k_i(s)h_i(s)$, is developed as a parallel to familiar single loop design techniques. It is shown, that stability can be analysed based on the Nyquist exact loci provided the return difference matrix is matrix dominant. The Nyquist exact loci give direct information about actual bandwidth, rise time, overshoot

and settling time.

The Nyquist exact loci (NEL) design technique was used to design constant compensator/controllers for a double effect evaporator, an open loop unstable chemical reactor, and a distillation column with significant time delays. The compensator/controllers designed using the NEL procedure are equivalent to those designed using other techniques.

Acknowledgements.

The author wishes to acknowledge the assistance and guidance of his thesis supervisors Dr. D.G. Fisher and Dr. S.L. Shah throughout the course of this research.

The author also want to thank the DACS centre personnel, in particular Mr. V. Berka and Mr. D. Furnell, for their assistance in the use of the University's computing facilities.

Thanks are also extended to my fellow graduate students, in particular Mr. N. Freitag and Mr. D.T. Lynch, for many intellectually stimulating discussions.

Financial support from the University of Alberta throughout this work is gratefully acknowledged. Finally, but not least, the travel grant from Civilingenior H. Jakob Nielsens Legat under the Danish Society of Chemical, Civil, Electrical and Mechanical Engineers, was deeply appreciated.

Table of Contents

Chapter	Page
1. Introduction and objectives	1
1.1 Introduction.	1
1.2 Objectives of this research.	2
1.3 Structure of thesis.	6
2. Interaction Analysis	7
2.1 Introduction and scope.	7
2.2 The nature of interaction.	8
2.3 The direct Nyquist array (DNA)	17
2.3.1 The DNA display and interaction.	17
2.3.2 The DNA display and variable pairing.	18
2.4 Critical review of published interaction measures.	19
2.4.1 The interaction quotient.	19
2.4.2 The relative gain array.	21
2.4.3 Tung and Edgar's approach.	23
2.4.4 The average dynamic gain array.	24
2.4.5 The relative transient response functions.	24
2.4.6 Other measures of interaction.	25
2.5 The DNA - an alternative to measures of interaction.	27
2.6 Conclusions.	39
3. Matrix dominance and transfer of dominance.	42
3.1 Introduction.	42
3.2 Definition of and test for matrix dominance.	43
3.2.1 Mathematical background and notation.	43
3.2.2 Previous work on extending MNA stability theorems.	43
3.2.3 Matrix dominance.	45
3.2.4 Graphical test for matrix dominance.	46

3.3	Implications for MNA design techniques	52
3.4	Duality of row and column dominance.	57
3.5	Transfer of dominance.	58
3.6	Conclusions.	60
4.	Nyquist exact loci (NEL) design technique.	62
4.1	Introduction.	62
4.2	The Nyquist exact loci of $h_i(s)$	64
4.3	The Nyquist exact loci (NEL) design procedure.	65
4.3.1	Transfer function model description.	66
4.3.2	Matrix dominance of the return difference matrix.	71
4.3.3	Choice of initial set of loop gains.	72
4.3.4	Nyquist exact loci plots.	73
4.3.5	Specify desired stability margins.	73
4.3.6	Calculate gains to satisfy stability margins.	74
4.3.7	Is the control system satisfactory.	74
4.4	Simultaneous controller constant evaluation.	75
4.5	Conclusions.	78
5.	Control system design using NEL.	79
5.1	Introduction.	79
5.2	Double effect evaporator.	79
5.3	Chemical reactor.	102
5.4	Distillation column.	114
5.5	Conclusions.	122
6.	Conclusions and recommendations.	124
6.1	Contributions of this work.	124
6.2	Further research.	125
7.	Nomenclature.	127
7.1	Technical abbreviations.	127
7.2	Nomenclature for chapter 1.	127

7.3 Nomenclature for chapter 2.	128
7.4 Nomenclature for chapter 3.	130
7.5 Nomenclature for chapter 4.	131
7.6 Nomenclature for chapter 5.	132
8. References	134
9. Appendices	139
9.1 Appendix A. Derivation of $h_i(s)$	139
9.2 Appendix B. Cofactor equivalence.	142
9.3 Appendix C. Proof of theorems 3.1 and 3.3.	144
9.4 Appendix D. Nyquist contours and encirclements.	146
9.5 Appendix E. Proof of theorem 4.1.	152

List of Figures

Figure		Page
1.1	Blockdiagram of main transfer function elements in a multivariable control system. $G_p(s)$ is the plant TFM, $G_L(s)$ is the load TFM, $K_1(s)$ is a compensator TFM, and $K_2(s)$ is a diagonal controller TFM. $Q(s) = G_p(s) \cdot K_1(s)$ is the compensated plant TFM.	3
1.2	Input-output relationship for a SISO system as shown by transfer function $g(s)$, and one pair of a MIMO system as shown by transfer function $h_i(s)$.	5
2.1	Blockdiagram representation to show classification of transmittances between $r_i(s)$ and $y_i(s)$ in a multivariable system (cf. equation 2.3).	10
2.2	Polar plot of Rijnsdorp's interaction quotient for the TFM given in equation 2.22. The arrow indicates increasing frequency.	29
2.3	Polar plots of the elements of the relative dynamic gain array for the TFM in equation 2.22. Axis are only shown on diagonal elements and the origin of off diagonal elements are indicated by a plus sign.	30
2.4	The direct Nyquist array for the TFM given in equation 2.22.	31
2.5	The relative dynamic gain array for the TFM given in equation 2.26.	33
2.6	The direct Nyquist array for the TFM given in equation 2.26.	34
2.7	The relative dynamic gain array for turboalternator using model of Ahson and Nicholson (1976).	35
2.8	The direct Nyquist array for turboalternator using model of Ahson and Nicholson (1976).	36
2.9	The relative dynamic gain array for turboalternator using model of Taiwo (1978).	37
2.10	The direct Nyquist array for turboalternator using model of Taiwo (1978).	38
2.11	The DNA for turboalternator using model of Ahson and	

	Nicholson (1976), and diagonal pre- and postcompensators.	40
3.1	Graphical test of pilot plant evaporator return difference matrix $F(s) = I + G(s)$ for column matrix dominance. Frequency in the range from 0.0038 to 7.73 rad/min. is the ordinate, and the abscissa the dimensionless numbers defined by equation 3.7.	48
3.2	Graphical test of pilot plant evaporator return difference matrix for row matrix dominance. Frequency range $0.0038 < \omega < 7.73$ rad/min.	49
3.3	Direct Nyquist array display of pilot plant evaporator TFM $G(s)$. Frequency range $0.0038 < \omega < 7.73$ rad/min.	50
3.4	Graphical test of pilot plant evaporator return difference matrix for row matrix dominance after compensation. Frequency range $0.0038 < \omega < 7.73$ rad/min.	53
3.5	Graphical test of return difference matrix of system in equation 3.10 for matrix dominance. Frequency range $0.1 < \omega < 10.0$.	55
3.6	Direct Nyquist array of 2×2 TFM $G(s)$ with Gershgorin circles superimposed on diagonal elements. Frequency range $0.1 < \omega < 10.0$.	56
4.1	Flow chart of NEL design procedure showing the different steps and design loops.	67
5.1	DNA of $G(s)K_1$ for continuous evaporator TFM $G(s)$ and compensator K_1 from equation 5.2. Frequency range $0.0038 < \omega < 7.73$ rad/min.	84
5.2	NEL of continuous evaporator with TFM $G(s)$, zero order hold with sampling time 64 seconds, compensator K_1 from 5.3 and $K_2 = I$. Frequency range $0.0038 < \omega < 7.73$ rad/min.	86
5.3	Row matrix dominance test of continuous evaporator with compensator K_1 from equation 5.3, zero order hold with 64 second sampling time, and proportional gain from calculation no.	

	4 of table 5.4.	87
5.4	Plots of $ k_i h_i(s) / 1 + k_i h_i(s) $ versus frequency for $i=1,2,3$ with proportional gains from calculation no. 6 of table 5.4.	89
5.5	Plots of $ k_i h_i(s) / 1 + k_i h_i(s) $ versus frequency for $i=1,2,3$ with proportional gains from calculation no. 7 of table 5.4.	90
5.6	Plots of $ k_i h_i(s) / 1 + k_i h_i(s) $ versus frequency for $i=1,2,3$ with proportional gains from calculation no. 8 of table 5.4.	91
5.7	Nyquist exact loci for continuous evaporator model after one iteration of gain calculation no. 8 of table 5.4.	92
5.8	Nyquist exact loci for continuous evaporator model after two iteration in gain calculation no. 8 of table 5.4.	93
5.9	Nyquist exact loci for continuous evaporator model after three iterations in gain calculation no. 8 of table 5.4.	94
5.10	Nyquist exact loci for continuous evaporator model after last (fourth) iteration in gain calculation no. 8 of table 5.4.	95
5.11	DNA of bilinear transformed discrete evaporator model $G(w)$. Discrete frequency range $0.01 < v < 2.80$ rad/min.	98
5.12	Simulated response of evaporator to a +10% change in product concentration. The fifth order discrete state space model and the compensator/controller of 5.3 were used.	99
5.13	Simulated response of evaporator to a +20% change in first effect hold-up. The fifth order discrete state space model and the compensator/controller of equation 5.3 were used.	100
5.14	Matrix dominance test of $F(s) = I + G(s)$ with the chemical reactor TFM $G(s)$ from table 5.7.	103
5.15	DNA of chemical reactor TFM $G(s)$ from table 5.7. Frequency range $0.002 < \omega < 30.5$ rad/1000s.	104
5.16	DNA of chemical reactor TFM $G(s)$ from table 5.7 after multiplication of column one by -100. Frequency range $0.002 <$	

	$\omega < 30.5 \text{ rad/1000s.}$	105
5.17	Matrix dominance test of $F(s) = I + G(s)K_1$ with the chemical reactor TFM $G(s)$ from table 5.7 and the compensator K_1 from equation 5.8.	106
5.18	DNA of compensated chemical reactor TFM model with Gershgorin circles, based on column sums, superimposed on the diagonal elements. Frequency range $0.002 < \omega < 30.5 \text{ rad/1000s.}$	107
5.19	DNA of similarity transformed compensated chemical reactor TFM model with Gershgorin circles, based on column sums, superimposed on the diagonal elements. Frequency range $0.002 < \omega < 30.5 \text{ rad/1000s.}$	109
5.20	Nyquist exact loci of compensated chemical reactor model with $k_1 = 0.15$ and $k_2 = 0.15$. Frequency range $0.002 < \omega < 30.5 \text{ rad/1000s.}$	110
5.21	Matrix dominance test of $F(s) = I + G(s)K_1 K_2$ with the chemical reactor TFM model from table 5.7, the compensator K_1 from equation 5.8 and $K_2 = \text{diag}\{0.15, 0.15\}$.	111
5.22	Plots of $ k_i h_i(s) / 1 + k_i h_i(s) $ for compensated chemical reactor model with $k_1 = k_2 = 1.0$. Frequency range $0.002 < \omega < 30.5 \text{ rad/1000s.}$	113
5.23	Matrix dominance test of $F(s) = I + G(s)$ with the distillation column TFM $G(s)$ from table 5.8.	115
5.24	DNA of compensated distillation column TFM model with Gershgorin circles, based on column sums, superimposed on the diagonal elements. Frequency range $0.005 < \omega < 1.0 \text{ rad/s.}$	117
5.25	Plots of $ k_i h_i(s) / 1 + k_i h_i(s) $ versus frequency for compensated distillation column model with proportional gain from calculation number 2 of table 5.9.	118

5.26	Plots of $ k_i h_i(s) / 1 + k_i h_i(s) $ versus frequency for compensated distillation column model with proportional gain from calculation number 3 of table 5.9.	119
5.27	Nyquist exact loci for compensated distillation column TFM model with proportional gain from calculation number 2 of table 5.9. Frequency range $0.005 < \omega < 1.0$ rad/min.	121
9.1	Blockdiagram of multivariable system with open loop transfer function marix $Q(s)K_2(s)$, and feedback matrix $S = \text{diag}\{s_i\}$, $s_i=0$, $s_k=1$, $k \neq i$, i.e. all loops except the i 'th loop are closed.	140
9.2	Nyquist D -contour in the s -plane	147
9.3	Modified Nyquist contour in the s -plane. a) D_1 -contour, and b) D_2 -contour.	147
9.4	Modified Nyquist contours in the z -plane. a) D'_1 -contour, and b) D'_2 -contour.	148
9.5	Modified Nyquist contours in the w -plane. a) D''_1 -contour, and b) D''_2 -contour.	148
9.6	Mappings of D_1 and D_2 by $G(s) = 1/s$.	150
9.7	Mappings of D'_1 and D'_2 by $G(z) = T/(z-1)$.	150
9.8	Mappings of D''_1 and D''_2 by $G(w) = -T/2 + T/2w$.	151

List of Tables

Table		Page
2.1	The elements of the closed loop transfer function matrix $R(s)$ for a 2×2 and a 3×3 system with open loop transfer function matrix $Q(s)K_2(s)$.	13
2.2	The transmittances along the primary physical transmission paths in a 2×2 and a 3×3 closed loop system with open loop transfer function matrix $Q(s)K_2(s)$.	15
3.1	Continuous transfer function model $G(s)$ of pilot plant evaporator. $G(s) = N(s)/d(s)$, where $N(s)$ is a polynomial matrix and $d(s)$ is the characteristic polynomial.	52
4.1	Summary of four different approaches to the design of a discrete control system for a continuous plant.	71
5.1	Discrete transfer function model $G(z)$ of pilot plant evaporator. $G(z) = N(z)/d(z)$, where $N(z)$ is a polynomial matrix and $d(z)$ is the characteristic polynomial.	82
5.2	Bilinear transformed discrete transfer function model $G(w)$ of pilot plant evaporator. $G(w) = N(w)/d(w)$, where $N(w)$ is a polynomial matrix and $d(w)$ is the characteristic polynomial.	82
5.3	Poles of evaporator TFM's $G(s)$, $G(z)$ and $G(w)$ obtained from fifth order state models.	82
5.4	Summary of proportional controller constant calculation for continuous evaporator model $G(s)G_h(s)K_1$.	88
5.5	Rise time, overshoot and settling time with proportional gain from calculation number eight of table 5.4.	96
5.6	Summary of proportional controller constant calculation for discrete evaporator model $G(w)K_1$.	101
5.7	TFM model of chemical reactor as given by Hung and Anderson (1979). The model $G(s)$ has the form $G(s) = N(s)/d(s)$, where $d(s)$	

	is the characteristic polynomial, and $N(s)$ is a polynomial matrix.	108
5.8	TFM model of binary pilot scale distillation column as given by Berry (1973).	116
5.9	Summary of proportional controller constant calculation for compensated distillation column model $G(s)K_1$.	120

1. Introduction and objectives.

1.1 Introduction.

The last fifteen years have brought extensions of the classical single variable frequency domain control system design techniques of Nyquist and Bode to the design of multivariable control systems. These developments have been spawned by practical difficulties in the use of modern control theory, which is to a large extent based on state variable formulations, in the design of multivariable process control systems, Foss (1973), Horowitz and Shaked (1975), and Lee and Weekman (1976).

The development of frequency domain methods in multivariable control system design has been conveniently summarized in a publication edited by MacFarlane (1979). Two well known multivariable design procedures, the inverse Nyquist array (INA) method due to Rosenbrock (1969) and the characteristic locus (CL) method due to MacFarlane and Belletrutti (1973) have been applied to industrial problems, but their use has been somewhat restricted because the requirement of diagonal dominance in the former is too strict for many industrial systems, and the characteristic values or eigenvalues of the latter have little physical meaning to the industrial designer. Furthermore the non-diagonal controller/compensator matrices these techniques often produce may reduce the integrity of the control system, especially toward actuator failures. Thus there is a need for a multivariable control system design method, which would be an exact parallel to single variable frequency domain design, and in a meaningful way use familiar terms like gain margin, phase margin and crossover frequency in a multivariable context. Also the method should allow the design of multiloop control systems for most chemical processes, thus giving high integrity toward both actuator and transducer failures. In the Department of Chemical Engineering at the University of Alberta research in multivariable frequency domain design techniques was initiated by Dr. D.G. Fisher after he had worked with Dr. H.H. Rosenbrock and Dr. A.G.J. MacFarlane during a sabbatical leave. Kuon (1975) conducted a survey of multivariable frequency domain design methods and formally developed the direct Nyquist array technique as a straightforward

design method for multivariable control systems that to the practitioner appears as a direct extension of familiar single variable techniques.

In parallel with the development of multivariable frequency domain design techniques a large research effort has gone into the analysis and measurement of interactions in multivariable systems, Rijnsdorp (1965), Bristol (1966, 1968, 1977, 1978, 1979) and others. The main goal of this research has been the development of methods for selecting the best pairing of manipulated and controlled variables in the design of a multiloop control system. However, these methods provide little fundamental insight into the nature of interactions and the way they are transmitted through a multivariable control system. Also, even though some of the variable pairing methods have been applied successfully, they do give incorrect answers for certain systems. Therefore the need exists for a better practical understanding of interactions and methods for reliably assessing interaction during control system design.

1.2 Objectives of this research.

Based on the above considerations the general area of interest in this investigation is the design of linear, multivariable, time-invariant, control systems in the frequency domain. The main transfer function elements of the class of systems considered are shown in figure 1.1. It is assumed the feedback transfer function matrix (TFM) $H(s) = I$, the identity matrix, since this represents no loss in scope.

For the class of systems defined by figure 1.1 the specific goals of this research are:

- i. to investigate the nature of closed loop signal transmission paths with the aim of clarifying closed loop transmittances and interactions.
- ii. to investigate the use of the direct Nyquist array (DNA) of $G_p(s)$ as a tool for pairing manipulated and controlled variables, and the DNA of $Q(s)$ as an indicator during the design phase of closed

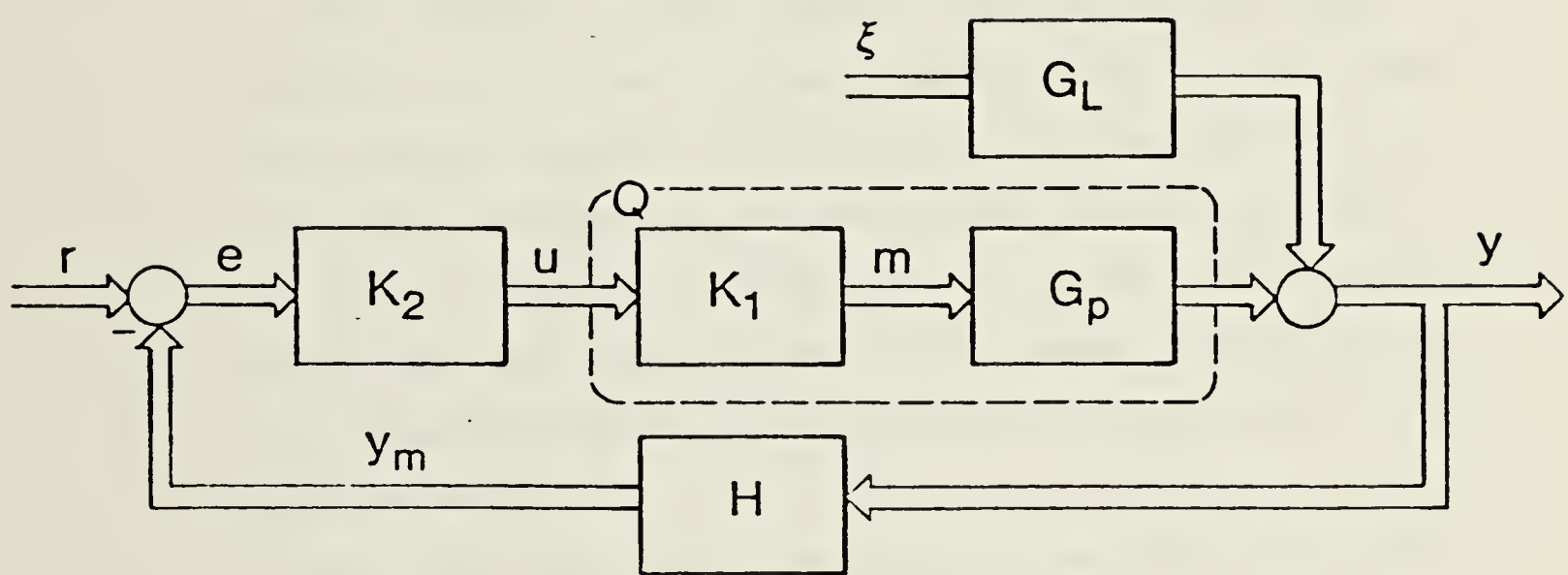


Figure 1.1 Blockdiagram of main transfer function elements in a multivariable control system. $G_p(s)$ is the plant TFM, $G_L(s)$ is the load TFM, $K_1(s)$ is a compensator TFM, and $K_2(s)$ is a diagonal controller TFM. $Q(s) = G_p(s) * K_1(s)$ is the compensated plant TFM.

loop interactions.

- iii. to review published measures of interactions, especially with respect to their application as design tools.
- iv. to formally introduce the use of M-matrices, as a TFM property called matrix dominance, in conditions for multivariable control system stability analysis using multivariable Nyquist array techniques.
- v. to develop graphical displays to test for matrix dominance and to aid in compensator design for non-matrix dominant systems.
- vi. to develop a multivariable control system design technique, which is a direct extension of the classical single variable techniques of Nyquist and Bode, and includes meaningful use of gain margin, phase margin, crossover frequency etc. in the multivariable context. This design technique will use the transfer function $h_i(s)$, which is the exact multivariable equivalent of the single variable transfer function $g(s)$, see figure 1.2. $h_i(s)$ is the transfer function between the i 'th input and the i 'th output when loop i is open and all other loops are closed.
- vii. to apply the NEL design procedure to the design of control systems for several linear plant models, and evaluate the resultant controllers, and compare the results with those of other design techniques.

Although it is not included as part of this thesis, this work has also involved the design specification for an interactive computer aided control system design package, Jensen (1980). Part of this program system has been implemented, and is designed to assist in the use of the proposed design technique and other multivariable frequency domain design techniques, such as the inverse Nyquist array method, the characteristic locus method, and the direct Nyquist array method. The programs have been written in a user oriented form, and the internal structure of the package is transparent to the user.

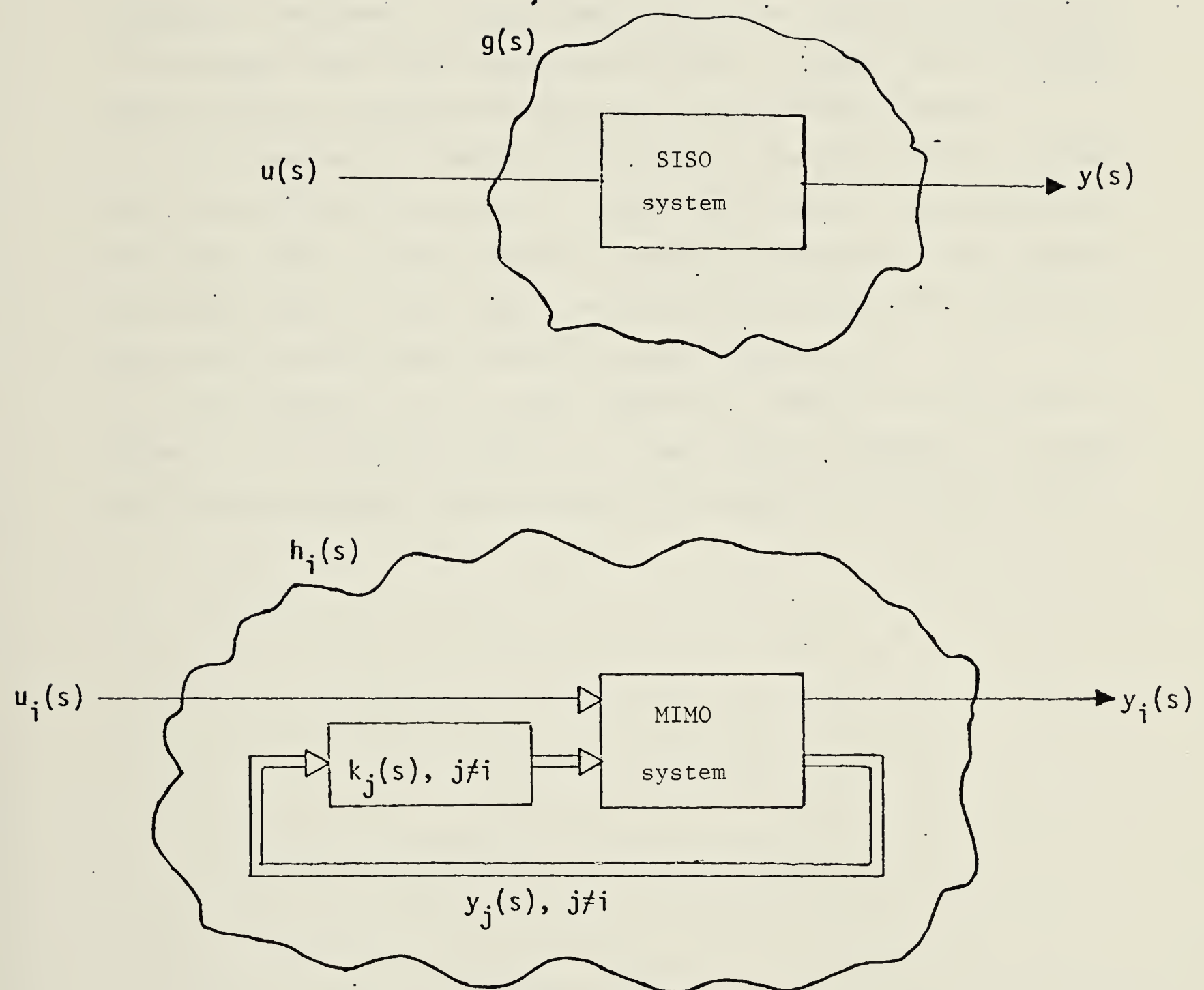


Figure 1.2 Input-output relationship for a SISO system as shown by transfer function $g(s)$, and one pair of a MIMO system as shown by transfer function $h_i(s)$.

1.3 Structure of thesis.

This thesis is divided into six chapters. Chapter two contains an analysis of interactions in closed loop linear multivariable control systems. The relaxation of the diagonal dominance requirement of the multivariable Nyquist array techniques is discussed in chapter three. Chapter four contains the development of the Nyquist exact locus (NEL) design procedure. In chapter five the proposed design procedure is evaluated by application to three different systems.

The treatment of interaction, dominance and the NEL method in chapters two, three and four are written, so each chapter can be read independently. This means there is some overlap or redundancy between the three chapters. Conclusions specific to each topic are stated at the end of each chapter, with the overall contributions and conclusions given in chapter six.

The application of the NEL method in chapter five is written to emphasize the practical aspects of the design procedure in handling non-dominant, open-loop unstable systems, and systems with pure time delays.

2. Interaction Analysis

2.1 Introduction and scope.

In recent years a great deal of research has gone into the analysis and measurement of interactions in multivariable systems, Rijnsdorp (1965), Bristol (1966, 1968, 1977, 1978, 1979), Davison (1969, 1970), Suchanti and Fournier (1973), Witcher and McAvoy (1977), Tung and Edgar (1977, 1978), Kominek and Smith (1979), Gagnepain and Seborg (1979), and Jaaksoo (1979). The main objective of this research was to develop methods for choosing the best pairing of manipulated and controlled variables as the first step in the design of a multiloop control system. However, the nature of interactions has not been clearly defined nor satisfactorily incorporated into an overall control system design scheme. Also the distinction between interactions and the various input/output transmission paths in a multivariable system has not been clearly made.

In this chapter the term interaction is defined and the nature of interaction is examined with respect to its measurement, implications for variable pairing, and its use in a multivariable control system design procedure. A classification of transmittances in closed loop multivariable control systems into direct, parallel, interaction and disturbance transmittances is introduced. Interaction transmittances are further shown to be a combination of 1st, 2nd and higher order terms, and the implications of low interactions for disturbance attenuation are discussed. A link between interaction transmittances and the return difference of Bode is established.

The direct Nyquist array (DNA) display of the open loop transfer function matrix is shown to give a measure of the amount of interaction to be expected in the closed loop system, and hence to be a useful tool for pairing controlled and manipulated variables.

Finally published tools for measuring interaction are critically reviewed, and it is shown, that several of them do not measure true interaction. Rijnsdorp's interaction quotient is extended to be applicable to systems with m -inputs and m -outputs, and the relation between Bristol's relative gain array and the

multivariable Nyquist array design techniques is discussed, and demonstrated by examples.

2.2 The nature of interaction.

In a multivariable system one output is in general influenced by more than one input or conversely one reference input (setpoint) will in general influence more than one output. This is normally the situation both in the open loop and in the closed loop system. The term interaction can then logically be defined as follows by an extension of MacFarlane's (1972) definition:

Definition: Interactions in a closed loop multivariable system are determined by the transmittances influencing the way in which a reference input $r_i(s)$ affects the set of outputs $\{y_j(s); j \neq i\}$, or alternatively the transmittances influencing the way in which an output $y_i(s)$ is affected by the set of reference inputs $\{r_j(s); j \neq i\}$.

Although interaction arises from the structure of the open loop system, it is evident, that the nature of interaction is best analysed by considering the closed loop transfer function matrix of a multivariable feedback control system, such as is shown in figure 1.1. As noted below much of the existing literature on interactions consider the multivariable system with the i 'th loop open. This does not appear to have much physical justification in interaction analysis. The above definition means, that any transmittance between a reference input $r_i(s)$ and the corresponding output $y_i(s)$ is not an interaction transmittance.

The closed loop relationship between the output vector $y(s)$, the reference input vector $r(s)$ and the disturbance vector $\xi(s)$ for the system in figure 1.1 is

$$\begin{aligned} y &= (I + G_p K_1 K_2 H)^{-1} G_p K_1 K_2 r + (I + G_p K_1 K_2 H)^{-1} G_L \xi \\ &= (I + Q K_2 H)^{-1} Q K_2 r + (I + Q K_2 H)^{-1} G_L \xi \\ &= F^{-1} Q K_2 r + F^{-1} G_L \xi = Rr + R_L \xi \end{aligned} \quad (2.1)$$

In the above equation and those following the Laplace argument, s , is omitted for convenience. From equation 2.1 the elements $r_{ij}(s)$ of the closed loop transfer function matrix $R(s)$ are given by

$$r_{ij} = \frac{\sum_{l=1}^m c_{li} k_j q_{lj}}{\det F} \quad (2.2)$$

where $c_{ii}(s)$ is the (i,i) 'th cofactor of the return difference matrix, $q_{lj}(s)$ is the (l,j) 'th element of $Q(s)$, and $k_j(s)$ is the j 'th diagonal element of $K_2(s)$. A similar expression can be obtained for the elements of the matrix $R_L(s)$.

The i 'th row of the closed loop transfer function matrix $R(s)$ in equation 2.1 can be viewed as a single loop system with reference input $r_i(s)$, other measurable inputs $r_j(s), j=1, \dots, m, j \neq i$, disturbances $\xi_k(s), k=1, \dots, p$ and output $y_i(s)$. Furthermore it is possible to express the diagonal element $r_{ii}(s)$ of $R(s)$ as a sum of two terms: one involving only $k_i(s)q_{ii}(s)/\det F(s)$, and one involving products of cofactors of the i 'th column of $F(s)$ and elements of the i 'th column of $Q(s)$. These two terms can be viewed as two signal transmission paths from $r_i(s)$ to $y_i(s)$, one being influenced only by the diagonal element $k_i(s)q_{ii}(s)$ of $Q(s)K_2(s)$, and one being influenced by two or more offdiagonal elements of $Q(s)K_2(s)$. The transmittances along the two paths are therefore labelled respectively the direct transmittance and the parallel transmittance. Thus the following result is obtained:

Remark 1: Transmittances in a closed loop multivariable system can be classified as direct, parallel, interaction and disturbance transmittance, as shown schematically in figure 2.1 and defined mathematically below.

The i 'th output can be expressed as a sum of four different terms due to respectively direct, parallel, interaction and disturbance transmittances:

$$y = \frac{k_i q_{ii}}{\det F} r_i + \sum_{k=1}^m \frac{(c_{ki} - \delta_{ki}) k_i q_{ki}}{\det F} r_i + \sum_{j=1}^m \left[\sum_{k=1}^m \frac{c_{kj} k_j q_{kj}}{\det F} \right] r_j + \sum_{j=1}^m \left[\sum_{k=1}^m \frac{c_{kj} g_{kj}}{\det F} \right] \xi_j \quad (2.3)$$

where g_{kj}^L is the (k,j) 'th element of $G_L(s)$. Equation 2.3 shows, that parallel, interaction and disturbance transmittances are all dependent on the properties of

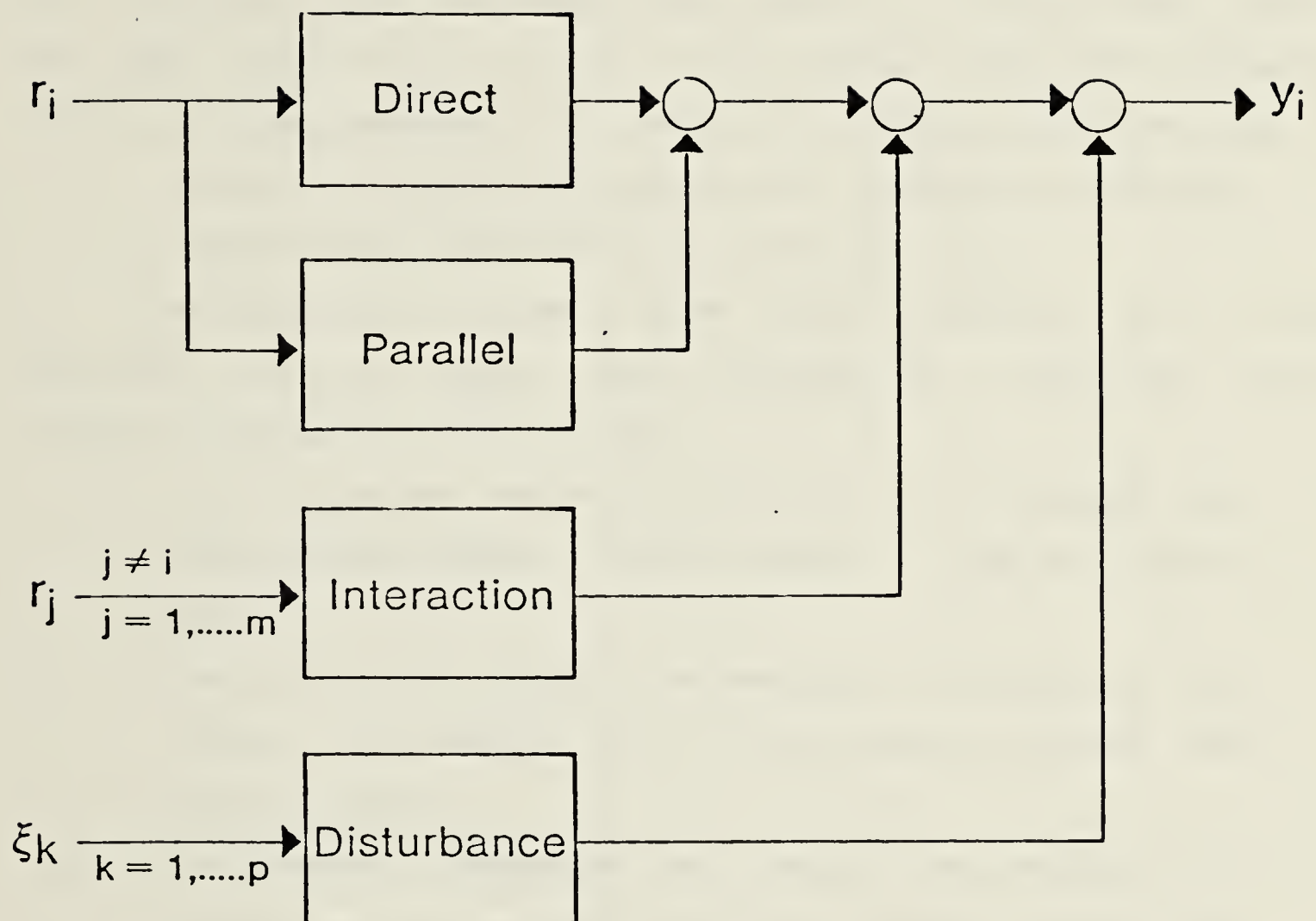


Figure 2.1 Blockdiagram representation to show classification of transmittances between $r_i(s)$ and $y_i(s)$ in a multivariable system (cf. equation 2.3).

the return difference matrix $F(s)$ through the cofactors $c_{ij}(s)$ of this matrix. The determinant of $F(s)$, $\det F(s)$, is common to all terms and can thus be factored out. Table 2.1 shows the elements of $R(s)$ for a 2×2 and a 3×3 system with $H(s) = I$. All elements are given with the determinant of the return difference matrix as common denominator, and the presence of direct, parallel and interaction transmittance terms are evident. From equation 2.1 it can be seen, that as the single loop gains $k_i(s)$, $i=1,\dots,m$ of $K_2(s)$ approach infinity, $R(s)$ approaches $H(s)^{-1}$, and $R_L(s)$ approaches 0. This leads to the following well known result:

Remark 2: Interaction transmittances and disturbance transmittances approach zero as all controller gains approach infinity.

The significance and role of these various transmittance terms is best appreciated when the common design objectives of a multivariable control system are expressed in terms of them:

Design objectives: The compensator $K_1(s)$ and the feedback controllers $\{k_i(s); i=1,\dots,m\}$ are normally designed to meet the following objectives:

- i. The disturbance transmittances are minimized. (The disturbance transmittances will approach zero as the feedback controller gains approach infinity).
- ii. The interaction transmittances are minimized. (The interaction transmittances will also approach zero as the feedback controller gains approach infinity).
- iii. Ideally the parallel transmittances would be designed to complement the direct transmittances. However, they cannot be designed independently of each other and of the interaction transmittances.
- iv. The direct transmittances are designed to achieve fast servo control.

Examination of table 2.1 reveals, that the numerators of the interaction transmittances $r_{ij}(s)$, $i \neq j$, for the 3×3 system consist of two terms, which are respectively 1×1 and 2×2 minors of the open loop transfer function matrix $Q(s)K(s)$. The 1×1 minor is associated with interaction transmitted directly from one loop to another loop. This is referred to as a first order interaction

Table 2.1 The elements of the closed loop transfer function matrix $R(s)$ for a 2×2 and a 3×3 system with open loop transfer function matrix $Q(s)K_2(s)$.

2×2 system:

$$r_{11} = (k_1 q_{11} + \det Q K_2)/\det F$$

$$r_{12} = k_2 q_{12}/\det F$$

$$r_{21} = k_1 q_{21}/\det F$$

$$r_{22} = (k_2 q_{22} + \det Q K_2)/\det F$$

3×3 system:

$$r_{11} = (k_1 q_{11} + k_1 k_2 (q_{11} q_{22} - q_{21} q_{12}) + k_1 k_3 (q_{11} q_{33} - q_{31} q_{13}) + \det Q K_2)/\det F$$

$$r_{12} = (k_2 q_{12} + k_2 k_3 (q_{12} q_{33} - q_{32} q_{13}))/\det F$$

$$r_{13} = (k_3 q_{13} + k_2 k_3 (q_{22} q_{13} - q_{12} q_{23}))/\det F$$

$$r_{21} = (k_1 q_{21} + k_1 k_3 (q_{21} q_{33} - q_{31} q_{23}))/\det F$$

$$r_{22} = (k_2 q_{22} + k_2 k_1 (q_{22} q_{11} - q_{12} q_{21}) + k_2 k_3 (q_{22} q_{33} - q_{32} q_{23}) + \det Q K_2)/\det F$$

$$r_{23} = (k_3 q_{23} + k_1 k_3 (q_{11} q_{23} - q_{21} q_{13}))/\det F$$

$$r_{31} = (k_1 q_{31} + k_1 k_2 (q_{31} q_{22} - q_{21} q_{32}))/\det F$$

$$r_{32} = (k_2 q_{32} + k_1 k_2 (q_{11} q_{32} - q_{31} q_{12}))/\det F$$

$$r_{33} = (k_3 q_{33} + k_3 k_1 (q_{33} q_{11} - q_{13} q_{31}) + k_3 k_2 (q_{33} q_{22} - q_{23} q_{32}) + \det Q K_2)/\det F$$

transmittance. The 2×2 minor is associated with the transmittance of interaction from one loop to another via a third. This is referred to as a second order interaction transmittance. For a m^{th} order multivariable system the interaction transmittances will contain minors of the open loop transfer function matrix of order up to $m-1$. This leads to the following:

Remark 3: Interaction transmittances in a $m \times m$ closed loop multivariable system can be expressed as a sum of minors of 1st, 2nd, ..., and $(m-1)^{\text{th}}$ order. The i^{th} order interaction transmittances are associated with $i \times i$ minors of the open loop transfer function matrix.

The general term 'associated with' is used deliberately above, since it is not possible to associate a physical transmission path with just the numerators of the elements of $R(s)$ as given in equation 2.2 or table 2.1. The physical transmission paths are revealed by dividing the numerators by $\det F(s)$ using long division, which shows there exist an infinite number of paths. The primary physical transmission paths can also be established by using combinatorics on a signal flow graph. Table 2.2 gives the transmittances along the primary transmission paths for a 2×2 and a 3×3 system. The term 'primary' is meant to indicate, that no section of the path is traversed more than once. The transmittances given in table 2.1 also show terms, which could be classified 1st and 2nd order interactions. Compared to the classification introduced above this would give an infinite number of interaction terms, which would make analysis of interaction more complicated.

The elements of $R(s)$ can be calculated from the the minors of the open loop transfer function matrix $Q(s)K_2(s)$ using the following general expression:

$$r_{ij} = \frac{1}{\det F} \left[Q_j^i + \sum_{l_1=1}^m Q_{j l_1}^{i l_1} + \sum_{l_1=1}^m \sum_{l_2=l_1+1}^m Q_{j l_1 l_2}^{i l_1 l_2} + \dots + \sum_{l_1=1}^m \sum_{l_m=l_{m-1}+1}^m Q_{j l_1 \dots l_m}^{i l_1 \dots l_m} + \dots + \delta_{ij} \det Q \right] \quad (2.4)$$

where l_1, l_2, \dots are always different from i and j . In equation 2.4 Q_j^i denotes the 1×1 minor of $Q(s)K_2(s)$ formed by deleting all rows except row i and all

Table 2.2 The transmittances along the primary physical transmission paths in a 2×2 and a 3×3 closed loop system with open loop transfer function matrix $Q(s)K_2(s)$.

2×2 system:

$$r'_{11} = k_1 q_{11} - k_1 k_2 q_{21} q_{12}$$

$$r'_{12} = k_2 q_{12}$$

$$r'_{21} = k_1 q_{21}$$

$$r'_{22} = k_2 q_{22} - k_1 k_2 q_{21} q_{12}$$

3×3 system:

$$r'_{11} = \frac{k_1 q_{11} - k_1 k_3 q_{31} q_{13}}{k_1 k_2 k_3 (q_{12} q_{23} q_{31} + q_{13} q_{32} q_{21})} + k_1 k_2 q_{21} q_{12}$$

$$r'_{12} = k_2 q_{12} - k_2 k_3 q_{32} q_{13}$$

$$r'_{13} = k_3 q_{13} - k_2 k_3 q_{12} q_{23}$$

$$r'_{21} = k_1 q_{21} - k_1 k_3 q_{31} q_{23}$$

$$r'_{22} = \frac{k_2 q_{22} - k_2 k_1 q_{12} q_{21}}{k_1 k_2 k_3 (q_{13} q_{32} q_{21} + q_{12} q_{23} q_{31})} + k_2 k_3 q_{32} q_{23}$$

$$r'_{23} = k_3 q_{23} - k_1 k_3 q_{21} q_{13}$$

$$r'_{31} = k_1 q_{31} - k_1 k_2 q_{21} q_{32}$$

$$r'_{32} = k_2 q_{32} - k_1 k_2 q_{31} q_{12}$$

$$r'_{33} = \frac{k_3 q_{33} - k_3 k_1 q_{13} q_{31}}{k_1 k_2 k_3 (q_{12} q_{23} q_{31} + q_{13} q_{32} q_{21})} + k_3 k_2 q_{23} q_{32}$$

columns except column j . δ_{ij} is the Kronecker delta, and $\delta_{ij} = 1$ for $i=j$, $\delta_{ij} = 0$ for $i \neq j$.

Much of the interaction analysis literature is concerned with the transmittances in a multivariable system in which the i 'th loop is open and all other loops are closed. In this situation the closed loop relationship between the reference input vector $r(s)$, the disturbance vector $\xi(s)$ and the output vector $y(s)$ is

$$\begin{aligned} y &= (I + QK_2 HS)^{-1} QK_2 r + (I + QK_2 HS)^{-1} G_L \xi \\ &= R'r + R'_L \xi \end{aligned} \quad (2.5)$$

where S is a diagonal matrix with the i 'th diagonal element zero and all other diagonal elements unity. If $k_i(s) = 1$ in equation 2.5, then the element $r_{ii}(s)$ of $R'(s)$ is the transfer function for which the i 'th loop controller $k_i(s)$ should be designed to take into account the multivariable nature of the system. A design procedure, which uses these transfer functions, is developed in chapter four and applied to several systems in chapter five. An expression similar to equation 2.3 for the i 'th output when all loops except the i 'th are closed can be stated as follows:

$$y_i = q_{ii} k_i r_i + L_i k_i r_i + \sum_{\substack{j=1 \\ j \neq i}}^m r'_{ij} r_j + \sum_{j=1}^p r'_{Lij} \xi_j \quad (2.6)$$

where $L_i(s)$ is the parallel transmittance between $u_i(s)$ and $y_i(s)$, and $u_i(s) = k_i(s)r_i(s)$, when the i 'th loop is open. The parallel transmittance $L_i(s)$ can be calculated by the following expression, which is derived in appendix A:

$$L_i = \sum_{\substack{j=1 \\ j \neq i}}^m \phi_{ij} q_{ij} k_j / k_i = \sum_{\substack{j=1 \\ j \neq i}}^m \phi_{ji} q_{ji} k_i \quad (2.7)$$

where $\phi_{ij}(s)$ is the ratio of the (i,j) 'th cofactor to the (i,i) 'th cofactor of the return difference matrix $F(s)$. Rosenbrock (1972) gives an expression for $h_m(s) = q_{mm}(s) + L_m(s)$, which is the transfer function with the m 'th loop open and all other loops closed. From this an expression for $L_m(s)$ can easily be derived. However, equation 2.7 is simpler and more flexible, since any one loop can be open, whereas Rosenbrock's result requires the m 'th loop to be open.

As discussed later the transmittances $h_i(s)$, $i=1,\dots,m$ in the limit as the gains in all closed loops approach infinity plays an important part in several published measures of interaction. However, from the foregoing treatment it is evident these limiting transmittances do not represent interaction transmittances, but, as defined in figure 2.1, only the limiting values of the sum of direct and parallel transmittance with one loop open and the rest closed. In the limit as the gain of all closed loops approach infinity the ratio of cofactors $\Phi_{ij}(s)$ approach a corresponding ratio of cofactors of the compensated plant transfer function matrix $Q(s)$. This means the parallel transmittance $L_j(s)$ does not in general approach zero under high gain feedback in all closed loops, and hence should not be used as a measure of true interaction.

Equations 2.3 and 2.6 also show, that parallel transmittance may prove helpful by increasing the controller bandwidth, whereas interaction transmittances must always be considered harmful. Since $r_i(s)$ and $r_j(s)$, $j \neq i$, can have opposing effects on $y_i(s)$, and the disturbances are in general arbitrary and unknown it is not possible to establish a priori whether a particular interaction transmittance is helpful or harmful. Ideally one would like to take advantage of the parallel transmittance and at the same time minimize interaction transmittances in all control loops. However, these are conflicting objectives, as evident by inspection of table 2.2. In practice it will only be possible to take advantage of the parallel transmittance in the design, or to minimize interaction transmittances in some loops at the expense of more interaction in other loops. Tools for accomplishing these objectives are developed in chapters three and four.

Although the above treatment has neglected disturbance transmittances they are closely related to interaction transmittances. In the servo problem the objective is to make a change in one input variable affect only one output variable, i.e. minimize all interaction transmittances. In the regulator problem the objective is to minimize the influence of a disturbance on all output variables, i.e. minimize all disturbance transmittances. Equation 2.3 shows, that the cofactors $c_{ij}(s)$ of the return difference matrix influence the interaction and disturbance transmittances in identical ways. Hence the objective of both the servo and the regulator problem can be met by minimizing the cofactors of the return

difference matrix. This would also minimize the parallel transmittances, but a practical procedure for affecting the minimization has not been developed yet.

2.3 The direct Nyquist array (DNA)

In the multivariable Nyquist type design techniques, such as the direct Nyquist array (DNA) technique and the inverse Nyquist array (INA) technique, classical single loop control system design approaches have been extended to the design of multivariable control systems. The use of the DNA display, which is an integral part of an established multivariable design technique, to give information about closed loop interaction and pairing of variables is discussed below.

2.3.1 The DNA display and interaction.

The DNA display in the direct Nyquist array technique is used to design a compensator $K_1(s)$, which reduces the interaction in the open loop system. The implication is that reducing open loop interaction will reduce closed loop interaction as well. In the previous section it was shown, that interaction transmittances can be classified as 1st., 2nd. and higher order, and that i 'th order interaction transmittances are associated with $i \times i$ minors of the open loop transfer function matrix. For most practical systems, such as chemical process systems, the magnitude of the minors will normally decrease as the order increases. Hence,

Remark 4: In most practical systems the first order interaction transmittances provide a reasonable approximation to the total interaction, i.e. the higher order interaction transmittances are generally negligible.

Since only first order interactions are found in 2×2 systems the above remark is clearly valid for all 2×2 systems. It is however possible to construct examples of 3×3 systems which contradict the above statement, i.e. have $|Q_{ii}^{ij}| > |Q_{jj}^{ij}|$ for some (i,j,l) , $i \neq i$, $j \neq j$. It is nevertheless always possible to compare direct transmittance and first order interaction transmittances in the closed loop system

by comparing a diagonal element and the corresponding offdiagonal elements of the open loop transfer function matrix $Q(s)K_2(s)$. The direct Nyquist array displays the elements of $Q(s)K_2(s)$ as a function of frequency in the form of an array of polar plots, hence

Remark 5: The DNA display of $Q(s)$ gives an exact measure of direct and interaction transmittances in the *open loop* system, as well as an indication of the direct transmittance and the first order interaction transmittances in the *closed loop* system.

Thus the DNA display of $Q(s)$ gives an indication of the closed loop interactions. The DNA plot of $Q(s)$ further has the advantage of being an integral part of an established multivariable control system design technique. No additional numerical calculations are necessary to get the first order interaction information, and the change in the amount of interaction can be followed as the control system design progresses. If desired higher order interactions can be calculated from the elements of $Q(s)K_2(s)$ and displayed as part of the DNA design procedure.

The INA does not offer as simple a physical interpretation of the display due to the complicated relationship between the elements of $R(s)$ and of $R^{-1}(s)$. Furthermore Clement (1980) has demonstrated, that the DNA-design procedure is preferable, when the plant transfer function matrix is experimentally determined.

2.3.2 The DNA display and variable pairing.

The first step in the frequency domain design of a multivariable control system usually is the pairing of manipulated and controlled variables. The aim is to find the pairing, which makes it possible to realize the control system objectives, e.g. minimize interactions and maximize disturbance attenuation, with the minimum amount of effort. Since the DNA display gives a measure of interaction the pairing objectives can be approached as follows:

Remark 6: Pair manipulated and controlled variables so the largest elements of the DNA display of $G_p(s)$ lie on the main diagonal.

This method will maximize the direct transmittance and minimize the first order interaction transmittances of the closed loop system. Also the above pairing

procedure is consistent with Bristol's (1977) relative dynamic gain array approach, but requires less numerical calculation. This is the case, because $G_p(s)$ being matrix dominant (cf. chapter 3) implies, that the relative dynamic gain array is matrix dominant, Fiedler and Ptak (1966).

2.4 Critical review of published interaction measures.

Most published measures of interaction have shortcomings such as: i) they are based on a system with one loop open rather than a fully closed loop system, and ii) they measure parallel transmittance rather than the true closed loop interaction.

2.4.1 The interaction quotient.

One of the first suggested measures of process interaction, was the interaction quotient proposed by Rijnsdorp (1965). Rijnsdorp considered only 2×2 systems with emphasis on distillation column control. For 2×2 systems the interaction quotient is defined to be

$$\kappa = g_{21}g_{12}/g_{11}g_{22} \quad (2.8)$$

where $g_{ij}(s)$ is an element of the plant transfer function matrix $G_p(s)$. The quotient is evaluated for $s = i\omega$ and plotted as a polar plot. The interaction quotient has the properties, that it is dimensionless and invariant under scaling. Rijnsdorp concludes, that when the static value $\kappa(0)$ is close to unity interaction causes poor control. This is also the case when $\kappa(s)$ shows increasing negative phase with frequency, and a magnitude close to one, e.g. a pure time delay. However, when $\kappa(s)$ is approximately constant and has a negative real part good control can be achieved with a multiloop control system. Poor integrity results if $\kappa(s)$ is approximately constant and has a real part greater than one.

The relationship, assuming $K_2(s) = 1$,

$$\kappa = \frac{q_{21}q_{12}}{q_{11}q_{22}} = \lim_{k \rightarrow \infty} \frac{q_{21}q_{12}}{\frac{q_{22}}{k_1} + q_{11}q_{22}} = \lim_{k \rightarrow \infty} \frac{1 + k_1 q_{11}}{q_{22}} = \lim_{k \rightarrow \infty} \frac{L_2}{q_{22}} \quad (2.9)$$

shows the interaction quotient is the limiting value of the ratio of parallel transmittance to direct transmittance for a system with one loop open and one loop closed. Hence the interaction quotient is not a measure of interaction, but a measure of the significance of parallel transmittance with one loop open. Rijnsdorp's conclusions about the interaction quotient provide an answer to the question 'Are problems likely to be encountered in the design of a multiloop control system for this plant?'. However, the interaction quotient does not give a reliable answer to the question 'Is interaction (as defined in section 2.1) significant?'. This will be further demonstrated by examples in section 2.5.

The interaction quotient as an indicator of possible difficulties in multiloop design can be extended to $m \times m$ system by the following definition:

$$K_i = \frac{\sum_{\substack{j=1 \\ j \neq i}}^m \psi_{ij} q_{ij}}{-q_{ii}} = \frac{\sum_{\substack{j=1 \\ j \neq i}}^m \psi_{ji} q_{ji}}{-q_{ii}} \quad (2.10)$$

where $\psi_{ij}(s)$ is the ratio of the $(i,j)'$ th cofactor to the $(i,i)'$ th cofactor of the compensated plant transfer function matrix $Q(s)$. The above extended definition follows from the expression for $L_i(s)$ and the fact, that as k in $K_2(s) = kl$ approaches infinity the ratio of cofactors of the return difference matrix approach the corresponding ratio of cofactors of the compensated plant transfer function matrix, i.e. with $K_2(s) = kl$

$$\lim_{k \rightarrow \infty} \phi_{ij} = \psi_{ij} \quad (2.11)$$

The proof of the above relationship is given in appendix B. It is easily verified, that the extended interaction quotient defined by equation 2.10 reduces to Rijnsdorp's for a 2×2 system. The extended interaction quotient has the same properties as Rijnsdorp's measure, and in addition reordering of inputs or outputs corresponds to an equivalent reordering of the set $\{K_i : i=1, \dots, m\}$. The extended interaction quotient also is only an indicator of possible difficulties in multiloop control system design, and not a measure of closed loop interaction.

It gives a measure for each row or column of the compensated plant transfer function matrix, that is, it gives a measure for each control loop.

Kominek and Smith (1978) gives the first extensive dynamic interpretation of the interaction quotient. They use polar plots of $K(s)$, $s = i\omega$, with a superimposed unit circle. They classify the plots as showing favourable and unfavourable interactions. From the preceding treatment it is evident, that Kominek and Smith are actually judging whether or not parallel transmittance will be advantageous or disadvantageous in a multiloop control system.

2.4.2 The relative gain array.

Bristol (1966, 1967) suggested a steady state interaction measure, which is a relative gain ratio:

$$\mu_{ij} = \frac{[(\Delta y_i / \Delta u_j) | \Delta u_k = 0 \text{ for } k \neq j]}{[(\Delta y_i / \Delta u_j) | \Delta y_k = 0 \text{ for } k \neq i]} \quad (2.12)$$

The numerator corresponds to the open loop gain between u_j and y_i , and the denominator is the gain between u_j and y_i with all other outputs perfectly controlled. $M = \{\mu_{ij}\}$ is called the relative gain array (RGA). The RGA, as Rijnsdorp's interaction quotient, is restricted to plants or compensated plants with an equal number of inputs and outputs. By virtue of the defining equation the elements of the relative gain array are dimensionless. This imply they are invariant under scaling, and since selection of final proportional controller gains is a scaling operation, the relative gain array is independent of the final multiloop controller gains $K_2(s)$. The RGA further has the property, that any row or column sums to one, and that reordering inputs or outputs implies a similar reordering of columns or rows of M . Bristol has shown, that only the open loop gains are necessary to evaluate the RGA, since

$$M = Q(0) \circ [Q(0)^{-1}]^T = \{q_{ij}(0) * \hat{q}_{ji}(0)\} \quad (2.13)$$

where the symbol \circ indicates the Hadamard or Schur product of the two matrices, see Johnson (1974). Bristol (1968) recommends, that controlled and manipulated variables with μ_{ij} positive and close to unity be paired. Also if any μ_{ij} is much larger than one or less than zero pairing the corresponding

variables will result in a loop, which is difficult to control. Bristol (1977) has also shown, that pairings, which gives negative relative gains on the diagonal should be avoided, since this would result in a control loop with nonminimum phase characteristics.

The steady state relative gain array has been successfully applied by several authors, e.g. Stainthorp (1972), Nisenfeld (1973), as a variable pairing tool in designing multiloop systems to give minimum closed loop interaction.

The steady state nature of the RGA neglects any high frequency dynamics, which could be important in certain systems, such as the turbo alternator considered by Ahson and Nicholson (1976) and by Taiwo (1978) and used in example 3 of section 2.5. Witcher and McAvoy (1977) and later Bristol (1978) therefore suggested an intuitive dynamic extension by defining a relative dynamic gain array (RDGA) as follows

$$M(s) = Q(s) \circ [Q(s)^{-1}]^T = \{q_{ij}(s) * \hat{q}_{ji}(s)\} \quad (2.14)$$

which possesses the same properties as the steady state equivalent, e.g. dimensionless. Witcher and McAvoy (1977) state, that interaction is small if the magnitude of the diagonal elements of $M(s)$ are close to one and the magnitude of all other elements are small. This is equivalent to saying $M(s)$ should be a diagonally dominant matrix.

The relationship, for a 2×2 system,

$$\mu_{22} = \frac{q_{22}}{q_{22} - \frac{q_{21}q_{12}}{q_{11}}} = \lim_{k \rightarrow \infty} \frac{q_{22}}{q_{22} - \frac{k_1 q_{21} q_{12}}{1 + k_1 q_{11}}} = \lim_{k \rightarrow \infty} \frac{q_{22}}{q_{22} + L_2} \quad (2.15)$$

shows that the relative dynamic gain array elements are the limiting values of the ratio of direct transmittance to the sum of direct and parallel transmittance for a system with one loop open and the rest closed. Therefore the relative dynamic gains also only indicate whether problems are likely to be experienced in design of a multiloop control system for a particular plant, but as the examples in section 2.5 will demonstrate no indication of closed loop interaction is given by the RDGA. A relationship similar to equation 2.15 exist for higher order systems.

The extended interaction quotient and the diagonal elements of the relative dynamic gain array are related as follows

$$\mu_{ii} = \frac{1}{1 - \kappa_i} \quad \text{or} \quad \kappa_i = \frac{\mu_{ii} - 1}{\mu_{ii}} \quad (2.16)$$

since

$$\frac{1}{1 - \kappa_i} = \frac{q_{ii}}{q_{ii} + \sum_{\substack{j=1 \\ j \neq i}}^m \psi_{ij} q_{ij}} = \frac{c_{ii} q_{ii}}{c_{ii} q_{ii} + \sum_{\substack{j=1 \\ j \neq i}}^m c_{ij} q_{ij}} = q_{ii} * \frac{c_{ii}}{\det Q} = q_{ii} * \hat{q}_{ii} = \mu_{ii} \quad (2.17)$$

where $c_{ij}(s)$ are the $(i,j)'$ th minor or $Q(s)$. The information contained in the RDGA is best seen by plotting it as an array of polar plots similar to the DNA display. From the above relationship with the extended interaction quotient, and the interpretation of the interaction quotient, it is evident, that the RDGA display should be interpreted as follows: If the magnitude of the diagonal elements are close to unity, and the magnitude of all other elements are small it will be possible to design a multiloop control system to give satisfactory control. Pairing of variables with magnitudes much different from unity should be avoided, and generally elements with negative real part should not be placed on the diagonal, since the corresponding control loop will show non-minimum phase properties.

2.4.3 Tung and Edgar's approach.

Tung and Edgar (1977, 1978) suggest basing the variable pairing upon open loop step responses with a compensator $K_1(s) = G(0)^{-1}$. The controlled and manipulated variables are to be paired, so the dominant coefficients of the time response arise from the diagonal elements of the transfer function matrix $G(s)G(0)^{-1}$. However, this procedure means, that in systems without high frequency interaction the variables will be paired so the first output is controlled by the first input and so on, i.e. no reordering of inputs or outputs. The resultant pairing can be considerably different from a similar analysis performed on the uncompensated plant. Tung and Edgar do not mention actually

implementing the precompensator on the physical system, hence the final controller performance could be unsatisfactory for systems with large low frequency interactions. This makes Tung and Edgar's approach less desirable than the RDGA.

2.4.4 The average dynamic gain array.

Gagnepain and Seborg (1979) also suggest using open loop step responses to pair variables. They extend the dynamic potential idea of Witcher and McAvoy (1977) using integrals of open loop step responses to define an average dynamic gain array. The average dynamic gain array (ADGA) is defined by

$$M(t) = D(t) \circ [D(t)^{-1}]^T \quad (2.18)$$

where each element of $D(t)$ is an integral of an open loop step response from time t_1 to time t_2 divided by the integration interval. t_1 is chosen as the smallest time at which the matrix $D(t)$ is not singular if integration was from time zero to time t_1 , and t_2 is chosen so the integration interval $t = t_2 - t_1$ is equal to the largest time constant of the plant transfer function matrix. The definition of the ADGA is in complete analogy with the definition of the RDGA, and it therefore has many of the properties of the RDGA. In particular it provides an answer to the same question as the relative gain array, i.e. since $D(t)$ is in effect a matrix of average open loop gains, the ADGA measures the significance of parallel transmittance in the same way and for the same situation as the RDGA. The difference between the RDGA and the ADGA is, that the latter tries to condense the dynamic information into a single constant matrix. Gagnepain and Seborg show, that the ADGA, even though it has a higher success rate than the steady state RGA, fails in the crucial situations, where stability considerations determine the best pairing of variables.

2.4.5 The relative transient response functions.

Jaaksoo (1979) presented an exact time domain equivalent of the relative dynamic gain array. Based on a discrete state space model of the form

$$\begin{aligned} x(k+1) &= Ax(k) + Bu(k) \\ y(k) &= Cx(k) \end{aligned} \quad (2.19)$$

relative transient response functions $\Phi_{ij}^{(k)}$ are calculated. These functions are defined by

$$\Phi_{ij}^{(k)} = \frac{\sum_{t=1}^k c_i A^{t-1} b_j}{\sum_{t=1}^k c_i (M_{ij} A)^{t-1} M_{ij} b_j} \quad (2.20)$$

$$\Phi_{ij}^{(k)} = \frac{c_i [\sum_{t=1}^k A^{t-1}] b_j}{c_i [\sum_{t=1}^k (M_{ij} A)^{t-1}] M_{ij} b_j}$$

where c_i is the i 'th row of C , b_j is the j 'th column of B and $M = I + B_j(C_i B_j)^{-1} C_i$ in which B_j is B without the j 'th column and C_i is C without the i 'th row. Due to the exact equivalence with Bristol's (1966) approach the relative transient response functions gives a measure of the significance of parallel transmittance with one loop open and the rest closed, and not an indication of closed loop interaction. Jaaksoo (1979) suggests using only the arrays obtained with $k=1$ and $k \rightarrow \infty$ in the analysis. This corresponds to using the RDGA with only $s \rightarrow \infty$ and $s=0$ respectively. Jaaksoo introduces this limitation because of difficulties in the analytical investigation of a set of time functions. For example the matrix power series in equation 2.20 will only converge if all eigenvalues of A and $(M_{ij} A)$ have absolute values less than one, and the denominators can only be calculated from the numerators for $k=1$, cf. relative dynamic gain array. Further drawbacks of the relative transient response functions are: it is not clear how the function should be displayed or interpreted as functions of the time parameter k ; and they require a significant amount of numerical calculations to evaluate.

2.4.6 Other measures of interaction.

None of the measures or indices discussed so far require any knowledge of the control system structure, the type of final controllers or the associated gains. The result is, that the indices so far reviewed are more of warnings about potential difficulties, than indicators of closed loop interaction. Three measures, which require the control system structure and the final controllers

to be known, will now be reviewed.

Davison (1969) suggests a non-minimum phase index and interaction index based on a state space model. The non-minimum phase index is evaluated from eigenvalues of two matrices for each input - output pair, so the variable pairing must be known, and the only type of controller considered is proportional feedback. The interaction index is the difference between the closed loop non-minimum phase index and the open loop non-minimum phase index. The interaction index is interpreted in terms of favourable and unfavourable interactions. Since as has been shown in section 2.2 interaction transmittances cannot be classified as good or bad for all possible load or setpoint changes Davison's interpretation is wrong. The interaction index can only be seen as a measure of parallel transmittance. The non-minimum phase index is really a measure of the importance of the process deadtime relative to the dominant time constant, and as such has little to do with interaction. Both the non-minimum phase index and the interaction index are of limited value during control system design, partly due to the calculational effort involved in evaluating them.

Davison and Man (1970) suggest an interaction index based on the difference between a single closed loop response and the multiloop closed loop response. The index is based on a state space model and is calculated by solving two matrix equations iteratively and calculating the maximum eigenvalues of the resulting matrices, for each closed loop. If the value of the index is small for a given control loop interaction is not severe in that loop. Even though the index actually measures interaction in the closed loop system the amount of numerical calculation involved in evaluating it seems prohibitive for use in control system design. Also since a state space model is required and the complete control system must be known, it appears to be simpler to conduct some closed loop simulations in order to evaluate the resultant control system performance before implementation.

Suchanti and Fournier (1973) suggest the interaction coefficients defined for each loop as

$$I_j = [(\bar{IE}) - (IE)_j]/(IE)_j \quad (2.21)$$

where $(IE)_j$ is the error integral of the j 'th output for a unit step change in the j 'th input with loop j closed and all other loops open. Similarly $(\bar{IE})_j$ is the error integral of the j 'th output for a unit step change in all inputs with all loops closed. All integrals are evaluated with proportional plus integral controllers tuned using single loop techniques. There is little doubt, that the index gives a measure of closed loop interaction, and it is possible to evaluate the coefficient for any control system. However, calculation of the index requires $m+1$ closed loop simulations for a $m \times m$ system, and that amount of closed loop simulation should reveal any interaction problems without the need to calculate error integrals. Furthermore, a trial and error approach must be adopted to use the coefficients during control system design, i.e. pairing of variables.

2.5 The DNA - an alternative to measures of interaction.

In this section the type of results obtained from the use of measures of interaction, such as the interaction quotient of Rijnsdorp, the RGA, the RDGA and the ADGA, are compared with the information obtained from the DNA without calculating these measures.

Example 1:

A simple 2×2 transfer function matrix will show, that interaction transmittances can be severe even when parallel transmittance with one loop open is small. Consider the plant:

$$G_p(s) = \begin{bmatrix} \frac{1}{1s+1} & \frac{0.05}{10s+1} \\ \frac{1}{2s+1} & \frac{1}{1s+1} \end{bmatrix} \quad (2.22)$$

and assume $K_2(s) = H(s) = 1$ and $G_L(s) = 0$. Then Rijnsdorp's interaction quotient and the (2,2)-element of Bristol's RDGA are respectively

$$\kappa = 0.05 \frac{1+2s+1s^2}{1+12s+20s^2} \quad \mu_{22} = \frac{1+12s+20s^2}{0.95+11.9s+19.95s^2} \quad (2.23)$$

$\kappa(s)$ and the RDGA $M(s)$ are plotted as functions of frequency in figures 2.2

and 2.3 respectively. The magnitude of $\kappa(s)$ is small at all frequencies, and the magnitude of the diagonal elements of $M(s)$ are close to one at all frequencies. Thus both measures indicate there should be no difficulty in designing a multiloop control system, which is expected, since the TFM in equation 2.22 is almost triangular.

The closed loop equation for the second output with two proportional controllers is

$$y_2 = \frac{1}{\det F} \left[k_2 \frac{1}{s+1} r_2 + k_2 k_1 \left(\frac{1}{(s+1)^2} - \frac{0.05}{1+12s+20s^2} \right) r_2 + k_1 \frac{1}{2s+1} r_1 \right] \quad (2.24)$$

It is evident, that direct transmittance and interaction transmittance have very similar dynamics and magnitude. Further, the parallel transmittance is helpful and significant especially at low frequencies. With the second loop open the equation for the second output becomes

$$y_2 = k_2 \frac{1}{s+1} r_2 - k_2 \frac{0.05(s+1)}{(2s+1)(10s+1)(s+1+k_1)} r_2 + k_1 \frac{s+1}{(2s+1)(s+1+k_1)} r_1 \quad (2.25)$$

which shows insignificant parallel transmittance under these conditions, but comparable direct and interaction transmittances.

Rijnsdorp's interaction quotient and the RDGA suggest that a multiloop control system can be designed without difficulty, but they fail to give a reliable measure of the closed loop interaction. For this particular plant the DNA of $G_P(s)$ gives the same information for multiloop design, since $G_P(s)$ have no right half plane poles or zeros and is almost triangular. In addition the DNA of $G_P(s)$, shown in figure 2.4, indicates there is significant closed loop interaction in the second loop, but almost none in the first, which is expected, since the TFM is almost lower triangular.

Example 2:

Gagnepain and Seborg (1979) consider the following 2x2 system

$$G_P(s) = \exp(-s) \begin{bmatrix} \frac{2}{10s+1} & \frac{1.5}{1s+1} \\ \frac{1.5}{1s+1} & \frac{2}{10s+1} \end{bmatrix} \quad (2.26)$$

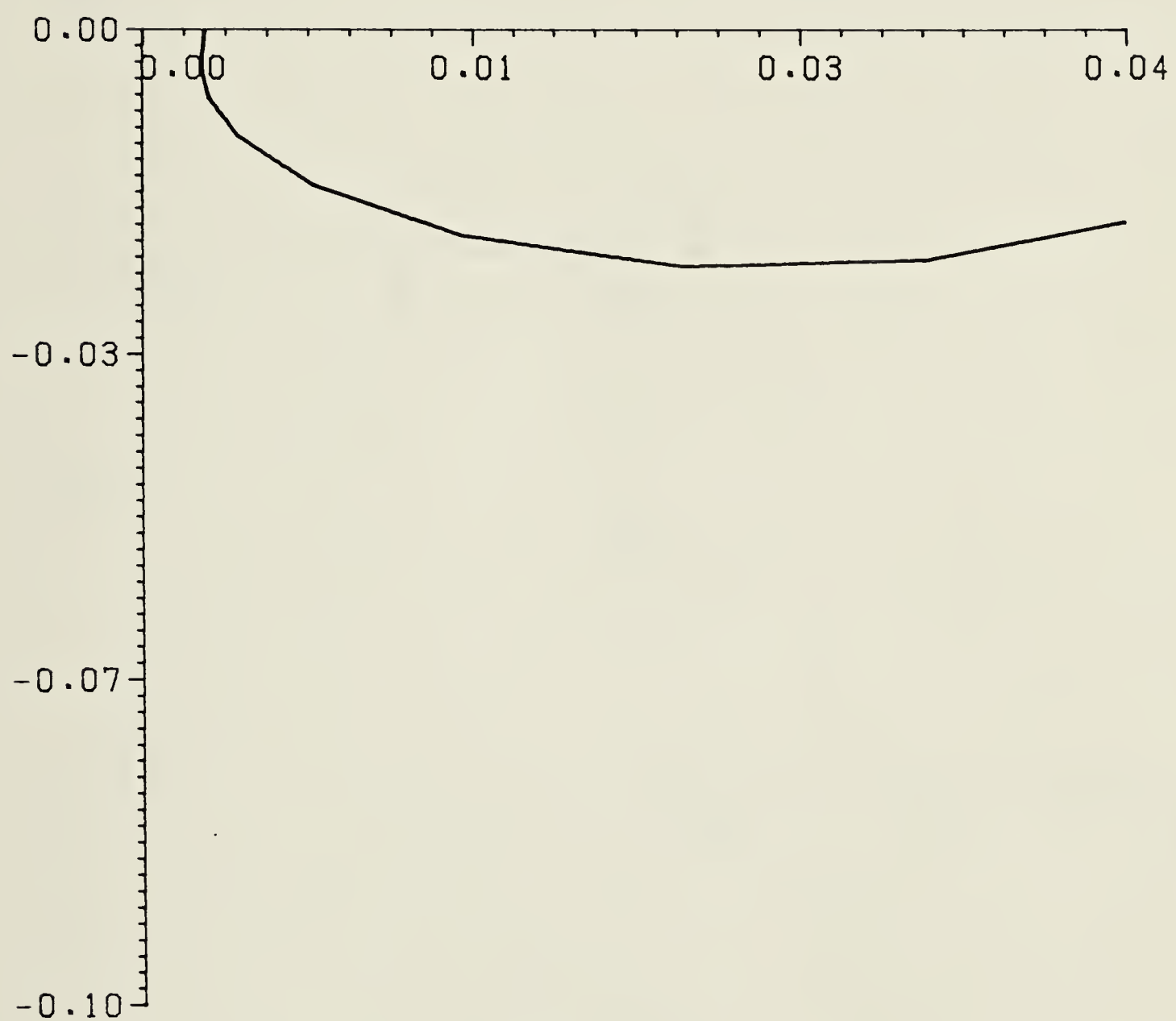


Figure 2.2 Polar plot of Rijnsdorp's interaction quotient for the TFM given in equation 2.22. The arrow indicates increasing frequency.

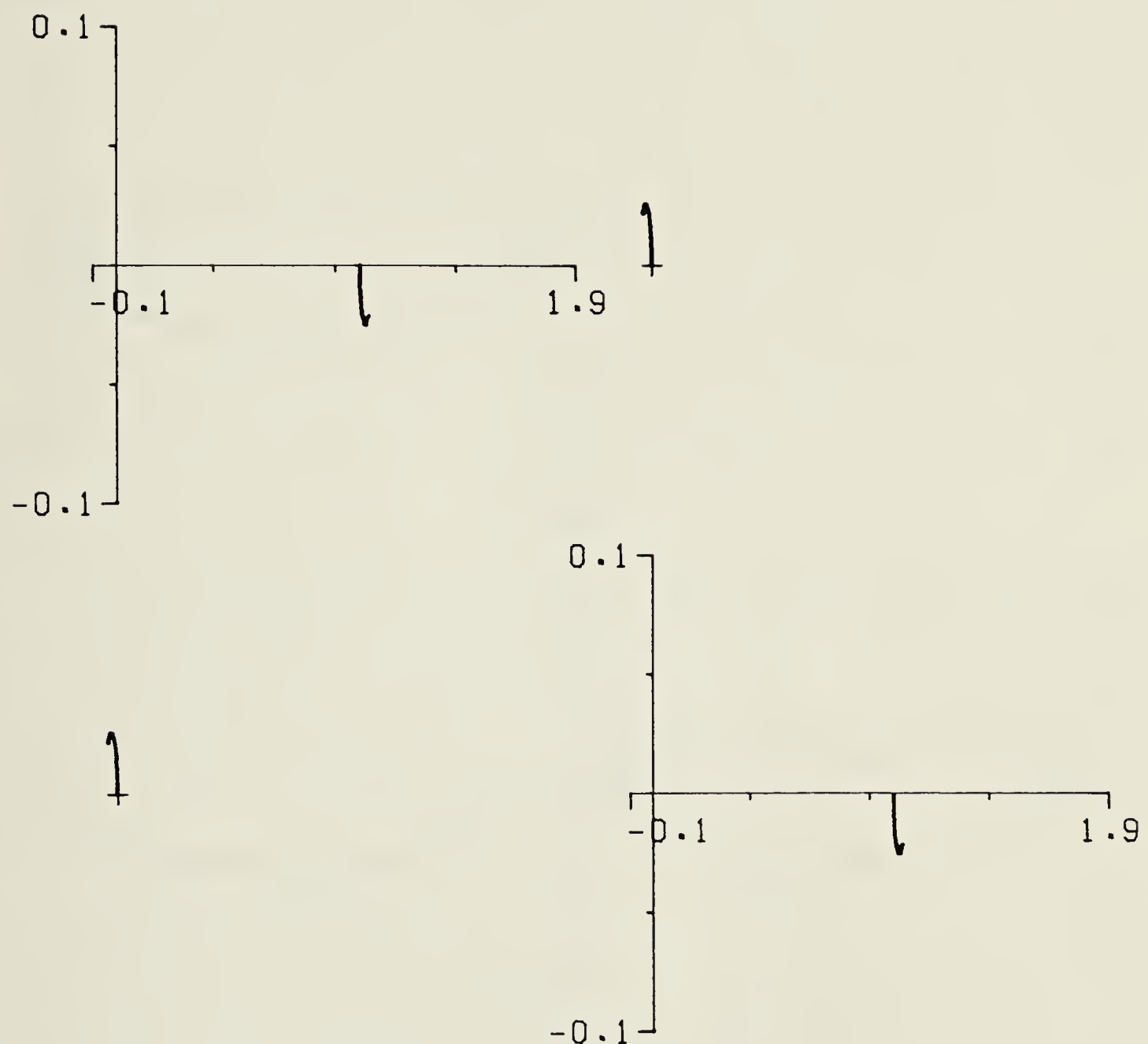


Figure 2.3 Polar plots of the elements of the relative dynamic gain array for the TFM in equation 2.22. Axis are only shown on diagonal elements and the origin of off diagonal elements are indicated by a plus sign.

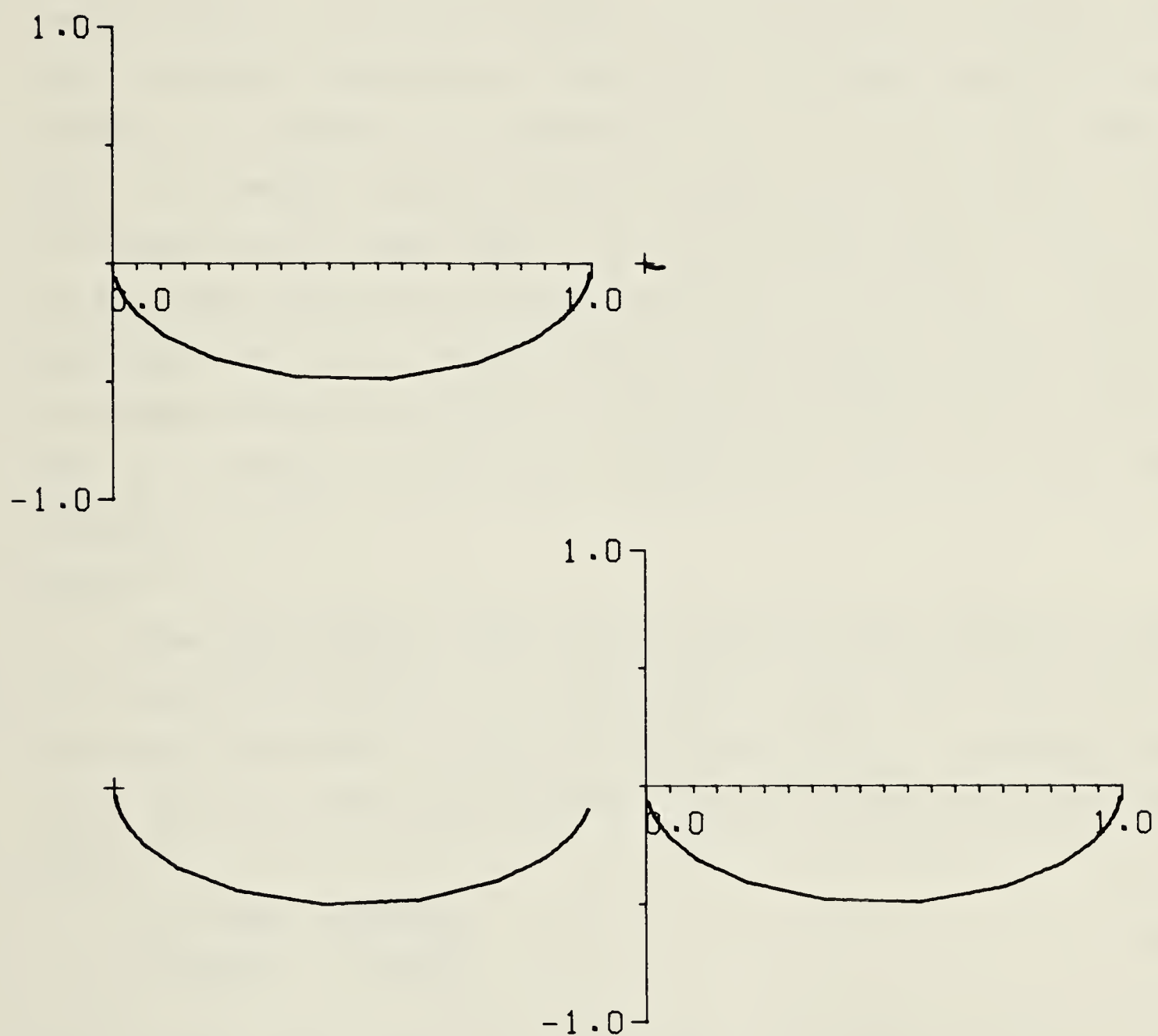


Figure 2.4 The direct Nyquist array for the TFM given in equation 2.22.

which has the following RGA and ADGA respectively

$$\begin{bmatrix} 2.29 & -1.29 \\ -1.29 & 2.29 \end{bmatrix} \quad \begin{bmatrix} -0.42 & 1.42 \\ 1.42 & -0.42 \end{bmatrix} \quad (2.27)$$

The two measures recommend different pairings. Gagnepain and Seborg (1979) show, the pairing recommended by the ADGA is structurally monotonic unstable according to a theorem due to Niederlinski (1971). The failure of the ADGA is due to the averaging integration process. The polar plot of the RDGA in figure 2.5 suggests, that at steady state the first input variable should be paired with the first output variable, but at higher frequencies with the second. The DNA of $G_p(s)$ leads to the same conclusion as seen from figure 2.6. The DNA plot not only supplies the same information for pairing as the RDGA but also provides a basis for designing the appropriate controller, e.g. using the DNA design procedure.

Example 3:

Ahson and Nicholson (1976) and later Taiwo (1978) consider the design of a compensator/controller for a turbo-alternator model with two inputs and two outputs. Simulations by Ahson and Nicholson show a multiloop control system gives very unsatisfactory control. However, the steady state relative gain array is

$$\begin{bmatrix} 1.0235 & -0.0235 \\ -0.0235 & 1.0235 \end{bmatrix} \quad (2.28)$$

which indicates there should be no difficulties in designing a multiloop control system. For this system the magnitude of the elements of the RDGA change significantly with frequency, as seen from figure 2.7, indicating different variable pairings at low frequency and at high frequency. The same information is also evident from the DNA-plot in figure 2.8, which also shows, that the difficulties are due to the small size of the (1,1)-element of the plant transfer function matrix. The transfer function model used by Taiwo (1978) is slightly different from the one used by Ahson and Nicholson (1976). The RDGA and DNA plots for the model used by Taiwo are shown in figures 2.9 and 2.10 respectively. While the DNA displays of figures 2.8 and 2.10 are very similar and readily

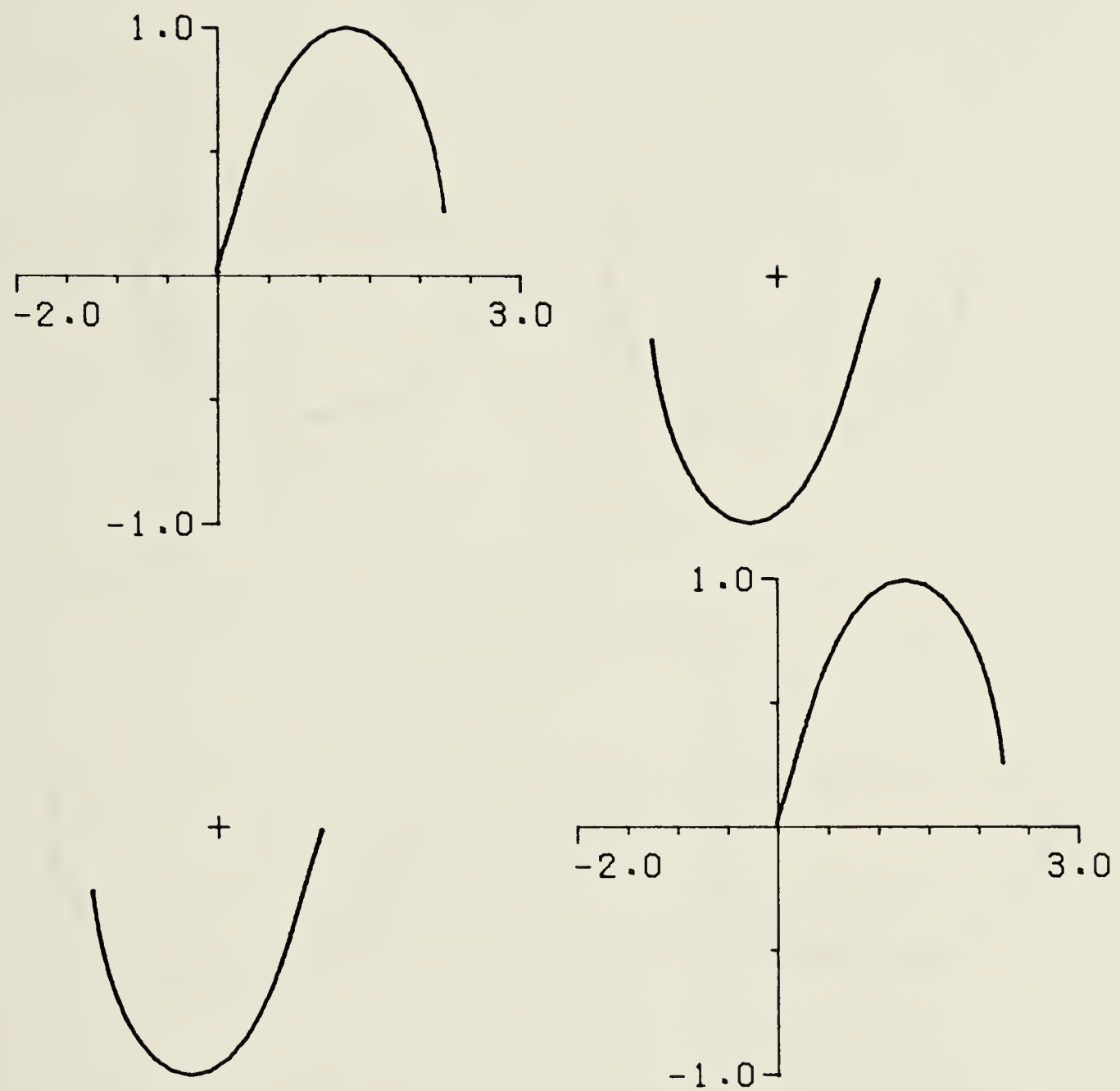


Figure 2.5 The relative dynamic gain array for the TFM given in equation 2.26.

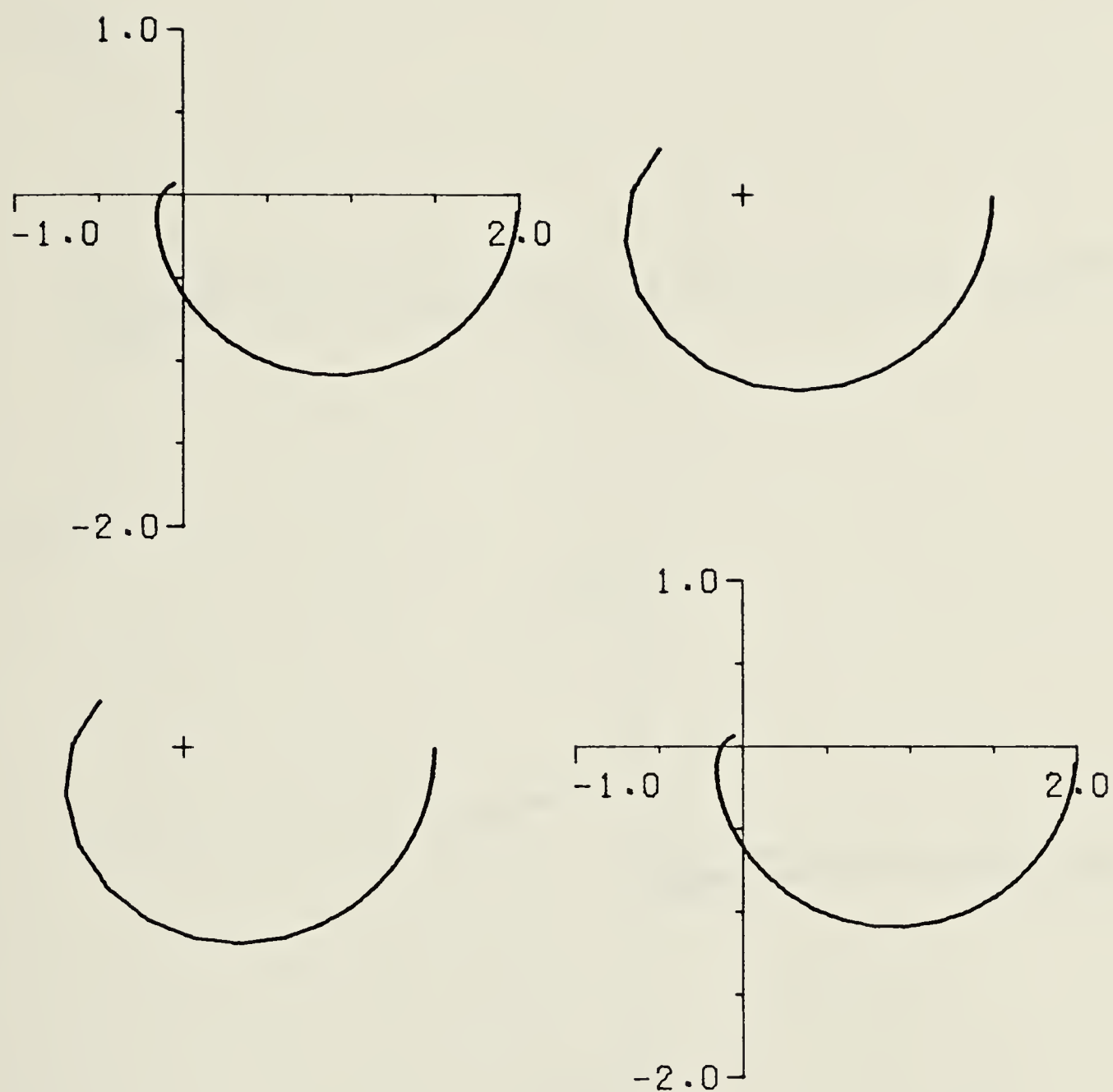


Figure 2.6 The direct Nyquist array for the TFM given in equation 2.26.

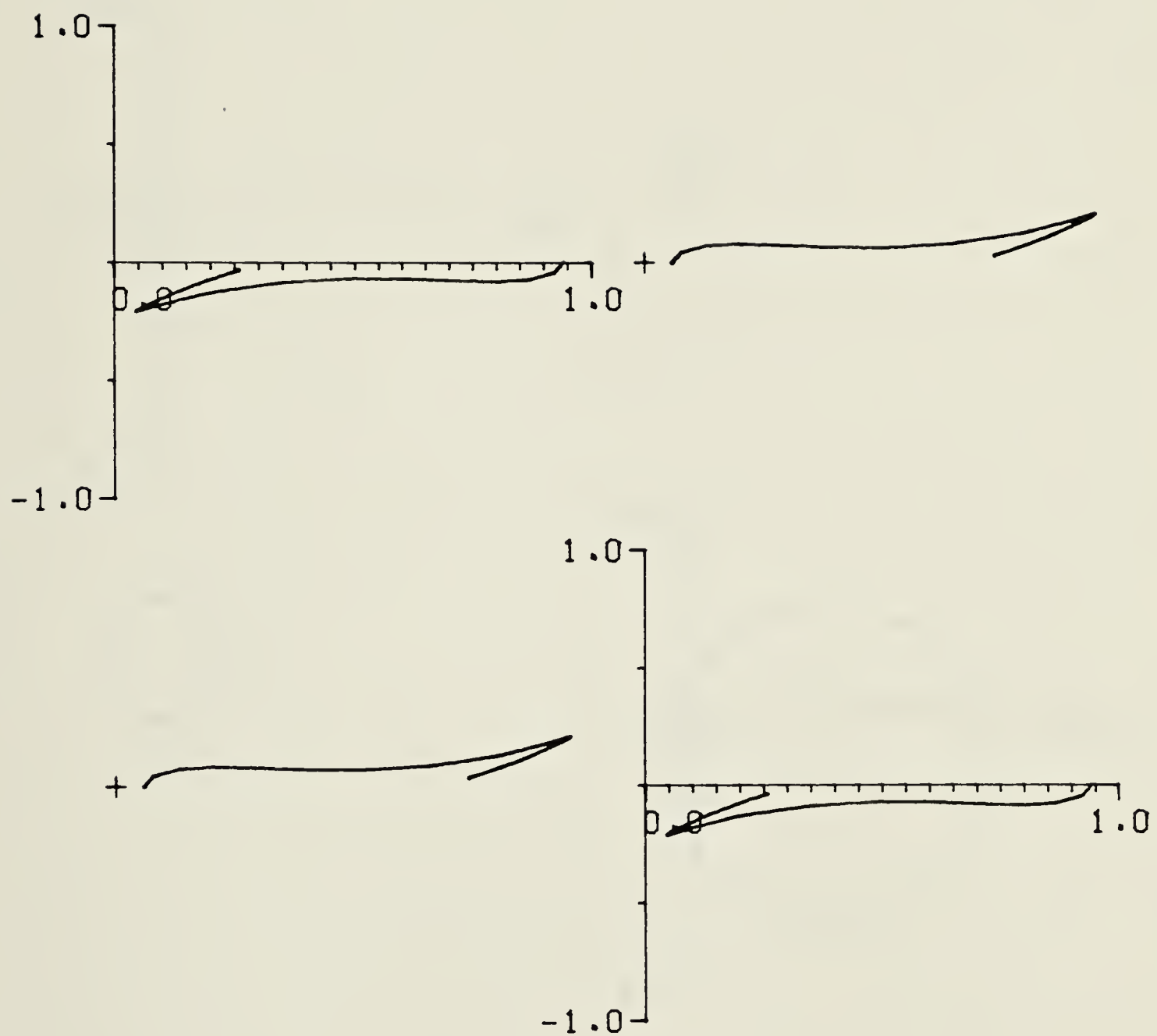


Figure 2.7 The relative dynamic gain array for turboalternator using model of Ahson and Nicholson (1976).

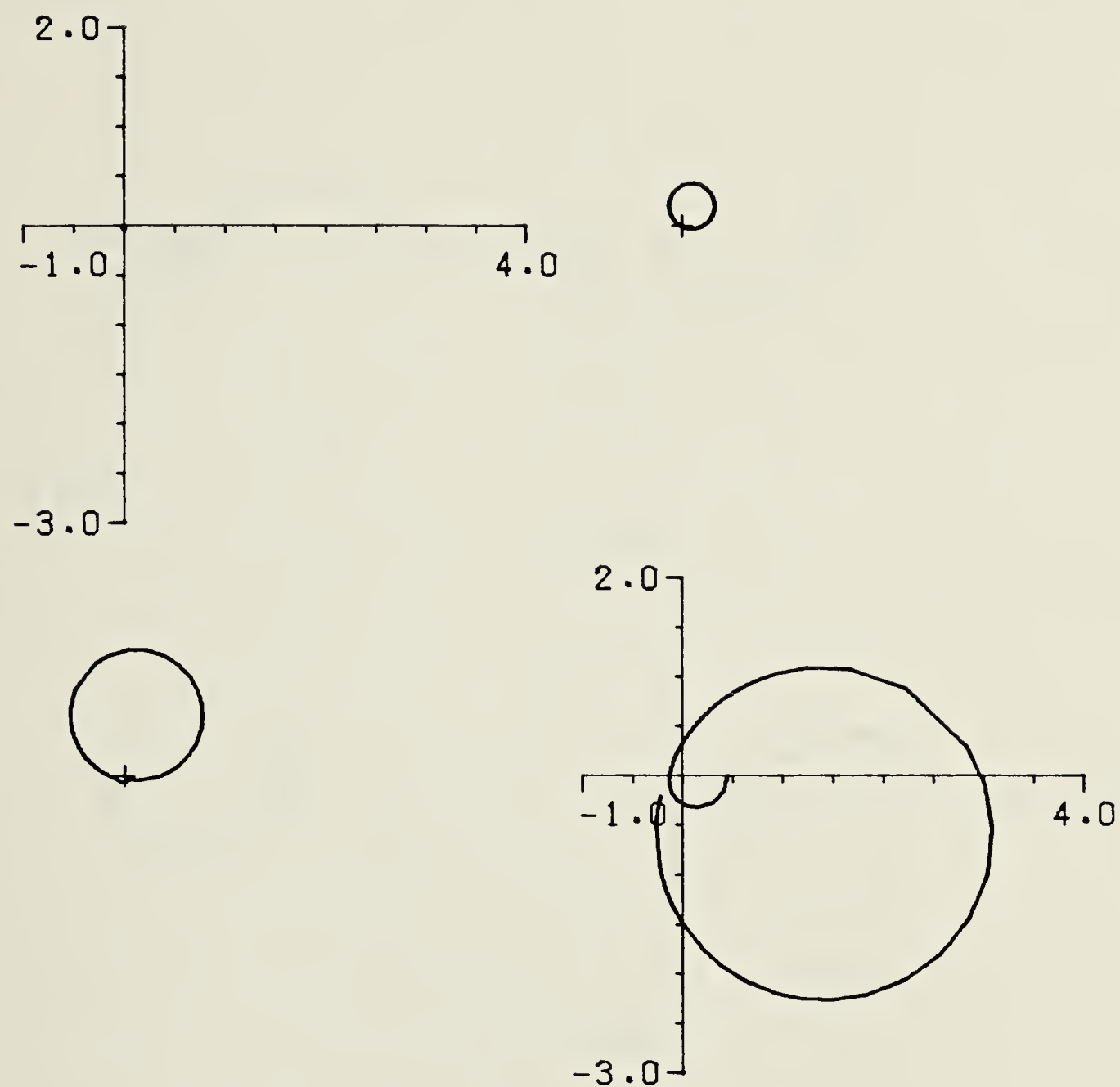


Figure 2.8 The direct Nyquist array for turboalternator using model of Ahson and Nicholson (1976).

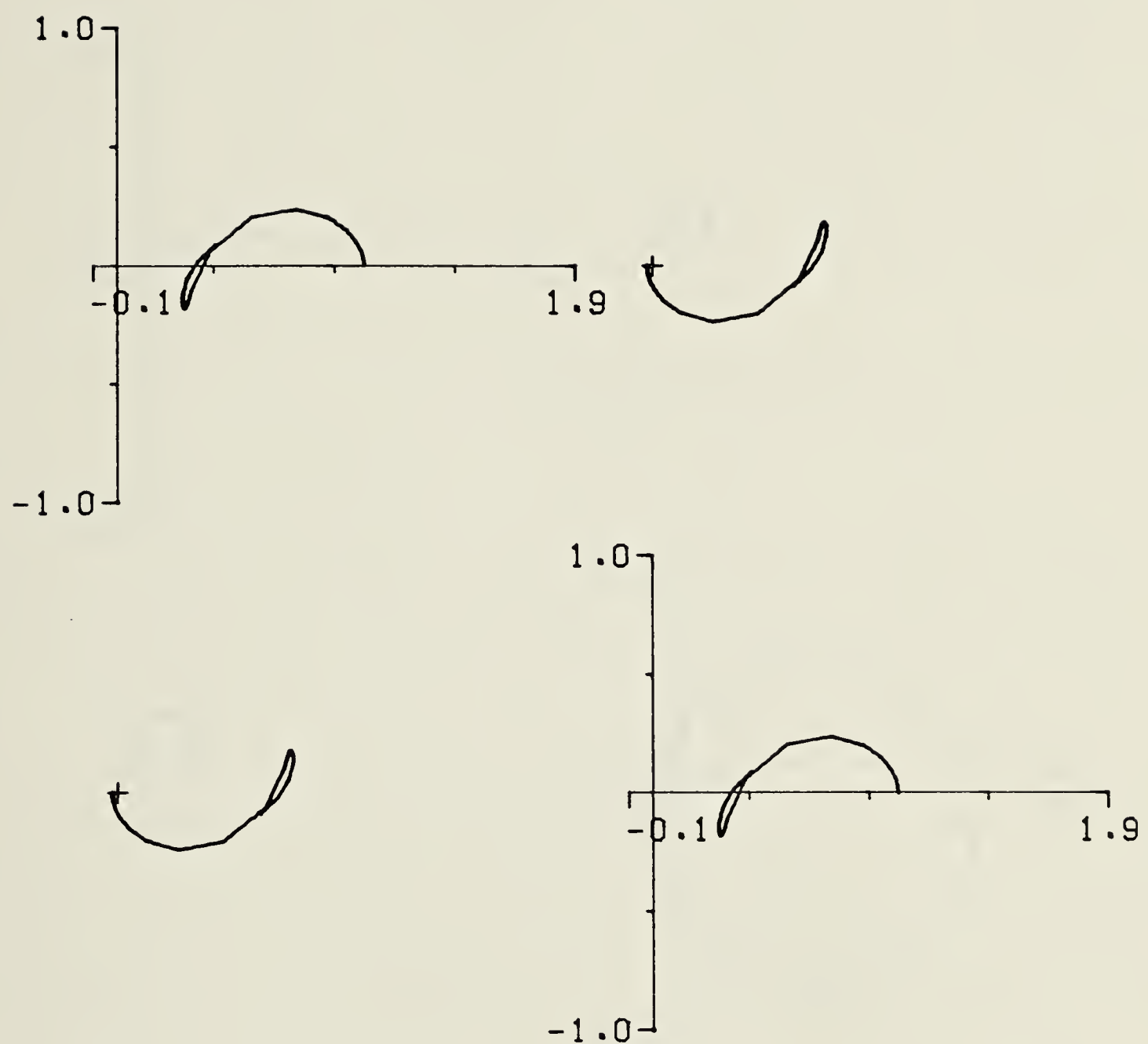


Figure 2.9 The relative dynamic gain array for turboalternator using model of Taiwo (1978).

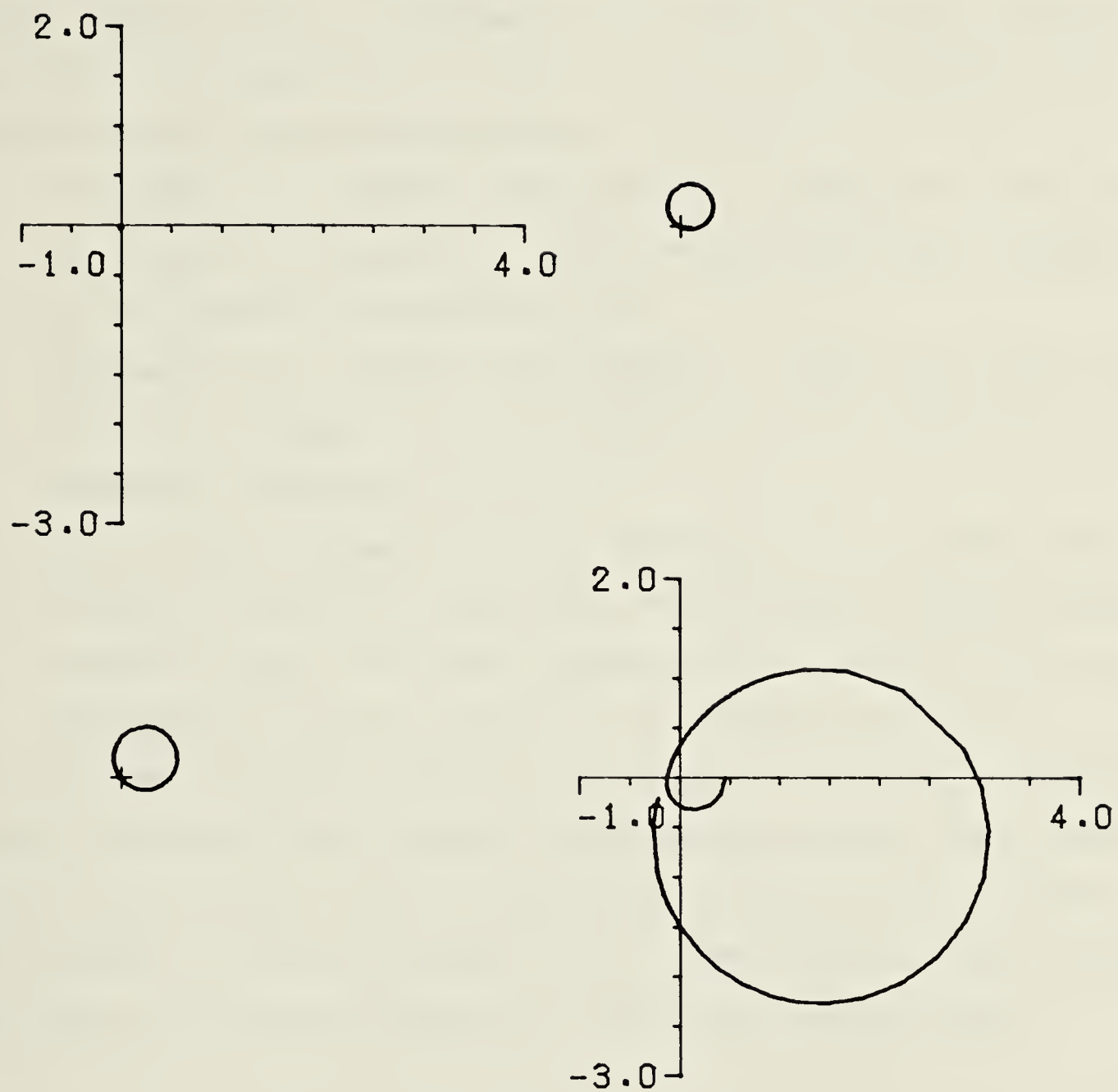


Figure 2.10 The direct Nyquist array for turboalternator using model of Taiwo (1978).

reveal the difference between the two models is in the (2,1)-element, the RDGA displays of figures 2.7 and 2.9 appear to come from two highly different models. The DNA displays of figures 2.8 and 2.10 further show, a full, dynamic compensator $K_1(s)$ is probably required for effective control. The complete design of such a compensator is not relevant here, but note that the classification of transmittances in figure 2.1 provides a convenient means of comparing some of the design alternatives:

- i. Introduction of a diagonal precompensator to multiply the first column of $G_p(s)$ by a constant, N_1 , which increases the direct, parallel and $r_1 \rightarrow y_2$ interaction transmittance by N_1 .
- ii. Introduction of a diagonal postcompensator to multiply the first row of $G_p(s)$ by a constant, N_2 , which increases the direct, parallel and $r_2 \rightarrow y_1$ interaction transmittance by N_2 .
- iii. For a given increase in direct transmittance it is probably best to combine the above two approaches, which increases the direct transmittance by $N_1 * N_2$, the parallel transmittance by $N_1 * N_2$, but the $r_1 \rightarrow y_2$ interaction by only N_1 , and the $r_2 \rightarrow y_1$ interaction by only N_2 .

Figure 2.11 shows the DNA resulting from using $N_1 = 2$ and $N_2 = 5$. The interactions could be further reduced through additional design steps. Also the diagonal postcompensator can be implemented as part of the controller and hence causes no practical difficulties. Thus it is seen, that the DNA provides a better basis for analysis and design of a compensator than the RDGA.

2.6 Conclusions.

Transmittances in a closed loop multivariable control system can advantageously be classified as: direct, parallel, interaction and disturbance transmittances. Interaction transmittances in an $m \times m$ system can further be expressed as a sum of 1st, 2nd, and up to $m-1$ 'th order interaction terms.

Several published measures of interaction were reviewed. The interaction quotient, the RGA, the RDGA, the ADGA and the relative transient response functions have the following shortcomings: i) they are based on a system with

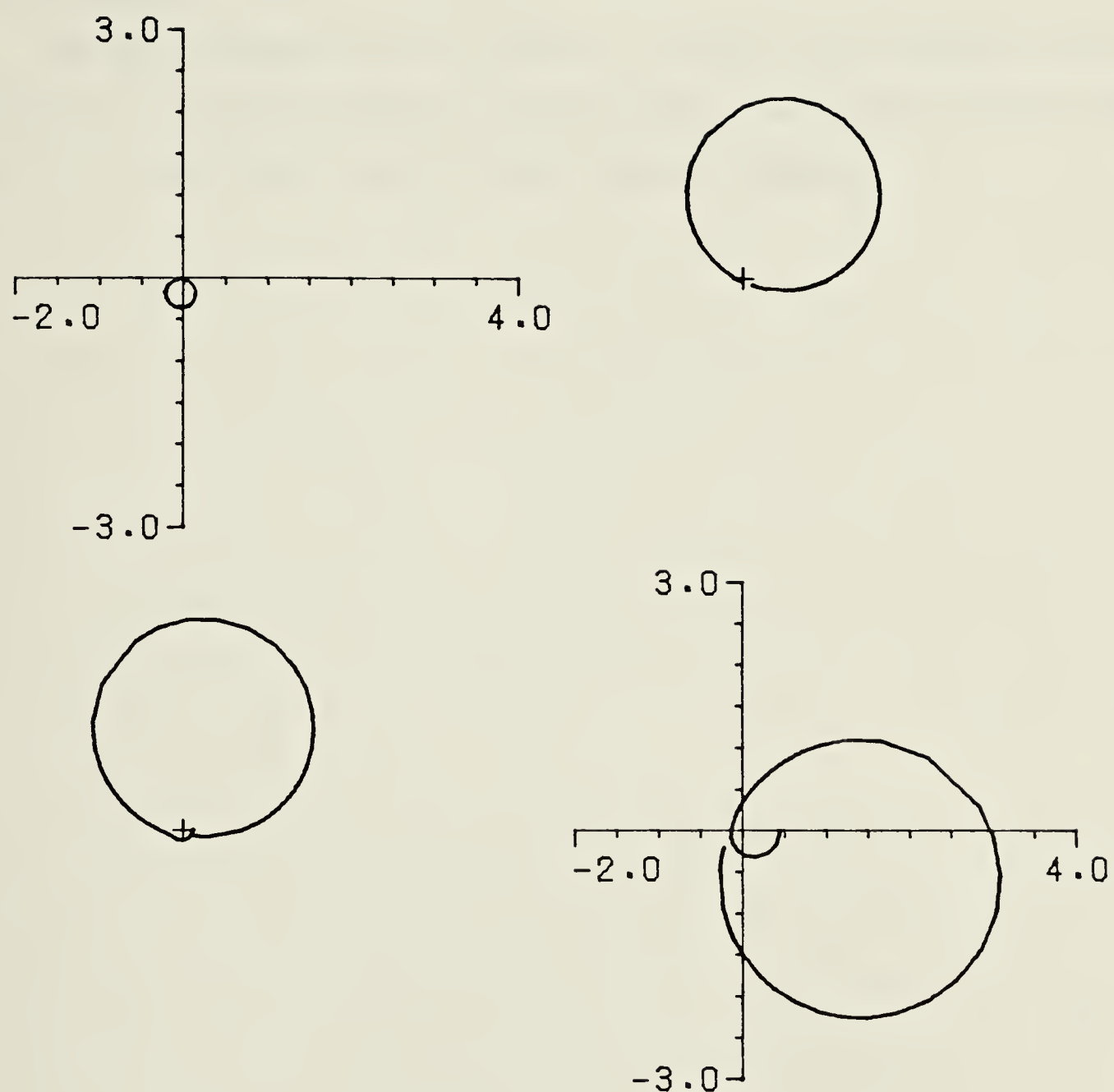


Figure 2.11 The DNA for turboalternator using model of Ahson and Nicholson (1976), and diagonal pre- and postcompensators.

one loop open rather than a fully closed loop system, and ii) they measure the parallel transmittance with all but one loop closed rather than the true interaction transmittance. They are more of a warning about potential difficulties in designing a multiloop control system, than a direct quantitative measure of system interaction.

The DNA display gives an indication of closed loop interaction and is a suitable tool for pairing variables as the first step in a multiloop control system design. It is recommended over the other reviewed measures.

3. Matrix dominance and transfer of dominance.

3.1 Introduction.

Multivariable frequency domain design techniques, such as the inverse Nyquist array (INA) method (Rosenbrock (1969)) and the direct Nyquist array (DNA) method (Kuon (1975)), base the final selection of controller constants and the stability analysis on only the diagonal elements of respectively the inverse open loop transfer function matrix (TFM) and the open loop TFM. In order to assess stability based only on the diagonal elements of a TFM, some condition must be put on this TFM. As first proposed the INA method required the open and closed loop inverse TFM's to be diagonally dominant, and the DNA method required the return difference matrix to be diagonally dominant, in the sense defined by Rosenbrock (1969). The application of the multivariable Nyquist array (MNA) techniques to industrial problems has been somewhat limited because the diagonal dominance requirement is too strict for many industrial systems, where integrity is a major concern. Recently several authors, e.g. Mee (1976), have explored ways of relaxing the condition for application of the multivariable Nyquist array stability theorems.

In this chapter past work on extending the applicability of the MNA stability theorems is reviewed. The results of previous work on M-matrices are formalized by the introduction of the concept of matrix dominance, and a necessary and sufficient test for a TFM to be matrix dominant is given. A graphical test for matrix dominance is developed, and the use of this test to aid in the design of a compensator for systems, which are not matrix dominant, is discussed.

The implications of matrix dominance for the MNA design techniques are demonstrated. Further, it is shown, that a row dominant system can be made column dominant by a diagonal similarity transformation. This duality is finally exploited in a selection procedure for final loop gains of matrix dominant systems.

3.2 Definition of and test for matrix dominance.

In the extension of the MNA stability theorems the concept of M-matrices plays a central role. The next subsection contains a very brief definition of an M-matrix and some associated mathematical tools. This is followed by sections reviewing previous work and developing tests for matrix dominance.

3.2.1 Mathematical background and notation.

A real $m \times m$ matrix $A = \{a_{ij}\}$ is an M-matrix if and only if the offdiagonal elements are nonpositive and all the principal minors are positive. The properties of M-matrices has been extensively treated by Ostrowski (1937, 1956) and by Fiedler and Ptak (1962, 1966, 1967), who also give alternative criteria for judging whether or not a real square matrix is an M-matrix. (Fiedler and Ptak use the term 'matrix of class K' to designate an 'M-matrix'). For a complex $m \times m$ matrix $Q = \{q_{ij}\}$ the companion matrix (Begleitmatrix (Ostrowski (1956))) $B = \{b_{ij}\}$ is defined as

$$b_{ii} = |q_{ii}| \quad \text{and} \quad b_{ij} = -|q_{ij}| \quad i \neq j \quad (3.1)$$

Further, $C = \{c_{ij}\}$ is a real matrix defined as

$$c_{ii} = 0 \quad \text{and} \quad c_{ij} = |q_{ij}| \quad i \neq j \quad (3.2)$$

and $W = \text{diag}\{w_i\}$ is a real $m \times m$ diagonal matrix with $w_i > 0$.

3.2.2 Previous work on extending MNA stability theorems.

The first published work on extending the class of TFM to which the MNA stability theorems are applicable is due to Araki and Nwokah (1975). Araki and Nwokah use the concept of M-matrices in establishing bounds on the transfer function $h_i(s)$ between the i 'th input and the i 'th output of a multivariable system with the i 'th loop open and all other loop closed. Their main result is, that for a open loop TFM $Q(s)$

$$|h_i(s) - q_{ii}(s)| < \lambda(s)w_i \quad (3.3)$$

where $\lambda(s)$ is the largest eigenvalue of CW^{-1} with C and W as defined in section 3.2.1. The authors also point out, that any one bound can be made arbitrarily small at the expense of making another bound arbitrarily large. Finally

Araki and Nwokah state without proof, that closed loop stability of an open loop stable system $Q(s)$ is guaranteed if the Nyquist loci of $q_{ii}(s)$ do not encircle the critical point and the companion matrix of the return difference matrix $F(s) = I + Q(s)$ is an M-matrix. Araki and Nwokah do not clarify the implications of their findings on the MNA design procedures, and give no simple way of ascertaining whether $F(s)$ has a companion matrix, which is an M-matrix.

Mee (1976) points out, that a practical disadvantage of the INA technique is, that high frequency response is usually not well known, giving rise to difficulties in establishing dominance at high frequencies. This practical difficulty is also reported by Leininger (1979a) and Clement (1980). Mee (1976) shows, that it is possible to test stability by considering the Nyquist loci over a finite frequency range $\omega_0 > \omega > -\omega_0$ instead of $\infty > \omega > -\infty$. Mee also introduces the use of diagonal similarity transformations $D(s) = \text{diag}\{d_i(s)\}$, $d_i(s)$ real and positive, to make a nondiagonally dominant system diagonally dominant during the design phase. Complex matrices with the property of being diagonally dominant after a diagonal similarity transformation are matrices, whose companion matrix is an M-matrix. The diagonal similarity transformation shares dominance among or transfers dominance to different rows or columns. The concept of dominance sharing is also discussed by Leininger (1978, 1979b), who remarks, that applying dominance sharing becomes analytically more difficult as the order of the transfer function matrix increases. Leininger (1979b) also restates the finite frequency range result of Mee (1976), and Leininger (1979a) develops a function minimization procedure, similar to pseudodiagonalization, to design a constant compensator, to achieve diagonal dominance. The dominance sharing results of Mee (1976) and Leininger (1978, 1979b) are essentially practical applications of the results previously stated by Araki and Nwokah (1975).

Kantor and Andres (1979) use a method identical to Araki and Nwokah's (1975) to calculate normalized Gershgorin bands. Kantor and Andres calculate the normalized Gershgorin radius, $\Theta(s)$, as the maximum eigenvalue of CW^{-1} or $W^{-1}C$ with $w_i = |q_{ii}(s)|$, where

$$\Theta^r(s) = \max_i \left[\sum_{\substack{j=1 \\ j \neq i}}^m |q_{ij}(s)| (c_j^r(s)/d_j^r(s)) / |q_{ii}(s)| \right] \quad (3.4)$$

and calculate individual radii as $\Theta^r(s)|q_{ii}(s)|$. The $d_j^r(s)$, $i = 1, \dots, m$, are positive real functions of s . These functions are the elements of a diagonal similarity transformation matrix $D(s)$. Kantor and Andres avoid calculating this transformation by transforming the problem of finding minimal Gershgorin radii into an eigenvalue problem. The largest eigenvalue must be chosen, since it is not possible to associate eigenvalues with rows or columns or the TFM $Q(s)$. The main result of Kantor and Andres is, that $Q(s)$ is similar to a diagonally dominant matrix, i.e. the companion matrix of $Q(s)$ is an M-matrix, if and only if $\Theta^r(s) < 1$. This makes it possible to determine from a simple graph of $\Theta^r(s)$ versus frequency whether or not the companion matrix of a given TFM is an M-matrix. However, if the test is negative the graphical display of $\Theta^r(s)$ gives no guidelines for designing a suitable compensator.

Nwokah (1980a) formally states the MNA stability theorems for TFM's, whose companion matrices are M-matrices. Nwokah (1980b) points out, that the results of Mee (1976) and Kantor and Andres (1979) are simple consequences of the properties of M-matrices. Nwokah (1980b) also misleadingly labels complex matrices, whose companion matrix is an M-matrix as Hadamard matrices. The term 'Hadamard matrix' is generally associated with matrices with all elements -1 or +1.

3.2.3 Matrix dominance.

Since the terms companion matrix and M-matrix do not clearly show the extension of the diagonal dominance idea of Rosenbrock(1969), and the term companion matrix in control is often defined differently from Ostrowski's (1956) definition, which is used here, it is proposed to call the extended class of systems to which the MNA stability theorems are applicable *matrix dominant* systems. Matrix dominance is defined as follows

Definition: A TFM $Q(s)$ is said to be matrix dominant if and only if

$$P_i = \sum_{\substack{k=1 \\ k \neq i}}^m \|q_{ik}(s)\|, R_i = \sum_{\substack{k=1 \\ k \neq i}}^m \|q_{ki}(s)\| \quad (3.5)$$

$$\text{and } \|q_{ii}(s)\| \|q_{jj}(s)\| > P_i P_j \quad \text{or} \quad \|q_{ii}(s)\| \|q_{jj}(s)\| > R_i R_j$$

for each pair $(i,j), i \neq j$.

The test contained in this definition is easily programmed on a digital computer and requires only a few more calculations than a diagonal dominance test. It also retains the sums of offdiagonal elements from diagonal dominance test. The above definition, which is adapted from a theorem of Fiedler and Ptak (1962), implies that the companion matrix of $Q(s)$ must be an M-matrix for $Q(s)$ to be matrix dominant. It is easily seen, that the class of diagonally dominant systems is contained in the class of matrix dominant systems, i.e. any diagonally dominant matrix $Q(s)$ satisfies inequalities 3.5.

The property of matrix dominance is identical to Mee's (1976) concept of similarity to a diagonally dominant system. The term *matrix dominance* is suggested here, since it shows the relationship to *diagonal dominance*, and indeed a 2×2 system is matrix dominant if the single inequality

$$\|q_{11}(s)\| \|q_{22}(s)\| > \|q_{21}(s)\| \|q_{12}(s)\| \quad (3.6)$$

involving all elements of the transfer function matrix is satisfied.

3.2.4 Graphical test for matrix dominance.

One of the major advantages of the MNA design techniques is the use of graphical displays to guide the designer and to test for diagonal dominance. A graphical test for matrix dominance, which would also give guidance as to the design of a compensator for a system, which was not matrix dominant, would be very desirable. The inequalities of the definition for matrix dominance do not immediately lend themselves to a graphical test. However, a slight rearrangement of the inequalities 3.5 gives

$$N_{ij}^r = P_i P_j / (\|q_{ii}(s)\| \|q_{jj}(s)\|) < 1 \quad \text{or} \quad N_{ij}^c = R_i R_j / (\|q_{ii}(s)\| \|q_{jj}(s)\|) < 1 \quad (3.7)$$

Hence, a system is matrix dominant if the real non-negative numbers N_{ij} are less than one for all pairs $(i,j), i \neq j$. Therefore a set of plots

of N_{ij} as a function of frequency, would show whether or not a system is matrix dominant. For a 2×2 system only one graph is involved, for a 3×3 system 3 graphs, and for a general $m \times m$ system the set of plots contains $m(m-1)/2$ graphs. This is less than the number of plots in the corresponding Nyquist array, but more than in a graphical test for diagonal dominance for $m > 3$.

To illustrate the use of the graphical test for matrix dominance as an aid in compensator design for non-matrix dominant systems a transfer function model of the pilot plant double effect evaporator in the Department of Chemical Engineering at the University of Alberta is considered. The transfer function model calculated from the continuous fifth order state space model given by Fisher and Seborg (1976) is shown in table 3.1. A set of three plots to graphically test $F(s) = I + G(s)$ for column matrix dominance is shown in figure 3.1, and the similar test for row matrix dominance is shown in figure 3.2. In figure 3.1 N_{12}^c , N_{13}^c and N_{23}^c are plotted as functions of frequency for frequencies in the range from 0.0038 to 7.73 rad/min. N_{13}^c and N_{23}^c are zero at all frequencies, and $N_{12}^c > 1$ for frequencies lower than 0.08 rad/min., hence the return difference matrix is not column matrix dominant at low frequencies. Figure 3.2 shows, that the return difference matrix is also not row matrix dominant at low frequencies. Since only N_{12}^c is different from zero in figure 3.1, this indicates, that the offdiagonal elements of columns 1 and 2 must be reduced to achieve matrix dominance of the return difference matrix at low frequencies. Figure 3.2 indicates, that the offdiagonal elements of row 3 should be reduced to attain matrix dominance. The direct Nyquist array (DNA) display of the TFM $G(s)$ is shown in figure 3.3 (Note: axis are only drawn on diagonal elements, and the origin of offdiagonal elements are indicated by a '+'). From figure 3.3 it appears, that the open loop TFM will become lower triangular by the following column operation

$$\text{column 2} = \text{column 2} + 0.73 * \text{column 1} \quad (3.8)$$

which will tend to cancel the influence of element (1,2) and at the same time increase the direct transmittance (cf. chapter 2) in the second loop, and slightly decrease the influence of element (3,2). After the above compensation the

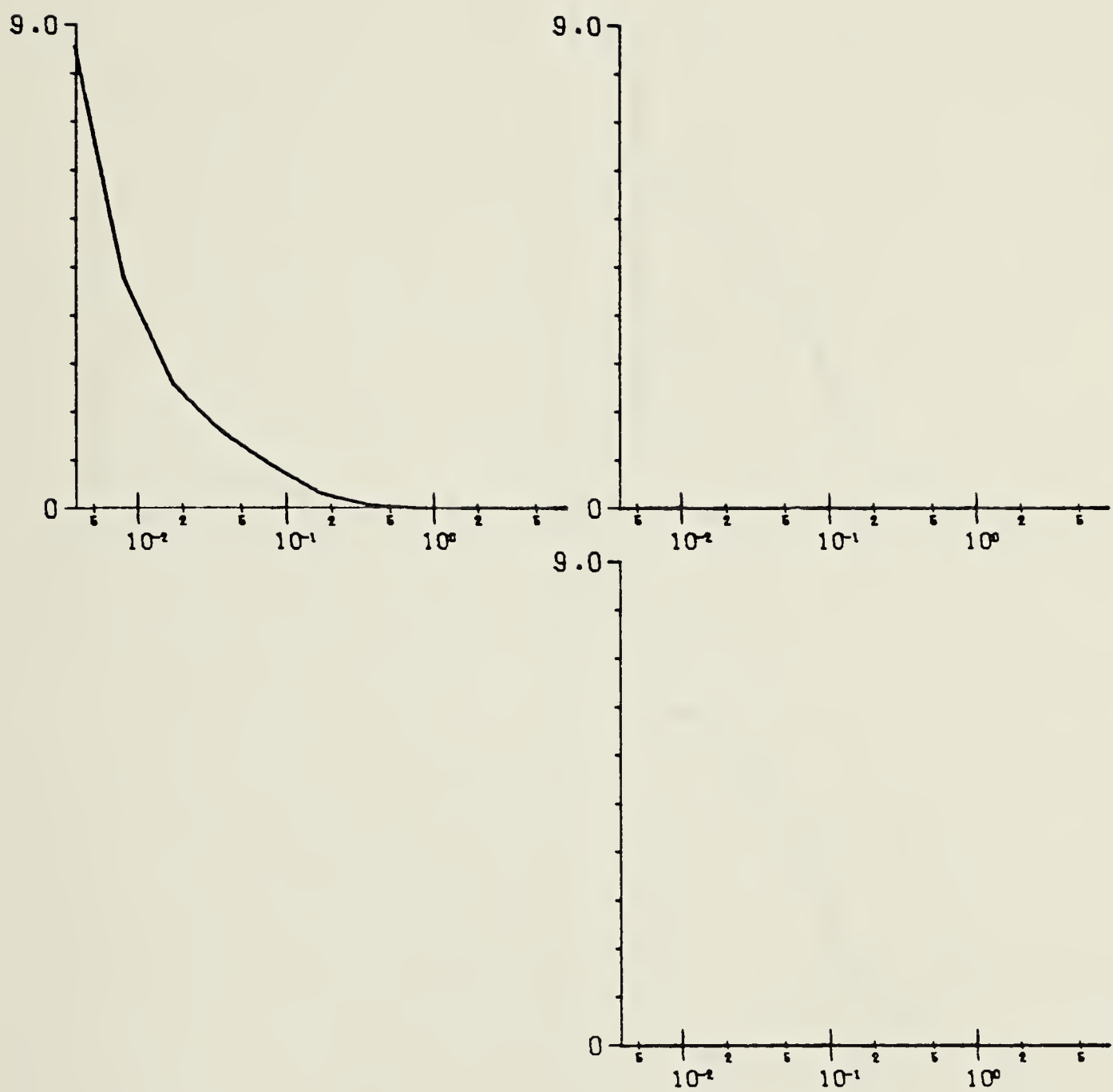


Figure 3.1 Graphical test of pilot plant evaporator return difference matrix $F(s) = I + G(s)$ for column matrix dominance. Frequency in the range from 0.0038 to 7.73 rad/min. is the ordinate, and the abscissa the dimensionless numbers defined by equation 3.7.

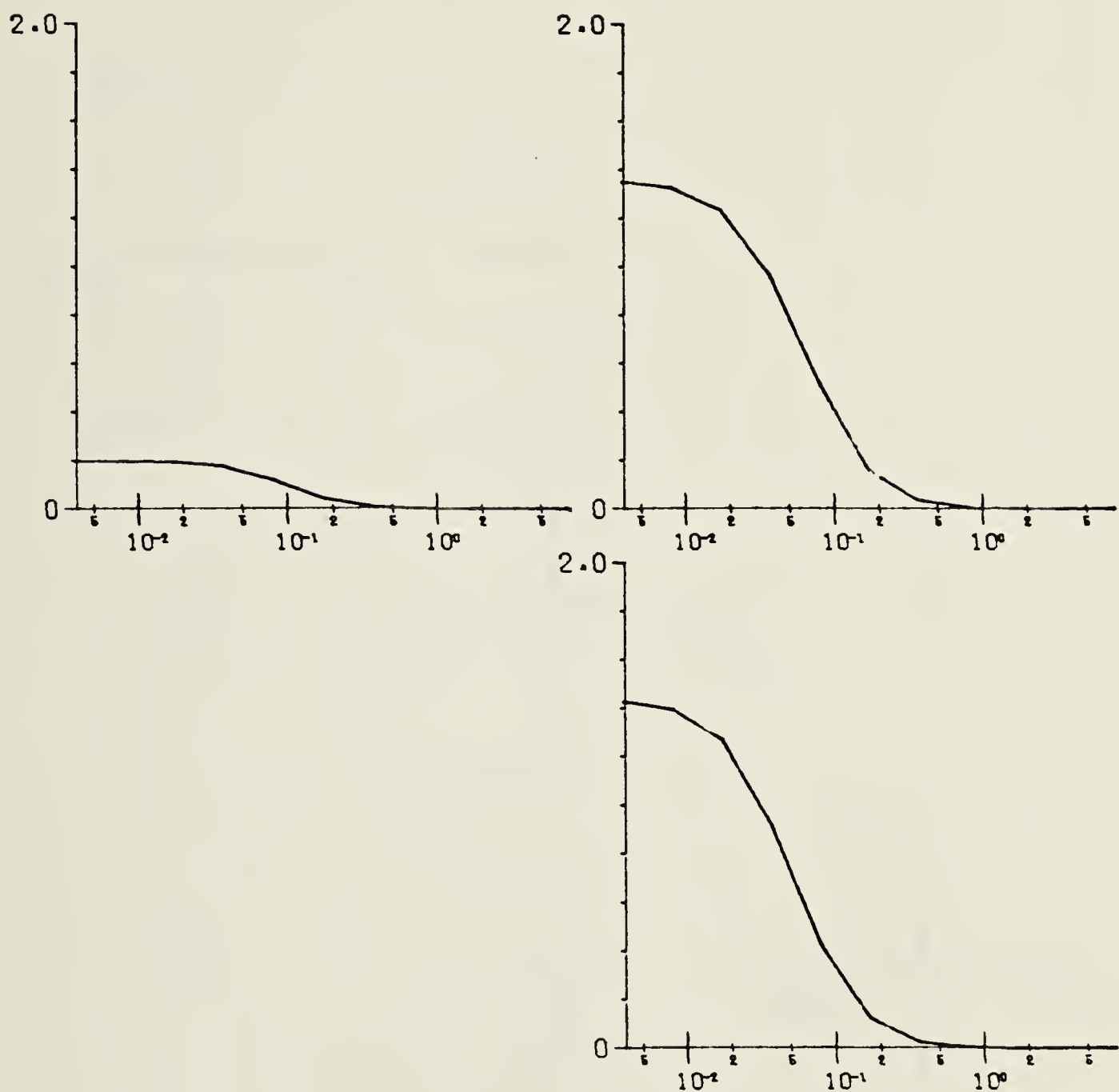


Figure 3.2 Graphical test of pilot plant evaporator return difference matrix for row matrix dominance. Frequency range $0.0038 < \omega < 7.73$ rad/min.

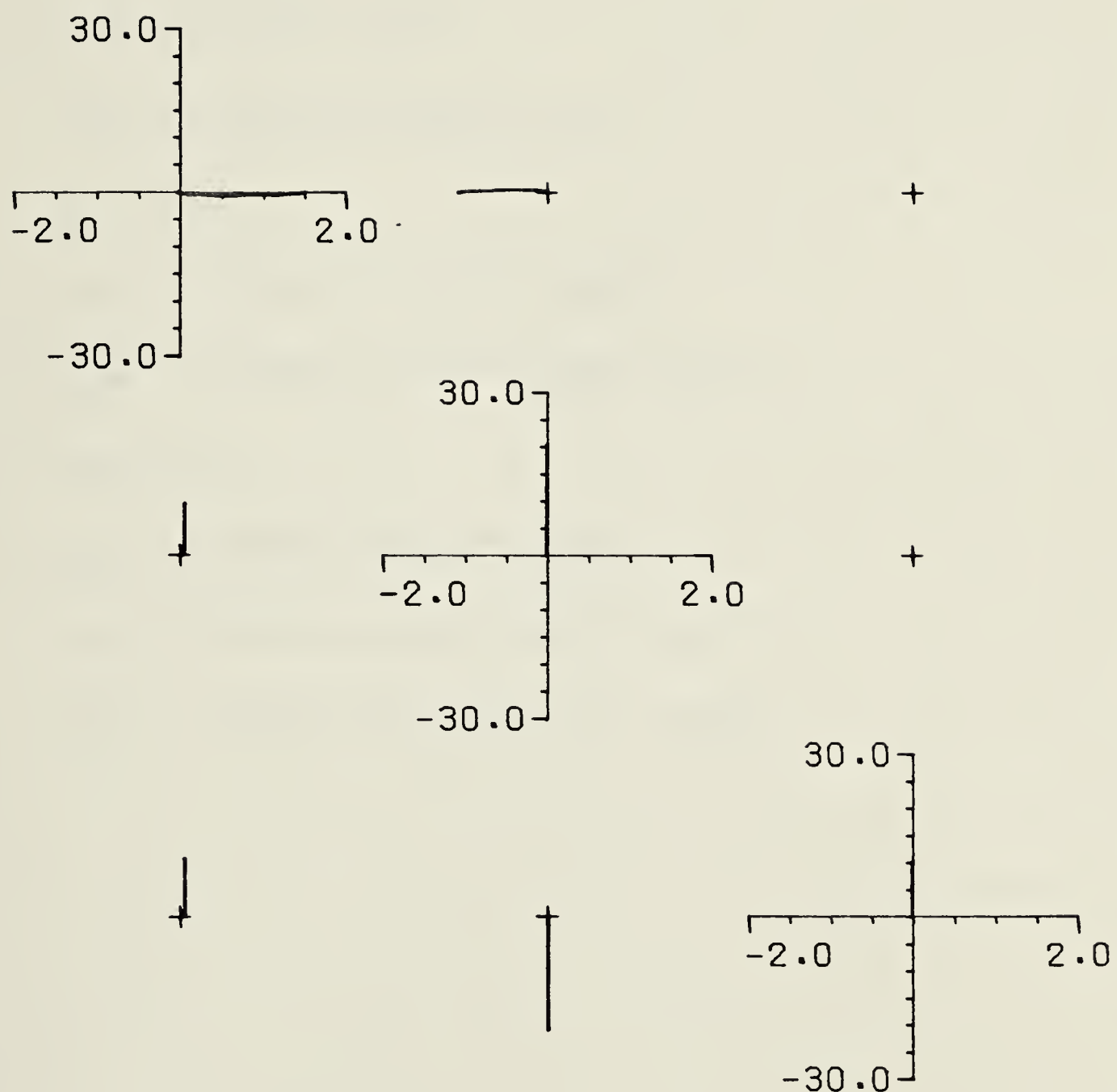


Figure 3.3 Direct Nyquist array display of pilot plant evaporator TFM $G(s)$. Frequency range $0.0038 < \omega < 7.73$ rad/min.

Table 3.1 Continuous transfer function model $G(s)$ of pilot plant evaporator. $G(s) = N(s)/d(s)$, where $N(s)$ is a polynomial matrix and $d(s)$ is the characteristic polynomial.

$$d(s) = 0.00025s^2 + 0.036s^3 + 0.82s^4 + 1.0s^5$$

$$n_{11}(s) = 0.0013s^2 + 0.032s^3$$

$$n_{12}(s) = -0.00027s^2 - 0.032s^3 - 0.041s^4$$

$$n_{13}(s) = 0.0$$

$$n_{21}(s) = -0.00001s^2 - 0.0013s^3 - 0.028s^4$$

$$n_{22}(s) = -0.00002s - 0.0028s^2 - 0.063s^3 - 0.077s^4$$

$$n_{23}(s) = 0.0$$

$$n_{31}(s) = -0.00001s - 0.0015s^2 - 0.032s^3$$

$$n_{32}(s) = 0.00002s + 0.0029s^2 + 0.065s^3 + 0.079s^4$$

$$n_{33}(s) = -0.00001s - 0.0014s^2 - 0.031s^3 - 0.038s^4$$

return difference matrix is row matrix dominant as shown in figure 3.4, but the return difference matrix is still not diagonally dominant.

3.3 Implications for MNA design techniques.

In this section it is shown, how the property of matrix dominance extends the applicability of the MNA stability theorems. The following theorem is the basis for applying the MNA stability theorems to matrix dominant systems:

Theorem 3.1: Let the square complex matrix Q be matrix dominant.

Then there exist a diagonal matrix D with positive diagonal elements, such that $D^{-1}QD$ is diagonally dominant.

A proof of this theorem is given in appendix C.

Since $|I(I+D^{-1}QD)| = |ID^{-1}(I+Q)DI| = |D^{-1}| |(I+Q)| |DI| = |(I+Q)|$ the return difference determinants of $F = I+Q$ and $F = I+D^{-1}QD$ are the same. The diagonal elements of Q and $D^{-1}QD$ are also identical, and it is well known, that the eigenvalues are preserved by a diagonal similarity transformation. Hence it follows from theorem 3.1 and existing results for diagonally dominant systems:

Theorem 3.2: Let $Q(s)$ be an open loop transfer function matrix for a system with m -inputs and m -outputs. Let the return difference matrix $F(s) = I+Q(s)$ be matrix dominant for all s on the closed right half plane Nyquist contour D , and let the diagonal elements of $Q(s)$ map D into Γ_i , $i=1,\dots,m$, which respectively encircle the $(-1,0)$ point n_i times clockwise. Then the closed loop system is asymptotically stable if and only if

$$\sum_{i=1}^m n_i = -p_0 \quad (3.9)$$

where p_0 is the number of open loop system poles in the closed right half plane.

The proof follows immediately from theorem 3.1 and published theorems for diagonally dominant systems.

A similar stability theorem in terms of matrix dominant $Q(s)^{-1}$ and $I+Q(s)^{-1}$ can be stated for the INA design procedure. However, $Q(s)$ or $F(s)$

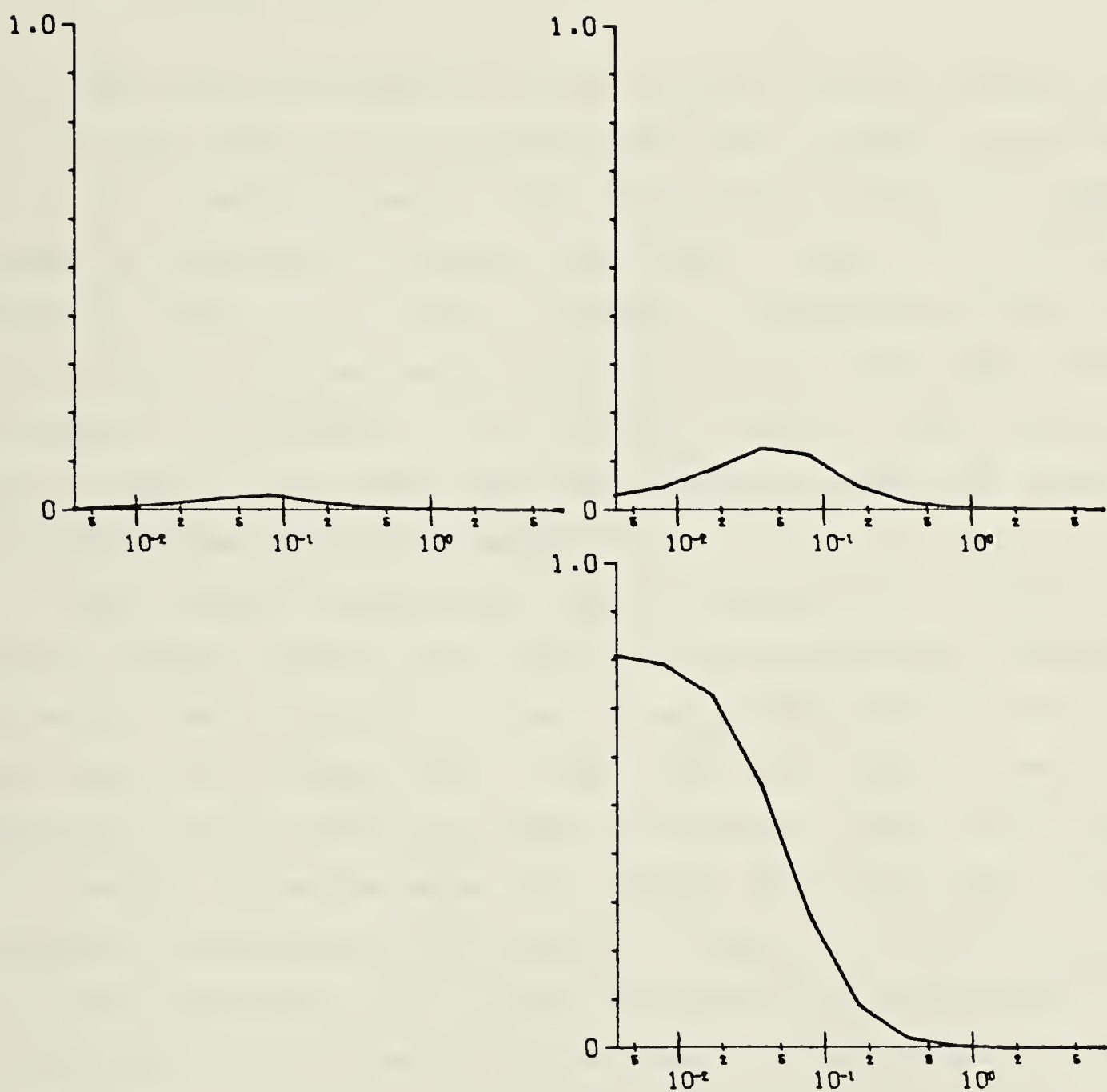


Figure 3.4 Graphical test of pilot plant evaporator return difference matrix for row matrix dominance after compensation. Frequency range $0.0038 < \omega < 7.73$ rad/min.

being matrix dominant does *not* imply $Q(s)^{-1}$ or $I+Q(s)^{-1}$ is matrix dominant.

To illustrate the application of theorem 3.2 consider the following 2×2 transfer function

$$G(s) = \frac{1}{s+1} \begin{bmatrix} 3 & 6 \\ 2 & 4.1 \end{bmatrix} \quad (3.10)$$

$F(s) = I+G(s)$ satisfies inequalities 3.5 for all s , so $F(s)$ is matrix dominant for all s . This is also evident from the graphical test shown in figure 3.5, since $N_{12} < 1$ at all frequencies. However, neither $G(s)$ nor $F(s) = I+G(s)$ are diagonally dominant, as shown by the Nyquist array display in figure 3.6. Nevertheless theorem 3.2 allows us to count the number of encirclements of the $(-1,0)$ point by $q_{ii}(s)$, $i=1,2$, when mapping the closed right half plane Nyquist contour. The number of encirclements of the $(-1,0)$ point is zero, and since $G(s)$ has no poles or zeros in the closed right half plane, the closed loop system is asymptotically stable according to theorem 3.2.

Figure 3.6 also illustrates the trade off between matrix dominance and diagonal dominance. The final loop gains must be selected so the characteristic loci encircle the $(-1,0)$ point clockwise the appropriate number of times, e.g. zero times for a system with no right half plane poles or zeros. The characteristic loci are known to lie inside the Gershgorin circles, and the bigger the Gershgorin circles the larger the uncertainty about the location of the characteristic loci. Because of this uncertainty the gain k_i of the i 'th loop must be chosen conservatively, so $-1/k_i$ lies to the left of the band swept out by the Gershgorin circles of the i 'th diagonal element (if the system has no right half plane poles or zeros). For the system considered here, this means, a high gain could be applied to loop 1, but a very low gain would have to be chosen for the second loop, i.e. a conservative gain would probably be selected for the second loop. Alternatively a trial and error procedure could be adopted in which gains are initially selected based on $q_{ii}(s)$, and the stability test, i.e. the matrix dominance test, repeated. For a diagonally dominant system the DNA-display would have smaller Gershgorin circles and hence there would be less uncertainty in the location of the characteristic loci, and therefore the

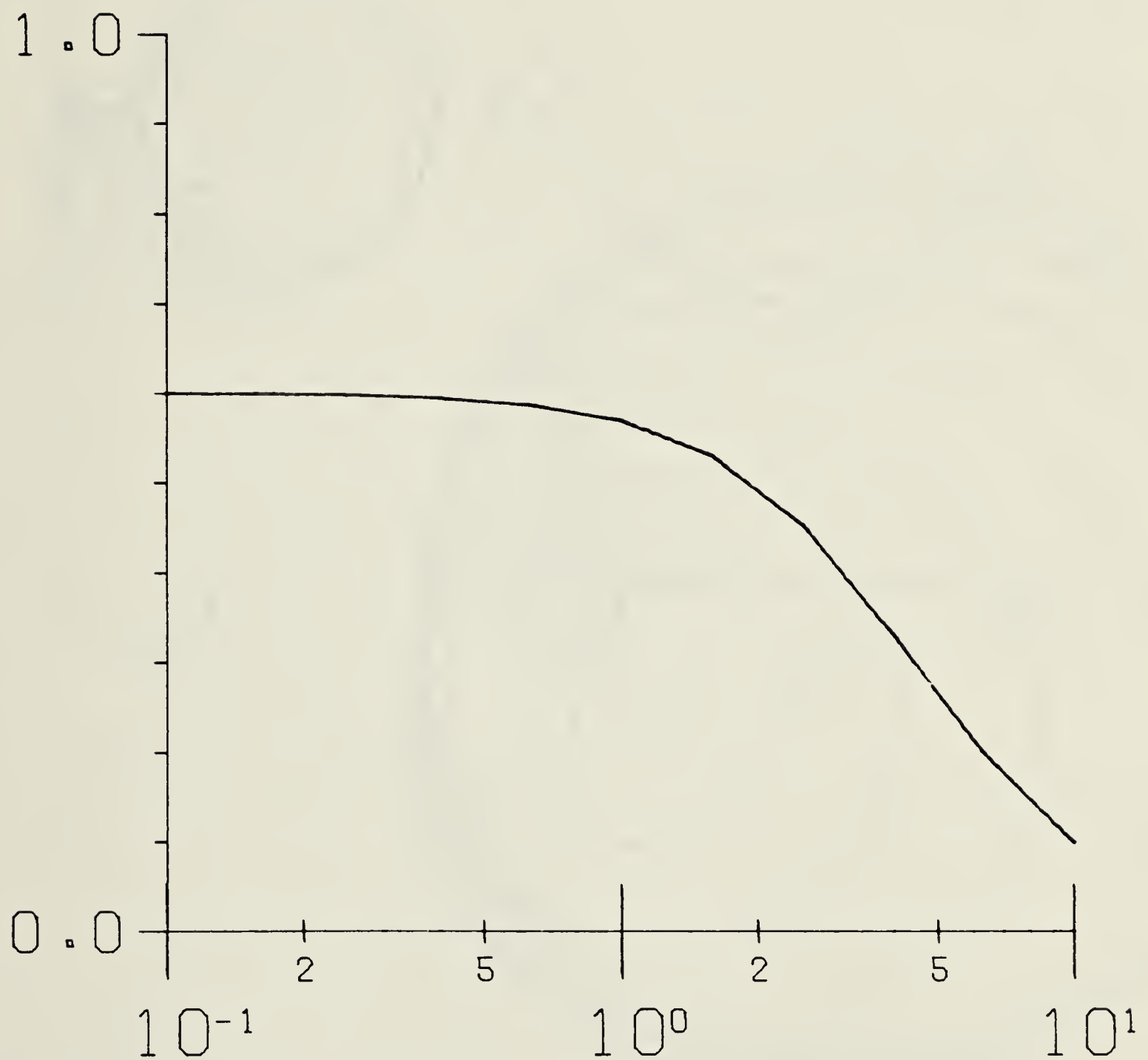


Figure 3.5 Graphical test of return difference matrix of system in equation 3.10 for matrix dominance. Frequency range $0.1 < \omega < 10.0$.

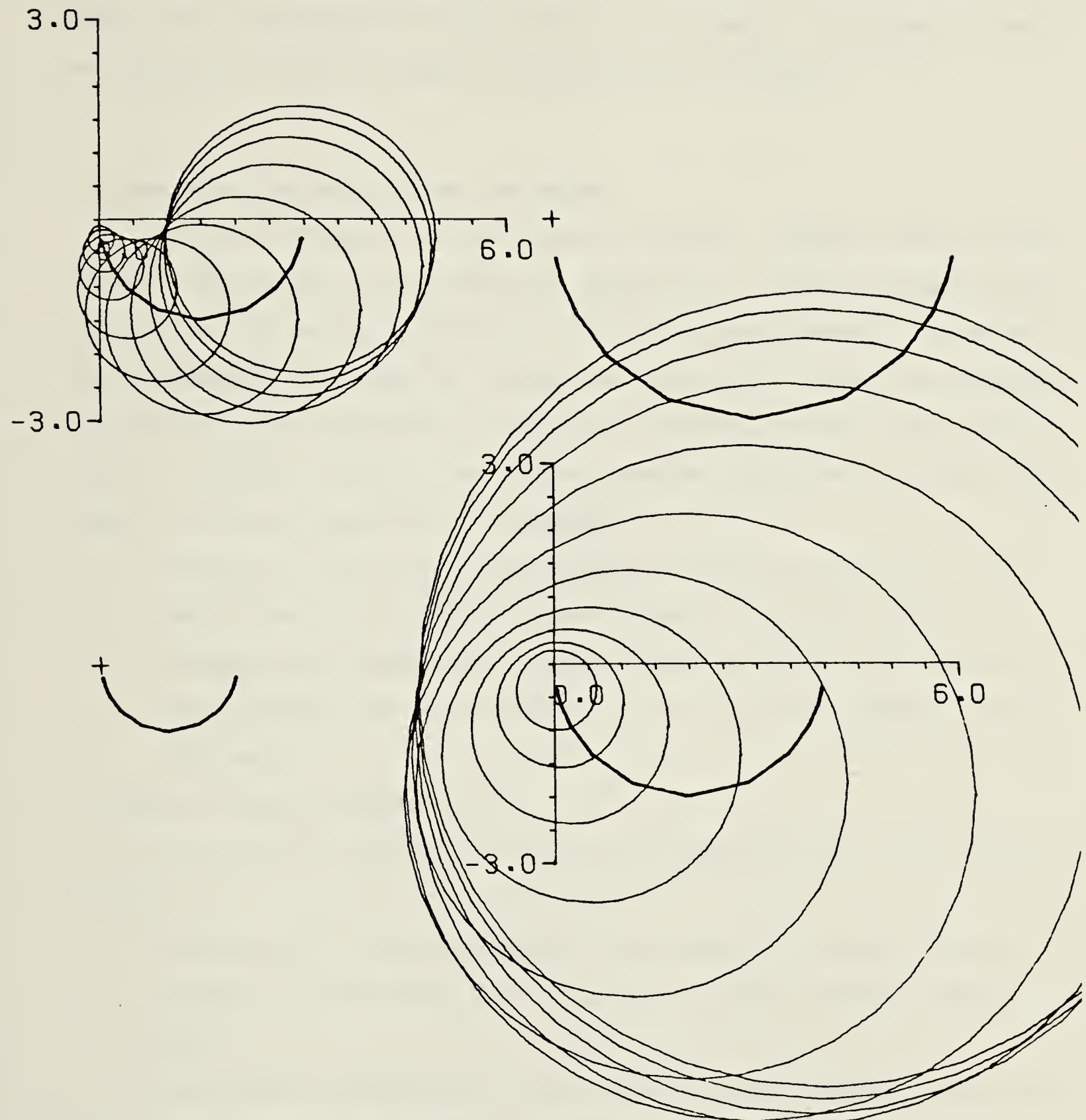


Figure 3.6 Direct Nyquist array of 2×2 TFM $G(s)$ with Gershgorin circles superimposed on diagonal elements. Frequency range $0.1 < \omega < 10.0$.

probability of choosing a conservative gain in any loop would be smaller. In section 3.5 a procedure based on transfer of dominance is developed to aid in the selection of final loop gains for matrix dominant systems.

3.4 Duality of row and column dominance.

The first theorem of the previous section showed how a matrix dominant system can be made diagonally dominant by a diagonal similarity transformation. In this section it is shown, that the diagonal similarity transformation can be designed to make the matrix dominant system either row diagonally dominant or column diagonally dominant. The following theorem establishes this, since row diagonal dominance and column diagonal dominance are both special cases of the more general matrix dominance.

Theorem 3.3: Row and column diagonal dominance are dual in the sense, that if a complex square matrix Q is column diagonally dominant, then there exist a diagonal matrix D with positive diagonal elements, such that $D^{-1}QD$ is row diagonally dominant, and vice versa.

The proof is given in appendix C.

The results of theorems 3.1 and 3.3 immediately lead to the following corollary:

Corollary 3.1: Diagonal similarity transformations to make a matrix dominant system either row or column diagonally dominant always exist.

The similarity transformation, which makes a matrix dominant system row diagonally dominant, will in general be different from the similarity transformation, which makes the same matrix dominant system column diagonally dominant.

The duality of row and column dominance can be viewed as further support of the idea, that the dominance requirements of the MNA design techniques are artificial requirements posed on the system for purely mathematical reasons. In general dominance, particularly diagonal dominance, is not a necessary requirement for a satisfactory control system design, although a

highly dominant system often means a system with little interaction.

The use of diagonal similarity transformations as an aide in controller design by transferring dominance is considered in the following section.

3.5 Transfer of dominance.

The final proportional loop gains of a matrix dominant multivariable system could be selected on the basis of the direct Nyquist array display of such a system with its associated wide Gershgorin bands. However, such a procedure could as discussed in section 3.3 lead to the selection of conservative gains or loose control in one or more loops. In order to overcome this deficiency a diagonal similarity transformation could be used to make the matrix dominant system diagonally dominant during the design. This approach was first brought forward by Mee (1976), who also pointed out, that the similarity transformation need not be implemented in the field, because it does not change any transmittances, but only redistributes dominance, taking from highly dominant rows and/or columns and giving to non-dominant rows and/or columns. Mee (1976) considered only 2×2 systems, where the redistribution or sharing of dominance was simple, but gave no procedure for calculating the necessary similarity transformation for a general $m \times m$ system. An algorithm for calculating the required similarity transformation for a general $m \times m$ system will be outlined below.

The similarity transformation of theorem 3.3 can be found as the solution to inequalities 9.22 and/or 9.23 of appendix C. The solution of these inequalities can be cast into a linear programming problem. Consider the $m \times m$ transfer function matrix $Q(s)$, which is assumed to be matrix dominant. The diagonal similarity transformation to maximize the row diagonal dominance is found by maximizing the following penalty function

$$J = d_{m+1}(s) \quad (3.11)$$

subject to the constraints

$$d_i(s) > 0 \quad i = 1, \dots, m+1 \quad (3.12)$$

and

$$|q_{ii}(s)|d_i(s) - \sum_{\substack{j=1 \\ j \neq i}}^m |q_{ij}(s)|d_j(s) - \beta_i(s)d_{m+1}(s) > 0 \quad (3.13)$$

for $i = 1, \dots, m$, and

$$d_i(s) \leq 1 \quad (3.14)$$

where $\beta_i(s)$ are row weighting factors. These weighting factors allow the designer to make certain rows strongly dominant at the expense of other rows, i.e. dominance is transferred between rows. An equivalent algorithm for transfer between columns is easily formulated, in which case $\beta_i(s)$ are column weighting factors. The optimization problem outlined above can be seen to have the structure of a general linear programming problem

$$\text{maximize } J = g(x) \quad (3.15)$$

subject to

$$Ax \geq 0 \quad (3.16)$$

which is easily solved using available standard procedures, such as the simplex algorithm. The solution is done numerically at a set of discrete frequencies $s = i\omega_k$, $k = 1, \dots, p$.

The algorithm allows certain rows or columns to be made strongly row or column diagonally dominant, thus decreasing the uncertainty about the stability margin for certain important input/output pairs. This might be an important consideration in many practical process control applications. The above algorithm also removes any analytical difficulties in sharing dominance as the order of the transfer function matrix increases, since the designer simply assigns weighting factors according to the importance of each output (row) or input (column).

The flexibility of the outlined algorithm as compared to the method of Kantor and Andres (1979) for calculation of minimal Gershgorin band radii is demonstrated by considering a constant 2×2 matrix. Consider the matrix

$$\begin{bmatrix} 3 & 6 \\ 1 & 4 \end{bmatrix} \quad (3.17)$$

Then the eigenvalues of CW^{-1} with C and W as defined in section 3.2.1 are $\pm 1/\sqrt{2}$, and the method of Kantor and Andres (1979) gives the following diagonally dominant matrix

$$\begin{bmatrix} 3 & 2.12 \\ 2.83 & 4 \end{bmatrix} \quad (3.18)$$

The linear programming scheme developed in this section gives different results depending on the choice of the weighting factors. For $\beta_1 = \beta_2 = 1$ the transformed system becomes

$$\begin{bmatrix} 3 & 2.50 \\ 2.40 & 4 \end{bmatrix} \quad (3.19)$$

or for $\beta_1 = 2$ and $\beta_2 = 1$ the transformed system becomes

$$\begin{bmatrix} 3 & 2.14 \\ 2.80 & 4 \end{bmatrix} \quad (3.20)$$

which is almost identical to 3.18. The higher weighting β_1 gives a smaller Gershgorin radius for the first row. Hence the example demonstrates, that with the transfer of dominance algorithm developed here the designer has the freedom to make the bands on certain important loops small at the expense of larger bands in other loops, i.e. dominance can be arbitrarily transferred from one row or column to another by the choice of appropriate weighting factors, $\beta_i(s)$.

3.6 Conclusions.

The past efforts in extending the class of transfer function matrices to which the MNA stability theorems are applicable were reviewed, and the common property of this class of matrices was defined as *matrix dominance*. A graphical test for matrix dominance, that also aides in compensator design was developed, and its application illustrated.

The implications of matrix dominance for the MNA design techniques were discussed, and row and column diagonal dominance shown to be dual with

respect to a diagonal similarity transformation.

A systematic algorithm for transferring dominance in transfer function matrices of any size were developed, and its flexibility illustrated by applying it to calculation of minimal Gershgorin radii. The transfer of dominance algorithm developed as part of this study gives the designer more freedom, than other published procedures for calculating minimal Gershgorin radii.

4. Nyquist exact loci (NEL) design technique.

4.1 Introduction.

In the past ten years the classical frequency domain, single-input, single-output control system design techniques of Nyquist and Bode have been extended to the design of multi-input, multi-output control systems. Many significant contributions to the development of frequency domain control system design techniques have been collected into a book edited by MacFarlane (1979). Kuon (1975) reviews the developments in multivariable frequency domain design techniques. The major differences between multivariable frequency domain design techniques, such as the multivariable Nyquist array methods, the characteristic loci method, and classical single variable techniques are discussed in the following paragraphs.

The first major extension of frequency domain design techniques to multivariable systems was the development of the inverse Nyquist array (INA) design procedure by Rosenbrock (1969). The inverse open loop and inverse closed loop TFM must be dominant before system stability can be evaluated. Dominance can (usually) be achieved by performing row or column operations on the set of Nyquist plots corresponding to the $m \times m$ elements of the open loop TFM. Once the desired degree of dominance has been achieved, stability can be determined by counting the encirclements of the origin and the critical point by the Nyquist loci of the m diagonal elements of the open loop TFM and the corresponding Gershgorin or Ostrowski circles. Because of the inverse nature of the plots and the uncertainty introduced by the Gershgorin or Ostrowski bands, the frequency and/or time domain relationship between a specific pair of input - output variables is not as clear as with the classical SISO Nyquist plots.

The second major extension of frequency domain control system design techniques was the introduction of the characteristic loci (CL) design procedure by MacFarlane and Bellettrutti (1973). The CL technique uses a set of plots of the eigenvalues of the open loop TFM to assess stability, and uses both the eigenvalues and eigenvectors of the open loop TFM to design a multivariable

compensator/controller. MacFarlane and Bellettrutti avoid "putting any conditions, such as dominance, on the open loop TFM by using the eigensystem of this matrix in the design procedure. The designer, using the CL technique, only has to work with m diagrams for a m -input, m -output multivariable system. However, these m -diagrams have no one to one relationship with the simple input/output relationships of SISO systems, since eigenvalues cannot in general be associated with specific input/output pairs. Furthermore the familiar SISO control system design terms, such as gain margin, phase margin, bandwidth, rise time, overshoot and settling time change meaning or cannot be evaluated directly from the characteristic loci diagrams.

Other significant extensions of classical frequency domain techniques to the design of multivariable control systems include the sequential return difference (SRD) design procedure proposed by Mayne (1972, 1973, 1974), and the direct Nyquist array (DNA) design procedure proposed by Rosenbrock (1974) and described in detail by Kuon (1975). The SRD technique, as the name suggests, constructs the multivariable controller from a sequence of single loop designs. The i 'th stage of this sequence designs a controller for the i 'th loop taking into consideration the already completed designs of loops 1 to $i-1$. The drawback of the SRD procedure is, that the final design depends on which sequence the loops are closed in, and no general method exists for choosing the best sequence. The DNA technique is similar to the INA technique, but uses the open loop TFM directly to design a multivariable compensator/controller, and requires the return difference matrix to be dominant before system stability can be evaluated. If the return difference matrix is strongly diagonally dominant familiar SISO control system design specifications can be evaluated directly from the diagonal elements of the direct Nyquist array. However, in the general case the meaning of terms, such as rise time, overshoot and settling time, still remain fuzzy, since the diagonal elements of the DNA do not represent the complete transmittance between input - output pairs with all other loops closed, but only the direct part (cf. chapter 2).

In this chapter a practical and systematic multivariable frequency domain design procedure, called the Nyquist exact loci (NEL) technique, is outlined. The

NEL design procedure, which is applicable to a large class of industrial systems, uses the transfer functions $h_i(s)$, $i = 1, \dots, m$ cf. figure 1.2, which represents the complete transmittance, direct and parallel, between the i 'th input and the i 'th output with the i 'th loop open and all other loops closed. The transfer functions $h_i(s)$ are direct multivariable parallels of the classical SISO transfer function $g(s)$. The transfer functions $h_i(s)$ are first introduced in the next section and the advantages of working with them discussed. This is followed by a general step by step outline of the NEL design technique. The different steps of the NEL procedure are then discussed in detail from a theoretical and a practical viewpoint. Finally the simultaneous gain calculation algorithms, which are a central part of NEL, are described.

4.2 The Nyquist exact loci of $h_i(s)$.

The central feature of the NEL procedure is the use of the transfer functions $h_i(s)$, $i = 1, \dots, m$, to simultaneously calculate the constants of m single loop controllers and to determine closed loop stability. The transfer function $h_i(s)$ represents the complete, direct and parallel, transmittance between the i 'th input and the i 'th output when the i 'th loop is open and all other loops are closed. It is thus the exact single-input, single-output system for which the i 'th controller should be designed to account for the multivariable nature of the system. The i 'th controller is the i 'th diagonal element of $K_2(s)$, cf. figure 1.1, and the transfer function $h_i(s)$ is the multivariable analogue of the SISO transfer function $g(s)$, cf. figure 1.2. It is therefore clear, that the transfer function $h_i(s)$ has physical meaning, and hence terms familiar from classical single variable design, such as gain margin, phase margin, bandwidth, rise time, overshoot and settling time, can be evaluated directly and meaningfully from Nyquist plots of $h_i(s)$.

The transfer functions $h_i(s)$ are nonlinear functions of the elements of the compensated plant TFM $Q(s)$ and the elements of the diagonal controller matrix $K_2(s)$. The following general expression for $h_i(s)$ is derived in appendix A:

$$h_i(s) = q_{ii}(s) + \sum_{\substack{j=1 \\ j \neq i}}^m \Phi_{ij}(s) k_j(s) q_{ij}(s) / k_i(s) = q_{ii}(s) + \sum_{\substack{j=1 \\ j \neq i}}^m \Phi_{ji}(s) q_{ji}(s) \quad (4.1)$$

where

$$\Phi_{ij}(s) = \frac{\text{cofactor of element } (i,j) \text{ of } F(s)}{\text{cofactor of element } (i,i) \text{ of } F(s)} \quad (4.2)$$

and $F(s) = I + Q(s)K_2(s) = I + G(s)K_1(s)K_2(s)$. The above expression for $i = m$ gives the same transfer function as an expression given by Rosenbrock (1972). However, for $i = m$ the expression given by Rosenbrock is the transfer function with loops $1, \dots, i-1$ closed and loops i, \dots, m open. Such a function has been used by Mayne (1974) in his SRD design procedure. The advantage of the above expression for $h_i(s)$ is, that it facilitates simultaneous design of the m controllers in $K_2(s) = \text{diag}\{k_i(s)\}$.

Equation 4.1 results in the following expression for $h_2(s)$ for a 2×2 system with loop 1 closed (cf. figure 1.1 and 1.2):

$$h_2(s) = q_{22}(s) + \frac{k_1(s)q_{21}(s)}{1+k_1(s)q_{11}(s)} q_{12}(s) \quad (4.3)$$

and similarly $h_1(s)$ with loop 2 closed is given by:

$$h_1(s) = q_{11}(s) + \frac{k_2(s)q_{12}(s)}{1+k_2(s)q_{22}(s)} q_{21}(s) \quad (4.4)$$

Since the transfer function $h_i(s)$ is the exact transmittance for which $k_i(s)$ should be designed to take into consideration the multivariable nature of the plant, the polar plot of $h_i(s)$ for s on the Nyquist D -contour is called a Nyquist exact locus, and the design procedure based on these loci is called the Nyquist exact loci (NEL) technique. The NEL design procedure is outlined in the next section.

4.3 The Nyquist exact loci (NEL) design procedure.

The NEL design procedure for the design of a multivariable controller for a general multivariable plant involves the following steps, which are discussed in greater detail in the following subsections:

- i. Obtain a transfer function model description of the plant or system.
- ii. Check if the return difference matrix is matrix dominant with $K_1(s) = K_2(s) = I$.
If yes then continue with the design of $K_2(s)$ leaving $K_1(s) = I$, or design $K(s)$ to reduce interaction,
e/se design $K_1(s)$ and/or reduce magnitude of elements of $K_2(s)$ to make $F(s)$ matrix dominant.
- iii. Choose a set of initial gains, k_i , $i = 1, \dots, m$.
- iv. Plot the Nyquist exact loci of $h_i(s)$, $i = 1, \dots, m$.
- v. Specify stability margins for each loop based on the Nyquist exact loci.
- vi. Simultaneously calculate controller constants, which satisfy the stability margins of all loops, cf. section 4.4.
- vii. Check if $F(s)$ is matrix dominant.
- viii. Determine if the design is satisfactory by plotting the Nyquist exact loci.
If yes and $F(s)$ is matrix dominant, then the design is completed after checking stability using the Nyquist exact loci,
e/se if yes and $F(s)$ is not matrix dominant, then check stability by method which does not require system dominance, e.g. characteristic loci.
e/se relax design specification and/or improve design of compensator $K_1(s)$ to meet the design specifications.

The flow chart in figure 4.1 summarizes the NEL design procedure, and the following subsection discusses each step in detail.

4.3.1 Transfer function model description.

The NEL procedure works with a TFM model of the system under consideration as the basis for the control system design. The TFM model can be either a continuous model $G(s)$, a discrete model $G(z)$, or a bilinearly

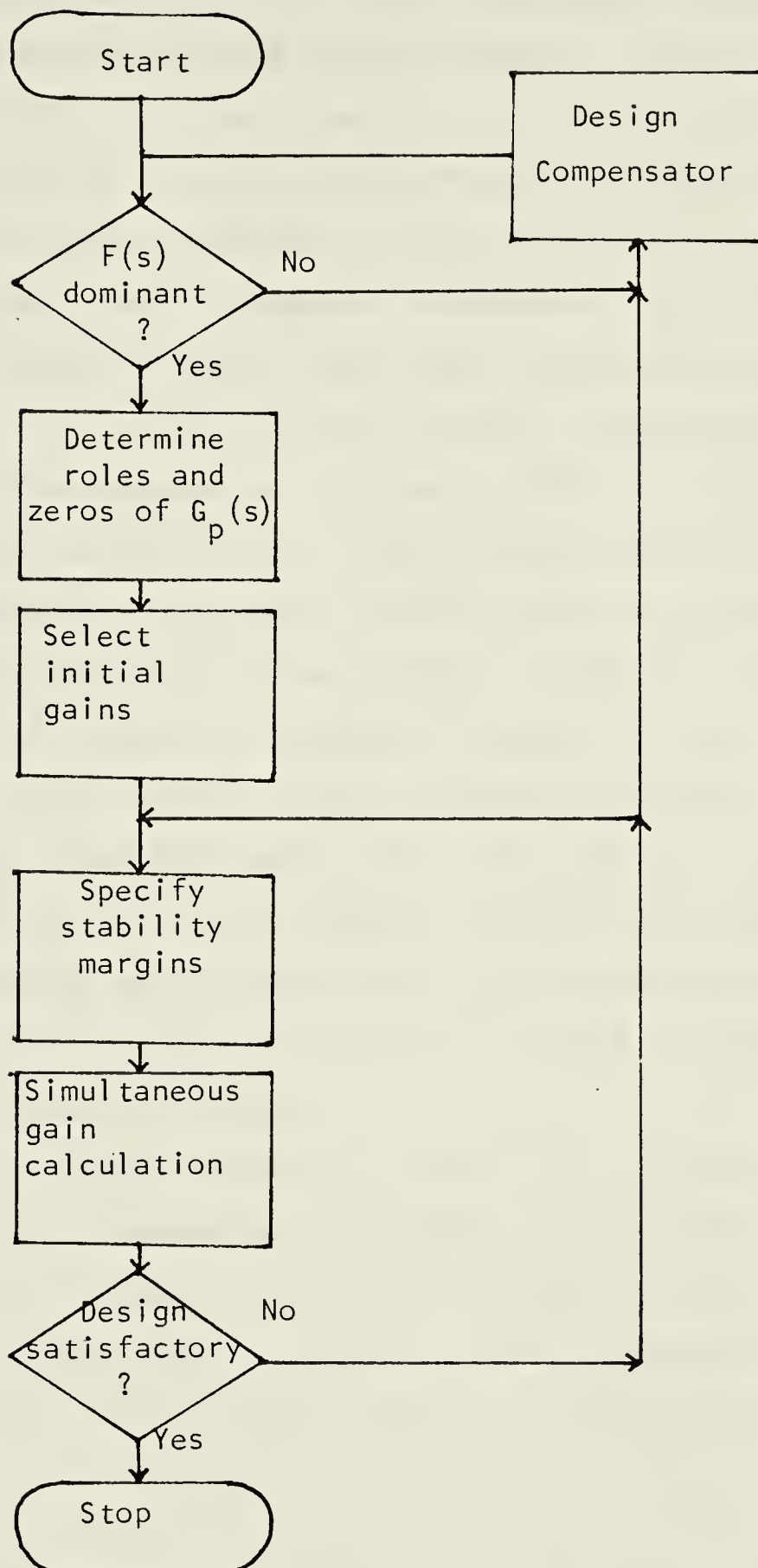


Figure 4.1 Flow chart of NEL design procedure showing the different steps and design loops.

transformed discrete model $G(w)$. If a system description is available in some other form, e.g. a partial differential equation model or a state space model, a transfer function model must be calculated from this form before the NEL procedure can be used. In a practical computer aided implementation of the NEL procedure the TFM model is evaluated at a set of discrete frequency points on the Nyquist D -contour, and all numerical calculations then proceed from the resulting set of complex matrices, rather than using algebraic manipulations of polynomials in s , z or w . The Nyquist D -contour, along which the transfer functions are evaluated depends on the type of TFM model. A discussion of the different Nyquist contours in the s -plane, z -plane and w -plane is given in appendix D. Theoretically the transfer functions must be evaluated along the appropriate complete Nyquist contour, however results by Mee (1976) and Leininger (1979b) show, that it is possible to use only a finite frequency range $0 < \omega < \omega_0$ in the Nyquist analysis, provided the transfer function matrix is bounded for all frequencies above ω_0 . The use of a finite frequency range makes the use of the NEL design procedure and other multivariable Nyquist array techniques more practical, since it is considerably easier to make e.g. the return difference matrix dominant over a finite frequency range, than over the complete Nyquist D -contour.

Many control systems, especially if $K_1(s) \neq I$, are implemented using a digital computer. Such implementations normally involve sampling of inputs and outputs at equidistant instants of time, and holding the plant inputs constant between sampling instants. Hence a continuous plant is controlled by a discrete controller. The design of this discrete controller can be approached in several ways:

- i. Based on a continuous TFM $G(s)$, a compensator/controller $K_1(s)K_2(s)$ is designed in the s -plane. The discrete implementation is then obtained by mapping the poles and zeros of $K_1(s)K_2(s)$ into the z -plane to obtain $K_1(z)K_2(z)$, and deriving a difference equation from $K_1(z)K_2(z)$ for time domain implementation. This procedure is theoretically incorrect, and as demonstrated by Franklin and Powell

(1980) for SISO system it does not give a control system, which is in agreement with the design specifications.

- ii. From the continuous TFM $G(s)$ a discrete TFM $G(z)$ is calculated by z -transformation of $G(s)G_h(s)$, where $G_h(s)$ is the transfer function of a zero order hold. Then a compensator/controller $K_1(z)K_2(z)$ is designed in the z -plane, and the difference equation obtained directly. This procedure is theoretically correct, and the discrete controller is as good as the model of the system. However, the z -plane analysis is different from the s -plane analysis, which most designer are more familiar with. Also the discrete transfer functions are not rational functions of frequency.
- iii. From the continuous TFM $G(s)$ a bilinearly transformed discrete TFM $G(w)$ is calculated by z -transformation of $G(s)G_h(s)$ to give $G(z)$, followed by bilinear transformation of $G(z)$ to give $G(w)$. Then a compensator/controller $K_1(w)K_2(w)$ is designed in the w -plane and the inverse bilinear transformation used to obtain $K_1(z)K_2(z)$, from which the difference equation is derived. This procedure is theoretically correct, and the resulting controller is as good as the model of the system. The advantage of performing the exact bilinear transformation from the z -plane to the w -plane is, that the analysis in the w -plane is very similar to the analysis in the s -plane, e.g. stable poles and zeros lie in the left half plane, and the transfer functions are again rational functions of frequency, cf. appendix D.
- iv. Based on a continuous TFM $G(s)G_h(s)$ a compensator/controller $K_1(s)K_2(s)$ is designed in the s -plane. The discrete implementation is then obtained by mapping the poles and zeros of $K_1(s)K_2(s)$ into the z -plane to get $K_1(z)K_2(z)$ from which a difference equation is derived for implementation. This procedure is not theoretically rigorous, but as discussed below, if the discrete transfer functions are calculated from the continuous using the Tustin rule, then this procedure is identical to iii) given above. However, readers should

be aware of some distortion in mapping from the s to the z-plane (Franklin and Powell (1980)) in using this approach. In the overall sense this approach is a good practical approximation, which accounts for the major feature of the discrete control systems implementation, the zero order hold. An alternative to this approach is the hold equivalence method also described by Franklin and Powell (1980).

The four approaches to design of a discrete controller system for a continuous plant are summarized in table 4.1. If a discrete TFM $G(z)$ or $G(w)$ is available the initial transformations of approaches ii or iii are of course omitted.

The variables s, z and w are related as follows (Franklin and Powell (1980)):

$$w = \frac{2}{T} \frac{z-1}{z+1} = \frac{2}{T} \tanh \frac{sT}{2} \quad (4.5)$$

where T is the sampling time, and the discrete frequency v in the w-plane and the continuous frequency ω in the s-plane are related by

$$v = \frac{2}{T} \tan \frac{\omega T}{2} \quad (4.6)$$

This means, that for small $sT/2$ or small $\omega T/2$ the following approximations

$$w \approx s \quad \text{and} \quad v \approx \omega \quad (4.7)$$

are valid. Furthermore if $G(z)$ is calculated from $G(s)G_h(s)$ using the Tustin bilinear substitution (Franklin and Powell (1980))

$$s = \frac{2}{T} \frac{z-1}{z+1} \quad (4.8)$$

and $G(w)$ is calculated from $G(z)$ using the bilinear transformation given in equation 4.5, then $s = w$, and hence $G(w) = G(s)G_h(s)$. Therefore evaluating $G(s)G_h(s)$ for $s = i\omega$, $0 < \omega < \omega_0$, gives approximately the same Nyquist loci as evaluating $G(w)$ for $w = jv$, $0 < v < v_0$. The approximation involved is valid only if ωT is small, which in practice means the sampling time should be small relative to the smallest open loop time constant. Franklin

Table 4.1 Summary of four different approaches to the design of a discrete control system for a continuous plant.

Model used	Design and analysis plane	Quality of approach
$G(s)$	s-plane	bad
$G(z)$	z-plane	good
$G(w)$	w-plane	good
$G(s)G_h(s)$	s-plane	fair

and Powell (1980) recommend a sampling frequency of 10 - 20 times the closed loop bandwidth, which will generally give a sufficiently small sampling time for the approximation to be valid. So when a continuous model is available the fourth approach to control system design outlined above is recommended.

The design examples of the next chapter will use the third and fourth above mentioned approaches to control system design.

4.3.2 Matrix dominance of the return difference matrix.

The determination of stability using the Nyquist exact loci requires (cf. section 4.3.4), that the return difference matrix is matrix dominant (cf. chapter 3). As an initial step in the NEL design procedure the return difference matrix $F(s) = I + G(s)$, i.e. $K_1(s) = K_2(s) = I$, is tested for matrix dominance as described in chapter 3.

If the return difference matrix is matrix dominant, the NEL design can proceed with the design of a diagonal controller matrix $K_2(s)$ as discussed in the following subsections, or a compensator $K_1(s)$ can be designed to further reduce interactions or satisfy other design specifications.

If the return difference matrix is not matrix dominant, the magnitude of the gains $k_i(s)$ in $K_2(s) = \text{diag}\{k_i(s)\}$ could be reduced, and/or a compensator $K_1(s)$ could be designed to make $F(s)$ matrix dominant (Note: In the limit $k_i(s) \rightarrow 0$, $i = 1, \dots, m$, $F(s)$ will be matrix dominant for any plant $G(s)$).

The design of the compensator $K_1(s)$ is done by applying either the direct Nyquist array technique using column operations or pseudodiagonalization, the inverse Nyquist array technique using row operations or pseudodiagonalization, or the characteristic loci technique using eigenvector alignment. These techniques are described in detail by Kuon (1975), who also applied them to the design of a control system for a pilot plant evaporator and compared the resulting controllers. Kuon (1975) found the three techniques to give very similar results if the main design criteria was to minimize closed loop interaction.

4.3.3 Choice of initial set of loop gains.

The initial choice of gains $k_i(s)$ in $K_2(s) = \text{diag}\{k_i(s)\}$ can be done in various ways, e.g. arbitrarily choose $k_i(s) = 1$, $i = 1, \dots, m$. However, one practical approach is to make $Q(s)$ as column dominant as possible by a diagonal similarity transformation $D(s)$, as discussed in chapter 3. Then plot the direct Nyquist array of $D(s)^{-1}Q(s)D(s)$ with Gershgorin circles superimposed on the diagonal elements, and choose a set of initial gains, which lie outside the band swept out by the Gershgorin circles. It should be noted, that the Nyquist exact loci of $h_i(s)$ lie inside the Gershgorin band on $q_{ii}(s)$, when $F(s)$ is dominant. That is the magnitude of $h_i(s)$ is bounded by:

$$(|q_{ii}(s)| - R_B(s)) < |h_i(s)| < (|q_{ii}(s)| + R_B(s)) \quad (4.9)$$

where, if $F(s)$ is dominant, $R_B(s)$ could be the Gershgorin radius:

$$R_B(s) = \sum_{\substack{j=1 \\ j \neq i}}^m |q_{ji}(s)| \quad (4.10)$$

It is possible to define even narrower bands for $h(s)$ than the Gershgorin band, whenever the cofactor $\phi_{ji}(s)$ contains a row or column of zeros. Such bands, called G^0 -circles, are discussed by Kuon (1975). These bands of course have the advantage of being independent of the elements of the diagonal controller

matrix $K_2(s)$. However, except for determining an initial set of loop gains bands are not used in the NEL design procedure, since the exact loci of $h_i(s)$ are easily calculated on a digital computer. In particular, Ostrowski circles are not used to check the final design because the Nyquist exact loci provide a better means of checking that design specifications are met.

4.3.4 Nyquist exact loci plots.

The Nyquist exact loci are the polar plots of $h_i(s)$ with s a function of frequency. These plots are used in the NEL procedure to check if the system is stable and if the control is satisfactory. The following theorem is the basis for assessing stability using the Nyquist exact loci:

Theorem 4.1: Let the return difference matrix $F(s)$ be matrix dominant and $k_i(s)h_i(s)$ map the right half plane Nyquist contour D into Γ_{h_i} encircling the critical point $(-1,0)$ n_{h_i} times clockwise.

Then the closed loop system will be stable if and only if

$$\sum_{i=1}^m n_{h_i} = -p_0 \quad (4.11)$$

where p_0 is the number of right half plane poles of the open loop system.

Proof of theorem 4.1 is given in appendix E.

Theoretically the transfer functions $k_i(s)h_i(s)$ should be evaluated along the complete Nyquist contour, but in practice they are evaluated only along a finite part of the imaginary axis (finite frequency range) and the contour completed by extrapolation. Also if $k_i(s)h_i(s)$ is bounded above a certain frequency the finite frequency range results of Mee (1976) and Leininger (1979b) apply.

4.3.5 Specify desired stability margins.

Based on the Nyquist exact loci, a desired stability margin is specified for each loop. This margin, as in classical SISO design, can be either a gain margin or a phase margin. The designer chooses the stability margins according to the design specifications, i.e. if tight control is desired in a certain loop a

small margin is specified and vice versa. The specific values of the margins of course depend on the individual application, but values of 4 - 8 db are typical for gain margins, and 30 - 45 degrees for phase margins.

4.3.6 Calculate gains to satisfy stability margins.

Controller constants, which satisfy all specified stability margins, are calculated simultaneously using one of the algorithms described in section 4.4. These algorithms will update the controller constants, so the location of the Nyquist exact loci approach the desired locations. This is done by linearizing the underlying optimization problem and solving a set of linear equations.

The updating of the controller constants continues, each time solving a set of linear equations, until the difference between the desired locations and the actual locations of the Nyquist exact loci becomes sufficiently small. Between each updating of the controller constants the designer can judge whether to continue or not by inspecting the Nyquist exact loci diagrams. The designer decides when to stop the iterative updating of the controller constants.

4.3.7 Is the control system satisfactory.

The final step of the NEL design procedure is to check, that the control system is satisfactory. This involves first of all checking for stability. If the final return difference matrix is matrix dominant, then stability can be judged from the Nyquist exact loci, by counting their encirclements of the critical point (-1,0). Since matrix dominance of $F(s)$ is a sufficient but not necessary condition for stability analysis based on the Nyquist exact loci, the system can be stable even though $F(s)$ is not matrix dominant. Therefore if the return difference matrix is not matrix dominant, stability can be checked by a method, which does not require system dominance, e.g. the characteristic loci technique.

Since the Nyquist exact loci represent the actual transmittances between given input - output pairs other control system performance criteria, such as bandwidth, rise time, overshoot and settling time for unit step change in input, can be evaluated from the NEL diagrams. These performance criteria can be calculated either from Nyquist plots of $h(s)$ using Nichols charts, or from Bode

plots of $|h_i(s)|/|1+h_i(s)|$. In a computer aided implementation of the NEL design technique the last approach is more convenient.

The transfer function $h_i(s)$ in general involve ratios of polynomials in s of degree greater than two. For such transfer functions it is not feasible to use analytical expressions for rise time, overshoot and settling time, but empirical correlations have been published, e.g. by Horowitz (1963). The following expressions are given by Horowitz:

Rise time t_r :

$$t_r = K \omega_b / 2\pi \quad 0.3 \leq K \leq 0.45 \quad (4.12)$$

Overshoot γ :

$$\gamma = 58(\omega_b / \omega_x)M - 39 \quad (4.13)$$

Settling time t_{s1} :

$$t_{s1} = (\omega_x / 4\pi)(7(\omega_b / \omega_x)M - 3) \quad (4.14)$$

where ω_b is the bandwidth frequency, that is the frequency at which $|h_i(s)|/|1+h_i(s)| = 0.707$, and ω_x is the frequency at which $|h_i(s)|/|1+h_i(s)| = 0.5$. M is the magnitude of $|h_i(s)|/|1+h_i(s)|$ at the resonance frequency.

The above expressions according to Horowitz are only accurate to within 15% - 30%, but they nevertheless give the significant features of the time response and are useful in comparing designs.

If the control system design is unsatisfactory the designer can either relax the specification with respect to stability margins or other criteria or improve the design of the compensator $K_i(s)$ to meet the design criteria. The latter will generally mean a more complicated compensator.

4.4 Simultaneous controller constant evaluation.

The simultaneous design of m single loop controllers $k_i(s)$, $i = 1, \dots, m$, each having n controller constants, to satisfy desired stability margins for the exact loci of $k_i(s)h_i(s)$, $i = 1, \dots, m$, is mathematically a $m \times n$ order nonlinear optimization problem. Algorithms to iteratively solve this problem for $n = 1$ or 2 are outlined below. These algorithms use the Nyquist exact loci and a standard Gaussian elimination procedure for adjusting the controller constants to

give designer specified stability margins.

The central step in the algorithms is the solution of a set of linear equations:

$$A \cdot x = b \quad (4.15)$$

where A is a Jacobian matrix containing the derivatives of the Nyquist exact loci w.r.t. the controller gains, x is a vector containing the necessary adjustments of the controller constants to satisfy the stability margins, and b is a vector of distances the loci have to be moved to give the desired stability margins, i.e. b_i is the change in location of $k_i(s)h_i(s)$. The elements of A and b are evaluated at the set of frequencies $s = j\omega_i$, $i = 1, \dots, m$, at which the current gain or phase margins are calculated. The distances between the current locations and the desired locations of the Nyquist exact loci are specified by the designer via specification of stability margins. The actual evaluation of the elements of A and b depend on whether $n = 1$ or $n = 2$.

For $n = 1$, proportional control, the elements of $A = a(s)$ are:

$$a_{ij}(s) = \frac{\partial (|k_i h_i(s)|)}{\partial k_j} \quad (4.16)$$

These real derivatives are of course evaluated numerically using a difference formula. For phase margins the distances contained in the vector b become $b_i = 1 - c_i$, where c_i is the current magnitude of $k_i h_i(s)$ at a phase of $(180^\circ - \text{phase margin})$. For gain margins, expressed as the factor the gain should be multiplied by for the loop to become unstable, the distances in the vector b become $b_i = (1/\text{gain margin}) - c_i$, where c_i here is the current magnitude of $k_i h_i(s)$ at a location closest to the critical point $(-1,0)$. The proportional controller constants are updated using

$$k_{pi} = k_{pi} + \alpha * x_i \quad (4.17)$$

where α is a relaxation factor less than one. The relaxation factor is introduced to avoid going too far, and possibly oscillating around the desired location because the linearity assumed in calculating the derivatives $a_{ij}(s)$, might not be valid for the full change in the controller constants.

For $n = 2$, proportional plus integral (PI) or proportional plus derivative (PD) control, the elements of $A = \{a_{ij}\}$ are:

$$a_{ij}(s) = \frac{\partial (k_i(s)h_i(s))}{\partial k_j(s)} \quad (4.18)$$

and again these complex derivatives are evaluated numerically using difference formula. For phase margins Θ_i , $i = 1, \dots, m$, the elements of the vector b become $b_i = (-\cos \Theta_i, -j\sin \Theta_i) - c_i$, where c_i is the location in the complex plane on the locus $k_i(s)h_i(s)$, which has a phase of $(180^\circ - \Theta_i)$. For gain margins the elements of the vector b become $b_i = (-1/gain\ margin + j*0) - c_i$, where c_i is the location in the complex plane on the locus $k_i(s)h_i(s)$, which is closest to the critical point. The updating of the controller constants is dependent on whether PI or PD controller constants are being calculated. For a PD-controller of the form

$$K_p(1+K_D s) \quad (4.19)$$

the gains are updated as follows:

$$k_{P_i} = k_{P_i} + \alpha * \text{Re } x_i \quad (4.20)$$

and

$$k_{D_i} = k_{D_i} + \alpha * (\text{Im } x_i / (\text{Re } x_i * \omega_i)) \quad (4.21)$$

where ω_i is the frequency at which b_i is calculated. For a PI-controller of the form

$$K_p(1+K_I/s) \quad (4.22)$$

the controller constants are updated as follows:

$$k_{P_i} = k_{P_i} + \alpha * \text{Re } x_i \quad (4.23)$$

and

$$k_{I_i} = k_{I_i} + \alpha * (\text{Im } x_i * \omega_i / \text{Re } x_i) \quad (4.24)$$

In the above equations $\text{Re } x_i$ and $\text{Im } x_i$ of course denote respectively the real and imaginary part of x_i .

The magnitudes of the elements of the matrix A provide measures of the sensitivity of the Nyquist exact loci to changes in any of the controller constants. Such sensitivity coefficients can be a helpful guide in field tuning of a multivariable control system. These coefficients are also an indirect measure of the sensitivity to the propagation of interactions. If the i 'th Nyquist exact locus has low sensitivity to changes in the j 'th controller constant, then it will likely also have low sensitivity to, for example, a setpoint change in the j 'th loop. Hence the matrix A gives a qualitative indication of which interactions are most likely to upset the system. The use of the matrix A as a sensitivity

measure warrants further investigation.

4.5 Conclusions.

The Nyquist exact loci and the transfer functions $h_i(s)$ were introduced. The transfer functions $h_i(s)$ were shown to be an exact multivariable parallel to the single variable transfer function $g(s)$. The Nyquist exact loci were demonstrated to be useful in stability analysis and to allow control system design criteria, such as rise time, overshoot and settling time, familiar from SISO design, to be used meaningfully in a multivariable context.

The Nyquist exact loci (NEL) design procedure was outlined and its different steps discussed in detail. The NEL procedure allows the designer to specify stability margins in familiar terms, such as gain or phase margin, and simultaneously design m single loop controllers. Algorithms for the simultaneous design of P, PI or PD controllers to give Nyquist exact loci, which satisfy designer specified stability margins, were developed and described.

Finally the use of the derivatives of the Nyquist exact loci as a sensitivity measure was discussed.

5. Control system design using NEL.

5.1 Introduction.

The final test of any control system design technique is its use in a commercial environment, such as a chemical plant. However, before this can happen a design technique's practicality must be demonstrated by applying it to the design of several control systems for widely different chemical plants, comparing the resultant designs with control systems designed using other techniques, and testing the designed systems by simulation and/or application to pilot plants. The purpose of this chapter is to carry out this first part of the test of the NEL design procedure.

The NEL design technique will be used to design control systems for three chemical processes: a double effect evaporator, a chemical reactor, and a distillation column. These three processes have been the subject of numerous control studies in recent years. This allows the control systems designed using the NEL procedure to be compared with published control systems, which were arrived at using other design techniques, such as the inverse Nyquist array method, the characteristic loci method, or the direct Nyquist array method.

In the next section the NEL design procedure is used to design a discrete control system for a pilot plant double effect evaporator. The design is approached using both the discrete TFM $G(w)$ and the continuous TFM $G(s)G_h(s)$, and the resulting control systems are compared. The resulting designs are also compared with the controllers designed by Kuon (1975). This is followed by application of the NEL design technique to the design of a control system for an open loop unstable chemical reactor. Finally the NEL procedure is used to design a control system for a distillation column with significant time delays.

5.2 Double effect evaporator.

The double effect evaporator pilot plant in the Department of Chemical Engineering at the University of Alberta has been the object of several control studies, which were collected into a case study by Fisher and Seborg (1976).

These studies involved techniques such as multiloop control, optimal feedback control, time optimal control, model reference adaptive control and multivariable Smith predictors. Frequency domain control studies involving the evaporator have been reported by Kuon (1975), who used the INA, DNA and CL techniques. Due to these past studies the evaporator is a good candidate for applying a new design technique, such as the NEL design procedure described in chapter 4, and comparing the resultant designs with control systems obtained using other methods.

Fisher and Seborg (1976) list several state space models of the evaporator. Among them are a continuous fifth order state space model and a discrete fifth order state space model using a sampling interval of 64 seconds. The continuous transfer function matrix (TFM) $G(s)$ calculated from the continuous state space model is shown in table 3.1 (Note: all coefficients have been truncated to two significant figures). The discrete TFM $G(z)$ obtained from the discrete state space model is listed in table 5.1, and the corresponding bilinearly transformed TFM $G(w)$ is given in table 5.2. The outputs are product concentration, first effect holdup and second effect holdup, and the inputs or manipulated variables are steam flowrate to first effect, bottoms flowrate from first effect and bottoms flowrate from second effect.

The poles of the TFM's $G(s)$, $G(z)$ and $G(w)$, i.e. the roots of the open loop characteristic polynomials, are tabled in table 5.3. The evaporator models are marginally stable, since $G(s)$ and $G(w)$ have two poles located on the imaginary axis, and $G(z)$ has the corresponding two poles located on the unit circle. The number of clockwise encirclements required by Nyquist type stability theorems hence depends on the particular Nyquist contour employed, as discussed in appendix D. In the following analysis the closed right half plane Nyquist contour will be used, this means two anticlockwise encirclements of the critical point, due to the poles at the origin in s -plane or the w -plane.

A graphical test of $F(s) = I + G(s)$ for column matrix dominance is shown in figure 3.1, and in figure 3.2 the corresponding test for row matrix dominance is shown. In figure 3.1 N_{12}^c , N_{13}^c and N_{23}^c , as defined by equation 3.6, are plotted as functions of frequency for frequencies in the range from

Table 5.1 Discrete transfer function model $G(z)$ of pilot plant evaporator. $G(z) = N(z)/d(z)$, where $N(z)$ is a polynomial matrix and $d(z)$ is the characteristic polynomial.

$$d(z) = -0.039 + 2.49z - 6.13z^2 + 7.35z^3 - 4.32z^4 + 1.0z^5$$

$$n_{11}(z) = -0.0093 + 0.017z + 0.0078z^2 - 0.029z^3 + 0.014z^4$$

$$n_{12}(z) = -0.017 + 0.094z - 0.18z^2 + 0.15z^3 - 0.043z^4$$

$$n_{13}(z) = 0.0$$

$$n_{21}(z) = 0.0080 - 0.015z - 0.0068z^2 + 0.025z^3 - 0.012z^4$$

$$n_{22}(z) = -0.032 + 0.17z - 0.33z^2 + 0.27z^3 - 0.082z^4$$

$$n_{23}(z) = 0.0$$

$$n_{31}(z) = 0.0093 - 0.017z - 0.0079z^2 + 0.029z^3 - 0.014z^4$$

$$n_{32}(z) = 0.033 - 0.18z + 0.34z^2 - 0.28z^3 + 0.085z^4$$

$$n_{33}(z) = -0.016 + 0.085z - 0.16z^2 + 0.13z^3 - 0.041z^4$$

Table 5.2 Bilinear transformed discrete transfer function model $G(w)$ of pilot plant evaporator. $G(w) = N(w)/d(w)$, where $N(w)$ is a polynomial matrix and $d(w)$ is the characteristic polynomial.

$$d(w) = 0.00005w^2 + 0.0070w^3 + 0.24w^4 + 1.0w^5$$

$$n_{11}(w) = 0.00007w^2 + 0.0023w^3 - 0.0039w^4 - 0.0011w^5$$

$$n_{12}(w) = -0.00005w^2 - 0.0026w^3 - 0.0067w^4 + 0.022w^5$$

$$n_{13}(w) = 0.0$$

$$n_{21}(w) = -0.00007w^2 - 0.0020w^3 + 0.0034w^4 + 0.00098w^5$$

$$n_{22}(w) = -0.00015w^2 - 0.0050w^3 - 0.012w^4 + 0.041w^5$$

$$n_{23}(w) = 0.0$$

$$n_{31}(w) = -0.00008w^2 - 0.0023w^3 + 0.0039w^4 + 0.0011w^5$$

$$n_{32}(w) = 0.00016w^2 + 0.0051w^3 + 0.012w^4 - 0.042w^5$$

$$n_{33}(w) = -0.00008w^2 - 0.0025w^3 - 0.0059w^4 - 0.020w^5$$

Table 5.3 Poles of evaporator TFM's $G(s)$, $G(z)$ and $G(w)$ obtained from fifth order state models.

s-plane	z-plane	w-plane
0.0	1.0	0.0
0.0	1.0	0.0
-0.0380	0.9603	-0.0380
-0.0766	0.9215	-0.0766
-0.773	0.4384	-0.732

0.0038 to 7.73 rad/min. N_{13}^c and N_{23}^c are zero at all frequencies, but $N_{12}^c > 1$ for frequencies less than 0.08 rad/min. Hence the return difference matrix is not column matrix dominant at low frequencies. Similarly in figure 3.2 N_{12}^r , N_{13}^r

and N_{23}^r , as defined by equation 3.6, are plotted as functions of frequency. N_{12}^r is less than one at all frequencies, but N_{13}^r and N_{23}^r are greater than one for frequencies less than 0.08 rad/min. Therefore the return difference matrix is also not row matrix dominant at low frequencies. The return difference matrix could be made matrix dominant by selecting gains k_1 and k_2 in $\text{diag}\{k_1, k_2, k_3\}$ less than one, for example with $k_1 = k_2 = 0.33$ and $k_3 = 1.0$ the return difference matrix is matrix dominant. However, such a scheme would give loose control over the most important output variable, i.e. product concentration, which is clearly not desirable. The design of a compensator to reduce interactions is thus warranted. Figure 3.1 indicates, that the offdiagonal elements of columns 1 and/or 2 should be reduced, where as figure 3.2 indicates, that the offdiagonal elements of row 3 should be reduced to lower the interaction. This combined with a design objective of tight control over product concentration points to reducing element (1,2). From the DNA of the TFM $G(s)$, which is shown in figure 3.3, it appears, that the open loop TFM will become lower triangular by the following column operation

$$\text{column 2} = \text{column 2} + 0.73 * \text{column 1} \quad (5.1)$$

As discussed in chapter 3 this operation will tend to cancel the influence of element (2,1) and at the same time increase the direct transmittance in the second loop and slightly decrease the influence of element (3,2). With the above compensation the return difference matrix is row matrix dominant, as shown in figure 3.4. The lower triangular open loop transfer function matrix, whose direct Nyquist array is shown in figure 5.1, means the closed loop transfer function matrix will also be lower triangular, hence product concentration is independent of the first and second effect bottoms flows and only dependent on steam flow to the first effect.

The simplest compensator, which decouple the product concentration from the bottoms flowrates, and at the same time give a matrix dominant return difference matrix, seems to be the following constant compensator

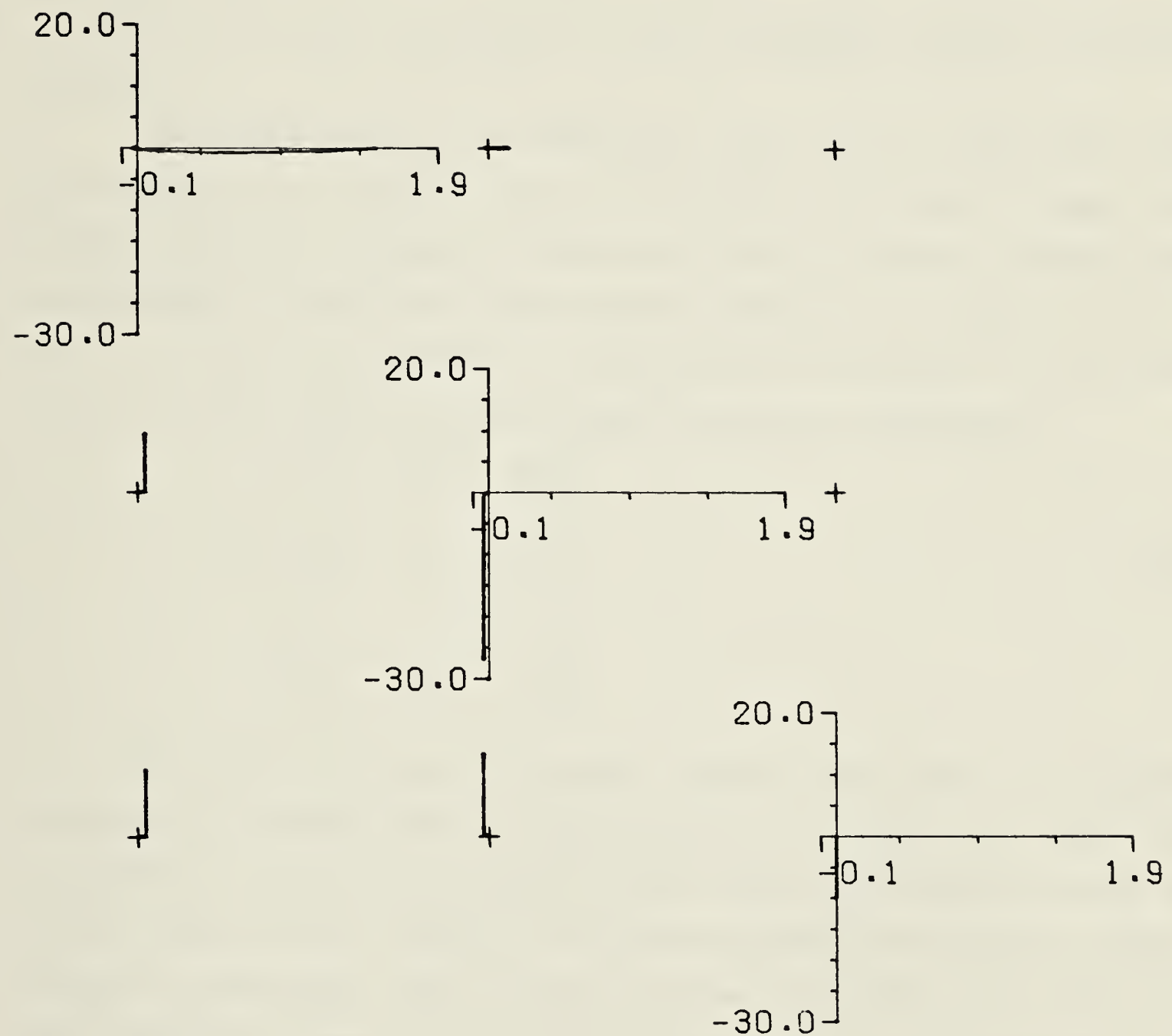


Figure 5.1 DNA of $G(s)K_1$ for continuous evaporator TFM $G(s)$ and compensator K_1 from equation 5.2. Frequency range $0.0038 < \omega < 7.73$ rad/min.

$$K_1 = \begin{bmatrix} 1.0 & 0.73 & 0.0 \\ 0.0 & 1.0 & 0.0 \\ 0.0 & 0.0 & 1.0 \end{bmatrix} \quad (5.2)$$

It should be noted, that $G(s)K_1$ is neither diagonally dominant nor matrix dominant.

The Nyquist exact loci of $G(s)K_1 G_h(s)$, where $G_h(s)$ is a zero order hold corresponding to a sampling time of 64 seconds, are shown in figure 5.2. Careful inspection of figure 5.2 shows, that none of the loci contribute any encirclements of the critical point, however multiplication of columns 2 and 3 by -1 will give the necessary two anticlockwise encirclements of the critical point (-1,0), one each by $q_{22}(s)$ and $q_{33}(s)$. Hence the compensator is

$$K_1 = \begin{bmatrix} 1.0 & -0.73 & 0.0 \\ 0.0 & -1.0 & 0.0 \\ 0.0 & 0.0 & -1.0 \end{bmatrix} \quad (5.3)$$

The simultaneous gain calculation algorithm was used to calculate proportional controller gains to give specified gain margins. The results are summarized in table 5.4. In all cases the initial gains were arbitrarily chosen to be one, and after five iterations the difference between the actual and desired locations of the Nyquist exact loci was less than 0.1. Except in the fourth and fifth calculation of table 5.4 the return difference matrix was dominant with the final gains. The two calculations in which $F(s)$ was not dominant, are the ones with the largest relative difference between the gain margin in loop 1, the concentration loop, and those in loops 2 and 3, the level loops. In the fourth calculation it is evident from the row matrix dominance plot, which is shown in figure 5.3, that $F(s)$ can be made matrix dominant by a slight increase in k_3 . The results of calculations number one and two, due to the large ratio k_3/k_1 , are not in agreement with the objective of tight control of product

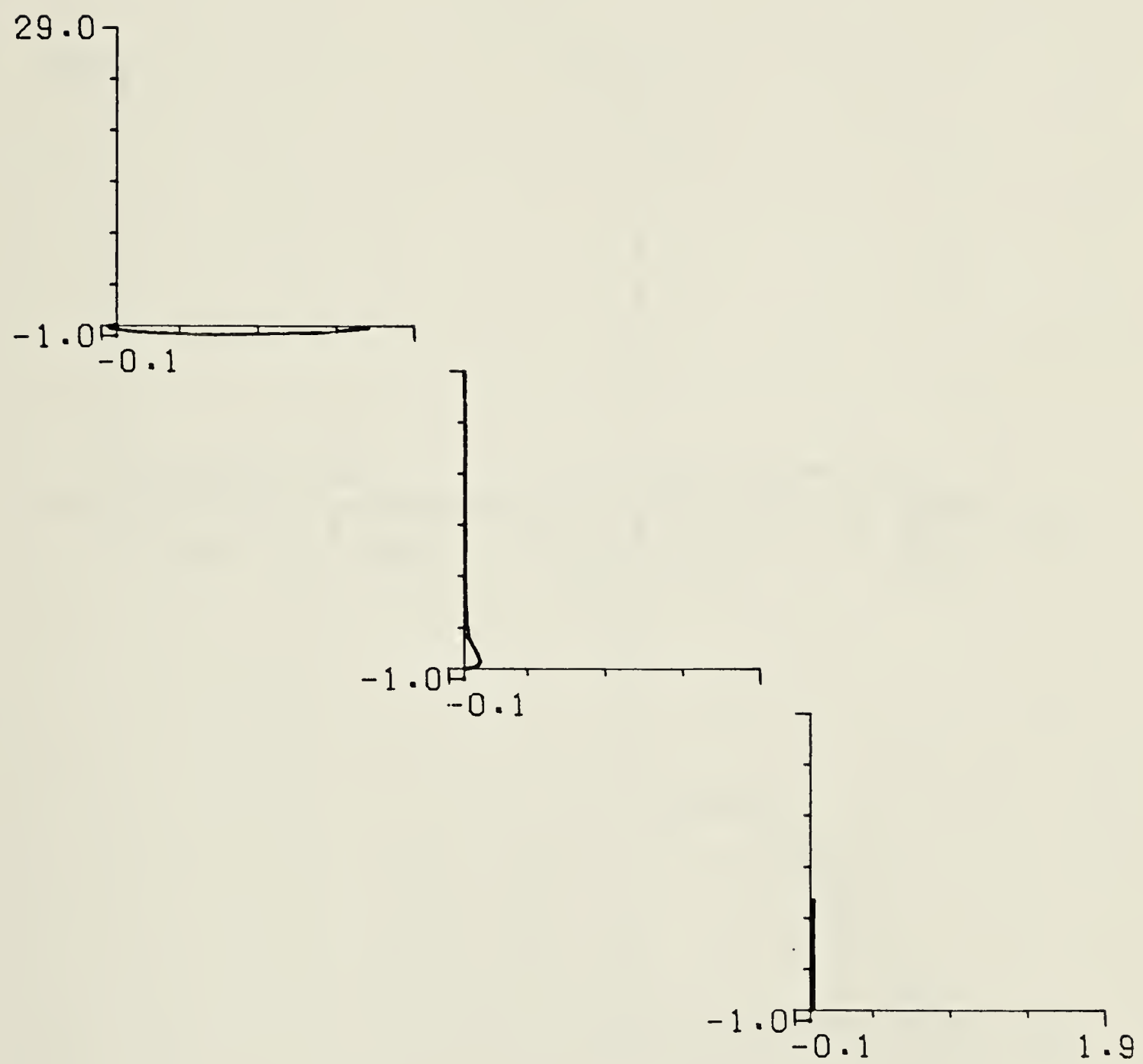


Figure 5.2 NEL of continuous evaporator with TFM $G(s)$, zero order hold with sampling time 64 seconds, compensator K_1 from 5.3 and $K_2 = 1$. Frequency range $0.0038 < \omega < 7.73$ rad/min.

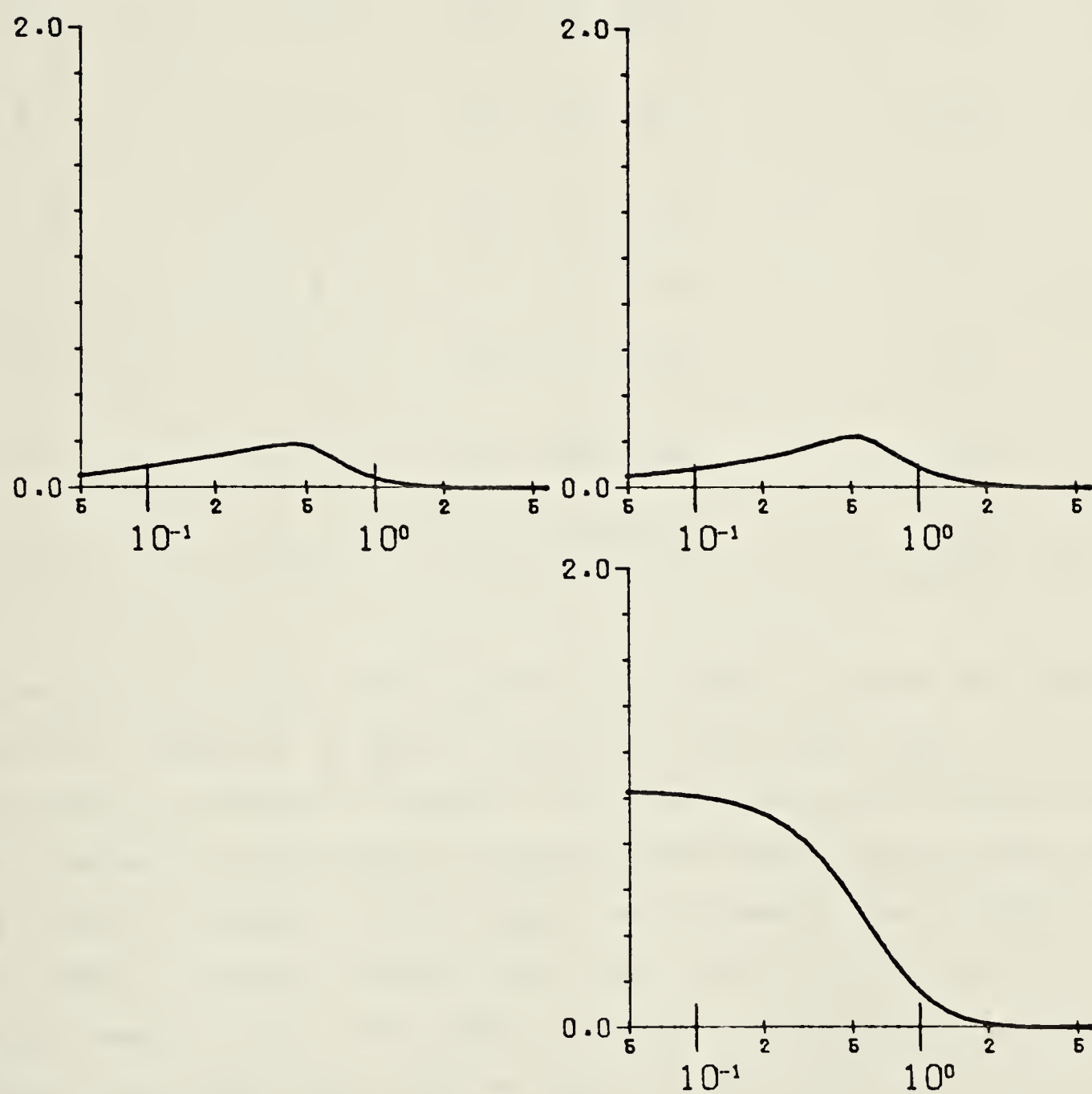


Figure 5.3 Row matrix dominance test of continuous evaporator with compensator K_1 from equation 5.3, zero order hold with 64 second sampling time, and proportional gain from calculation no. 4 of table 5.4.

Table 5.4 Summary of proportional controller constant calculation for continuous evaporator model $G(s)G_h(s)K_1$.

Calc. no.	gain margins			proportional constants			F(s) dominant ?
1	2	2	2	10.1	14.1	40.5	yes
2	2	3	3	9.9	5.9	23.5	yes
3	2	3	4	9.9	5.9	16.5	yes
4	2	4	4	10.6	3.4	16.5	no
5	2	5	5	11.3	2.3	12.6	no
6	3	4	4	5.6	4.1	15.6	yes
7	3	5	5	5.8	2.9	11.8	yes
8	2.5	4	4	7.2	3.6	15.6	yes

concentration, and loose control of the two levels. This leaves the results of calculations number six to eight. In figure 5.4 to 5.6 $|h_i(s)|/|1+h_i(s)|$ for $i = 1, 2, 3$ are plotted as functions of frequency. The proportional gains, which best fulfills the objective of tight control on product concentration and loose level control are those of calculation number eight. The simultaneous gain calculation took four steps to arrive at the final gain starting with $k_1 = k_2 = k_3 = 1$. The Nyquist exact loci after each iteration are shown in figures 5.7 to 5.10. It is evident from these figures, that the shape of the Nyquist exact loci do not change drastically from iteration to iteration, and figure 5.10 also shows the desired gain margins have been realized. Rise time, overshoot and settling time as calculated using equations 4.12 to 4.14 with the gains of calculation number eight are shown in table 5.5. Loop 1, the product concentration loop, responds purest to a unit setpoint change. However, since all variables are normalized deviation variables, a unit step in product concentration actually represents a doubling of the product concentration, which is physically more difficult to

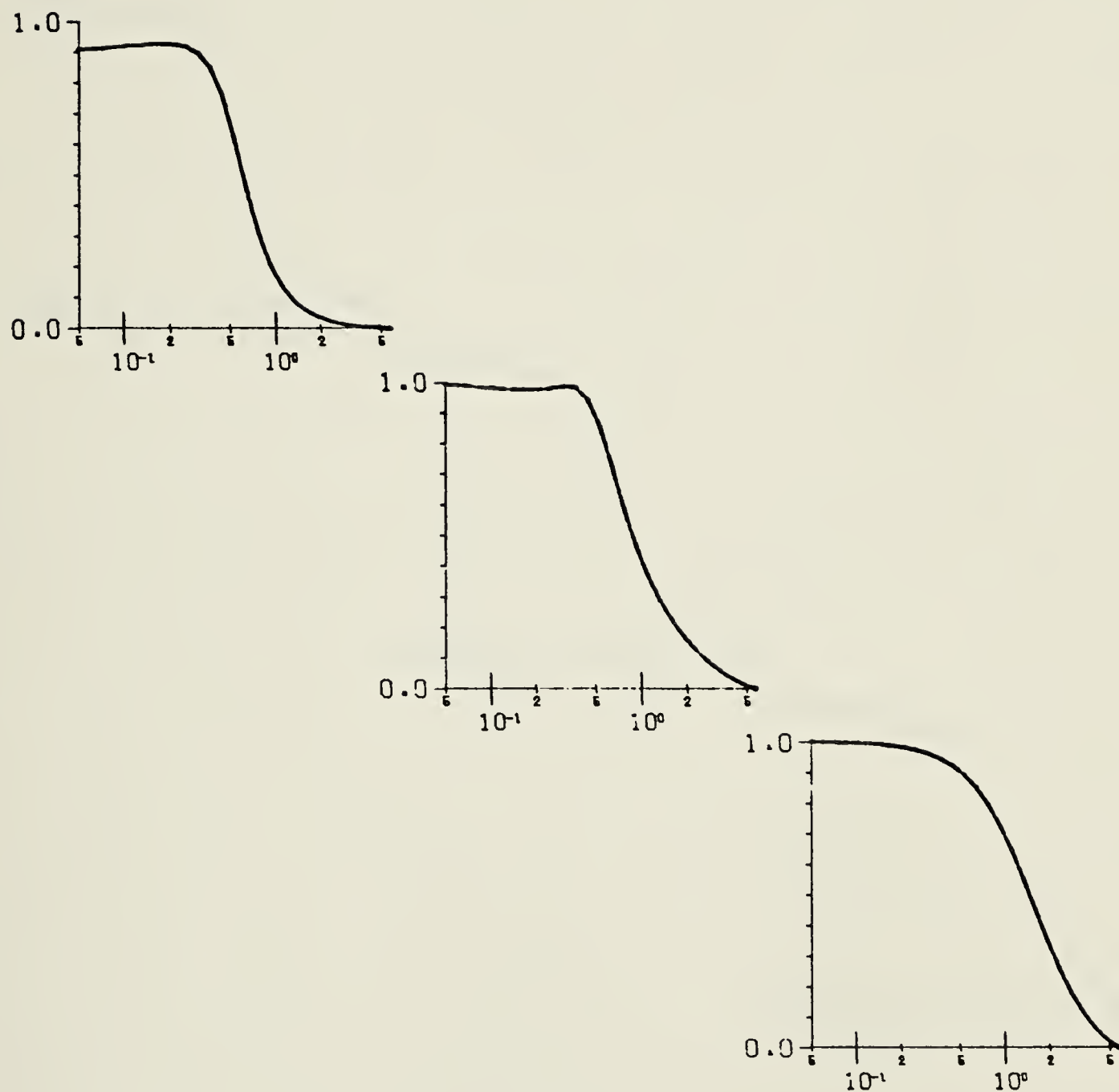


Figure 5.4 Plots of $|k_i h(s)| / |1 + k_i h(s)|$ versus frequency for $i=1,2,3$ with proportional gains from calculation no. 6 of table 5.4.

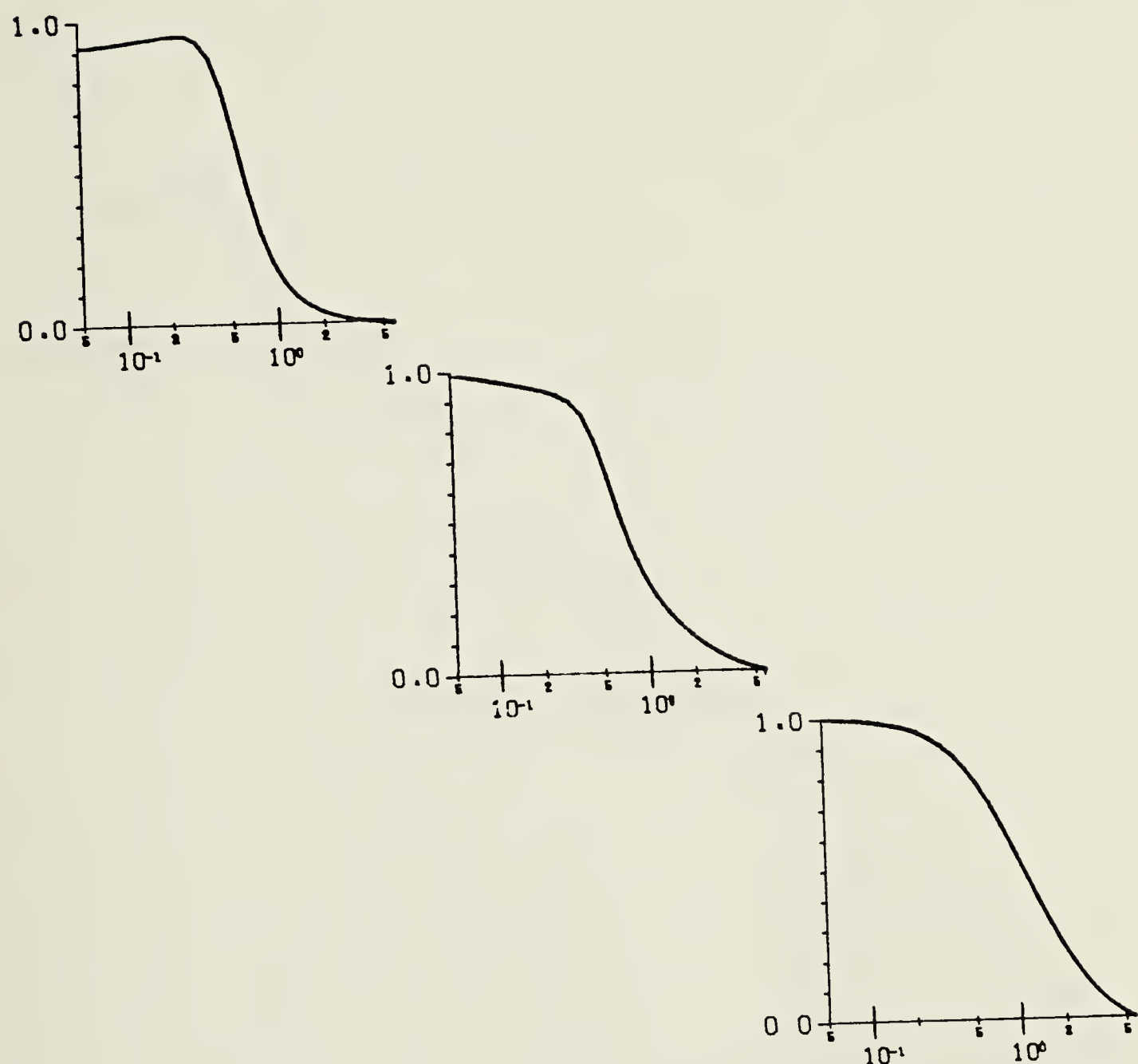


Figure 5.5 Plots of $|k_i h_i(s)| / |1 + k_i h_i(s)|$ versus frequency for $i=1,2,3$ with proportional gains from calculation no. 7 of table 5.4.

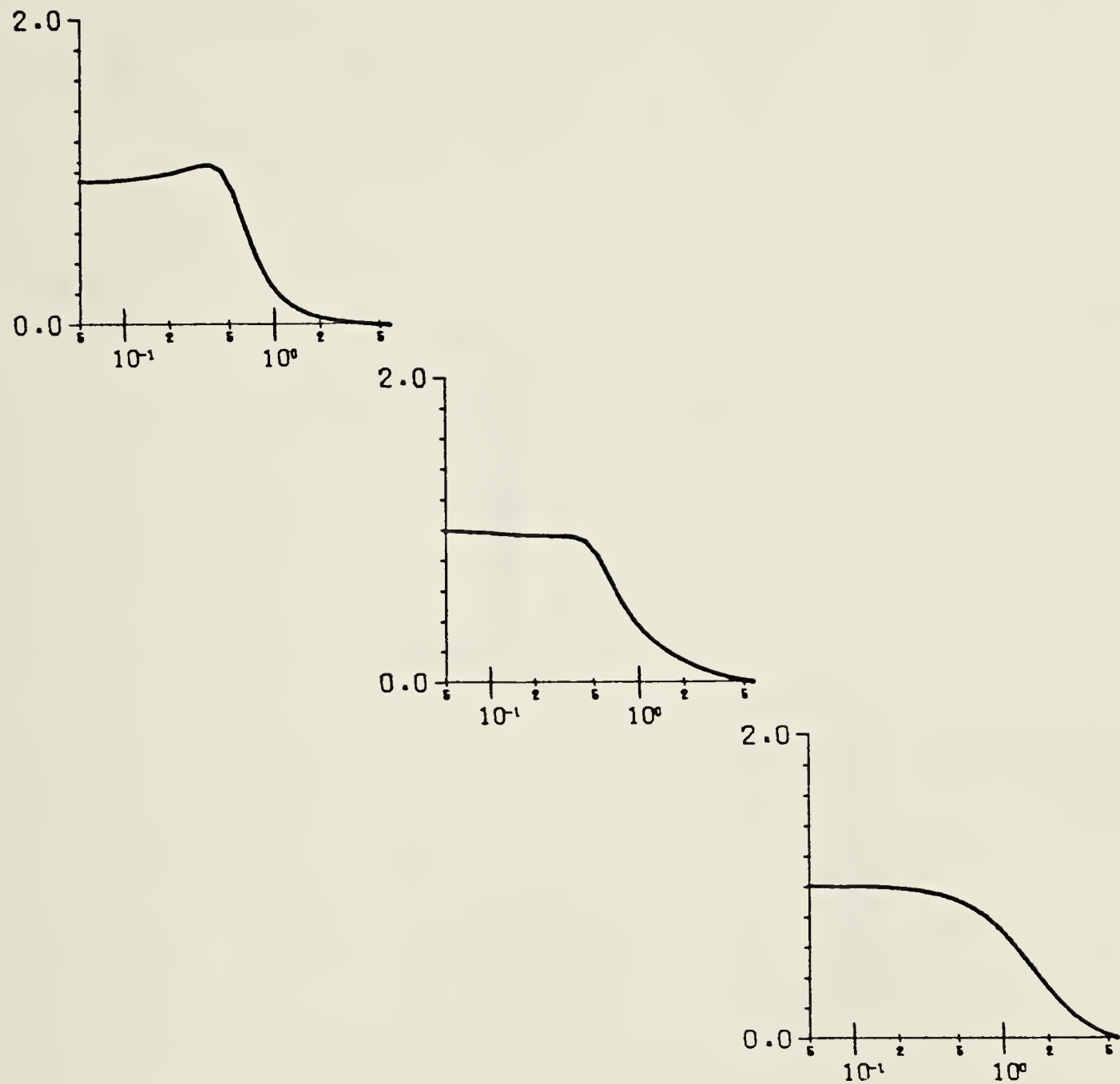


Figure 5.6 Plots of $|k_i h_i(s)| / |1 + k_i h_i(s)|$ versus frequency for $i=1,2,3$ with proportional gains from calculation no. 8 of table 5.4.

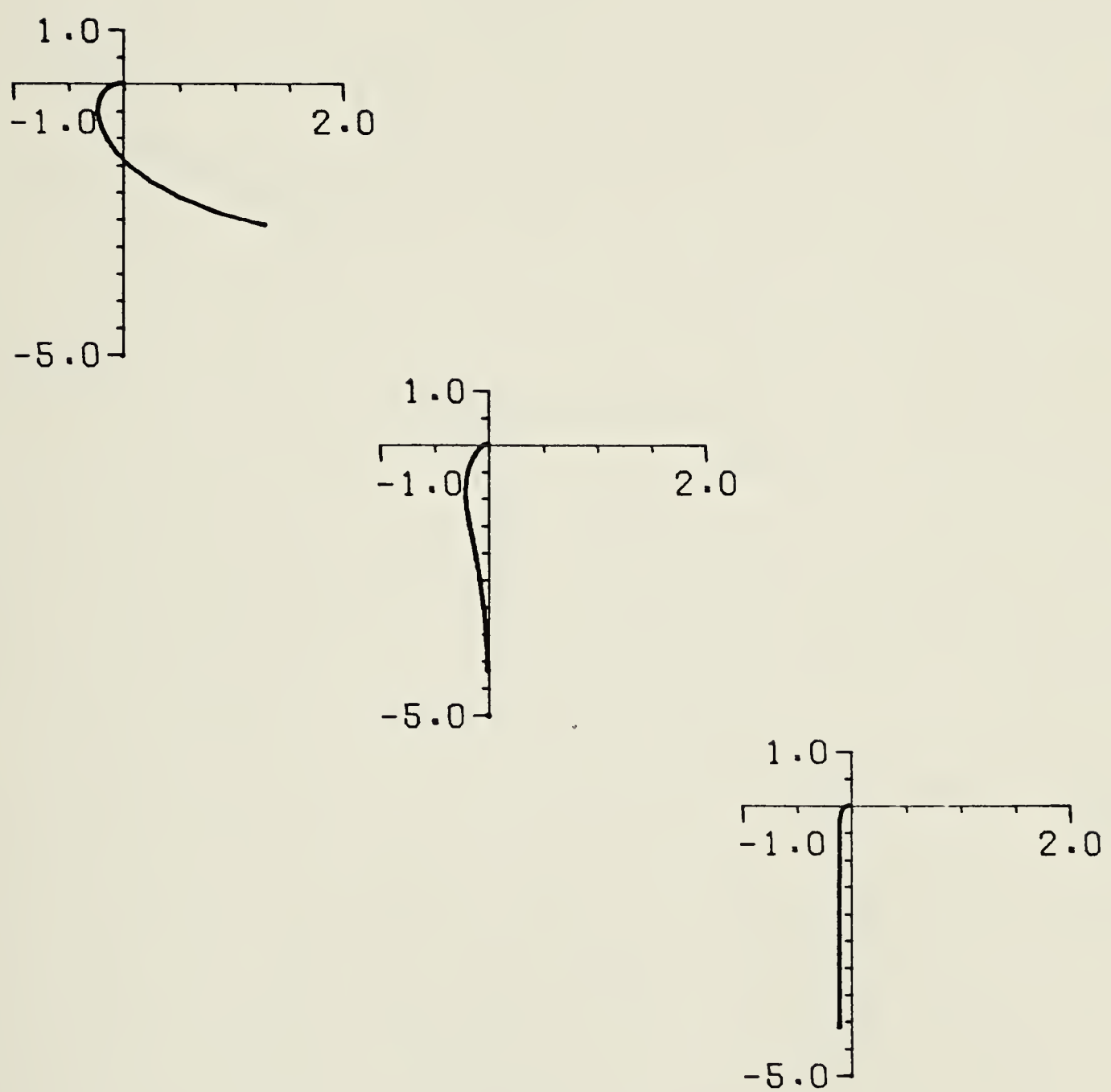


Figure 5.7 Nyquist exact loci for continuous evaporator model after one iteration of gain calculation no. 8 of table 5.4.

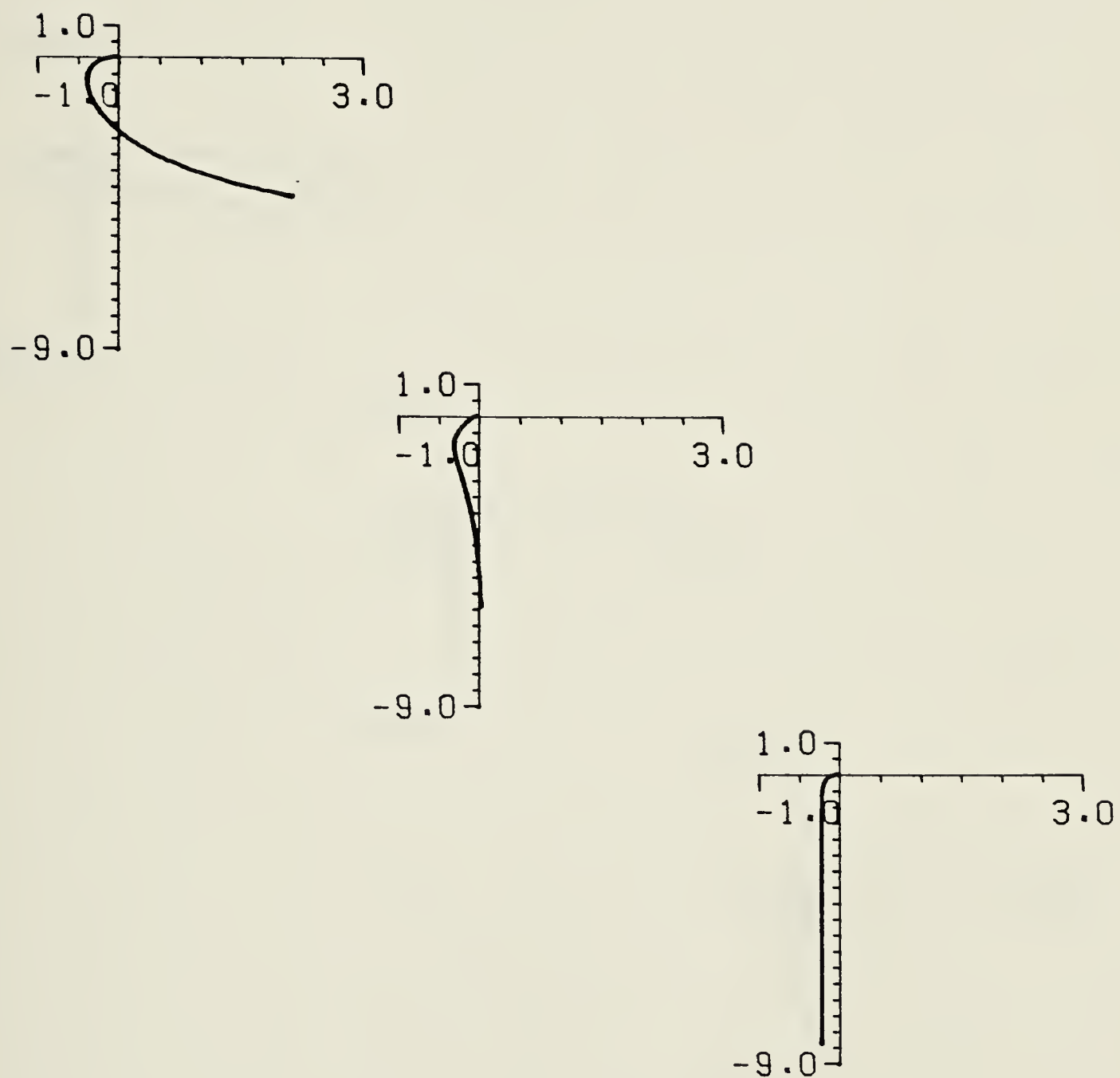


Figure 5.8 Nyquist exact loci for continuous evaporator model after two iteration in gain calculation no. 8 of table 5.4.

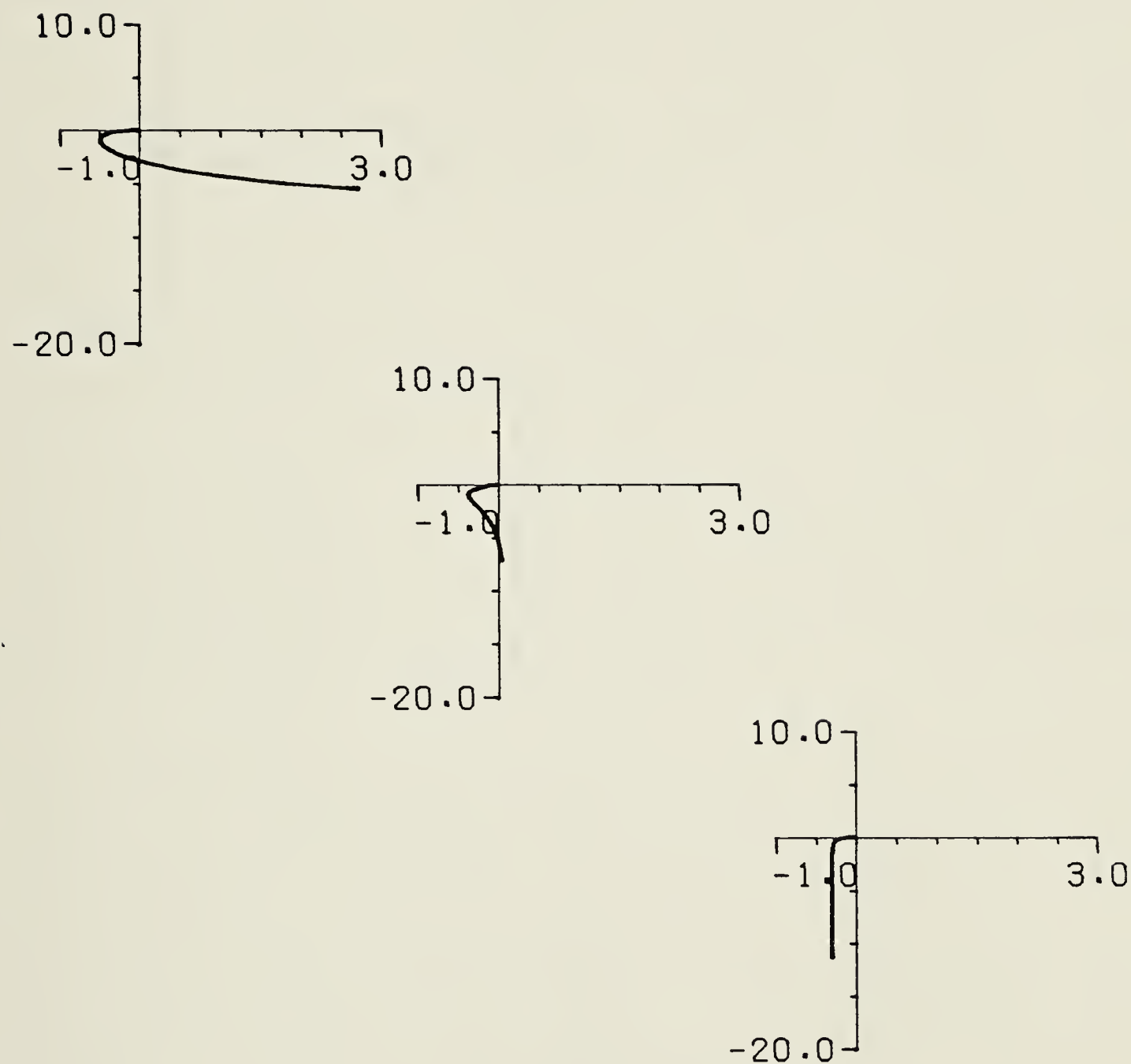


Figure 5.9 Nyquist exact loci for continuous evaporator model after three iterations in gain calculation no. 8 of table 5.4.

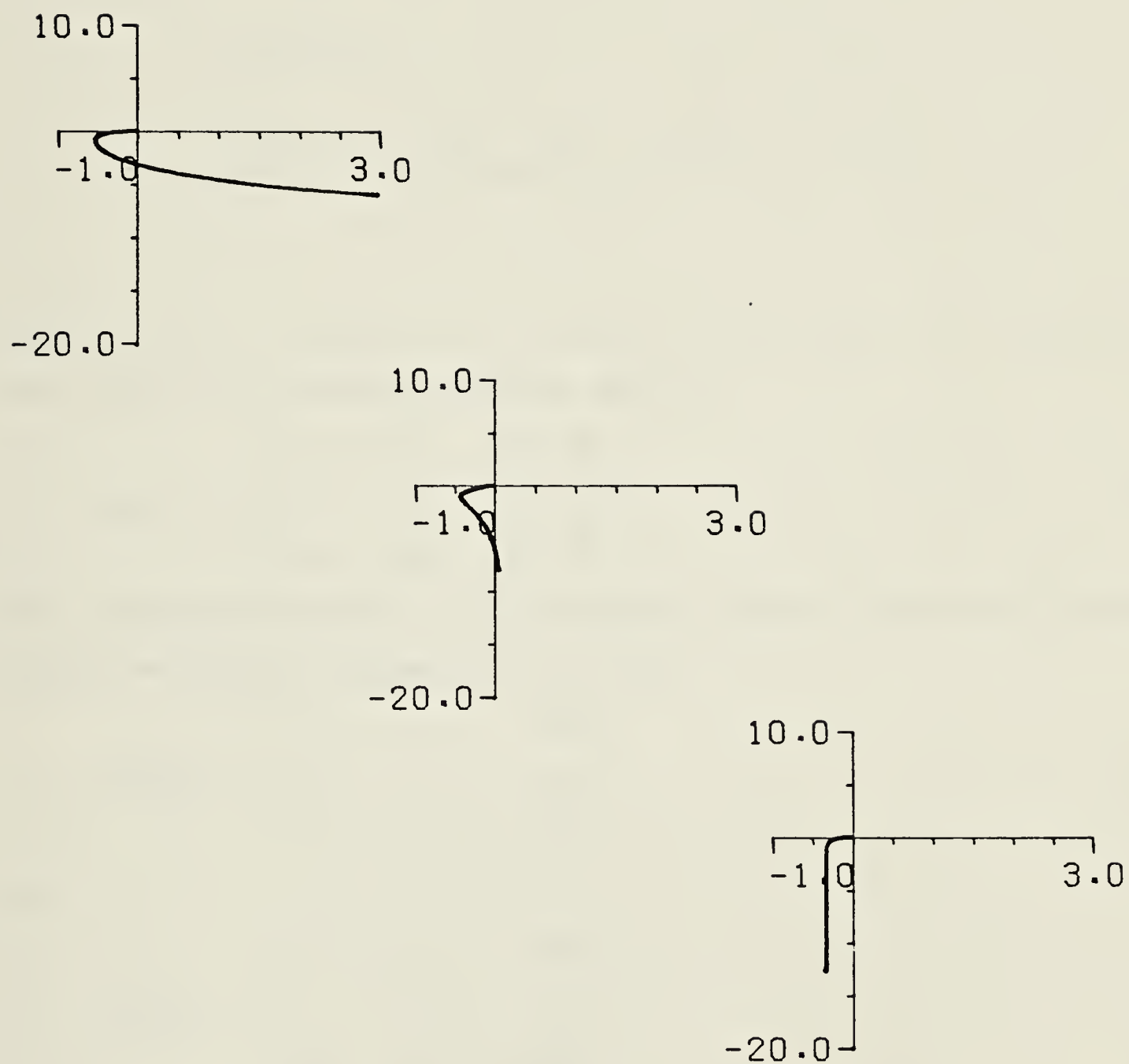


Figure 5.10 Nyquist exact loci for continuous evaporator model after last (fourth) iteration in gain calculation no. 8 of table 5.4.

Table 5.5 Rise time, overshoot and settling time with proportional gain from calculation number eight of table 5.4.

	loop 1	loop 2	loop 3
rise time, min.	4.7	3.4	1.9
overshoot, %	11	5	3
settling time, min.	12.5	8.7	4.5

accomplish than a doubling of the hold-ups of each effect. The recommended final proportional compensator/controller hence is

$$K_1 K_2 = \begin{bmatrix} 7.2 & -2.6 & 0.0 \\ 0.0 & -3.6 & 0.0 \\ 0.0 & 0.0 & -15.6 \end{bmatrix} \quad (5.4)$$

This compensator/controller can be compared with the proportional controllers FD0320 and FD0330 designed by Kuon (1975):

$$FD0320 = \begin{bmatrix} 5.6 & -3.1 & 0.0 \\ -2.2 & -3.7 & 0.0 \\ -9.8 & -4.9 & -9.8 \end{bmatrix} \quad (5.5)$$

and

$$FD0330 = \begin{bmatrix} 8.3 & -4.7 & 0.0 \\ -3.3 & -5.5 & 0.0 \\ -14.8 & -7.3 & -14.8 \end{bmatrix} \quad (5.6)$$

which were designed for gain margins of respectively 5 and 3.3 in all three loops. The additional non-zero elements below the diagonal in the compensator/controllers FD0320 and FD0330 will reduce level oscillations, but they will not influence the product concentration response to setpoint changes. Kuon used the discrete evaporator model $G(w)$ in designing FD0320 and FD0330, and the controllers were found to perform satisfactorily in experimental test. Compared with Kuon's compensator/controllers $K_1 K_2$ seems to have lower gains in loops 1 and 2 and higher in loop 3, when the gain

margins used in calculating K_1, K_2 are considered. This could be due to the use of the continuous model $G(s)G_h(s)$ in calculating K_1 . In order to investigate this possibility the calculations are repeated using the discrete model $G(w)$.

The DNA of the bilinear transformed discrete evaporator model of table 5.2 is shown in figure 5.11 for discrete frequencies from 0.01 to 2.80 rad/min., corresponding to continuous frequencies from 0.01 to 7.73 rad/min. A compensator identical to the one in equation 5.2 makes the return difference matrix dominant with $K_2 = I$. Proportional controller gains were calculated for the same conditions as were used with the continuous model. The results of the eight calculations with the discrete model are summarized in table 5.6. With respect to stability the results are identical, the gains of loop 1 and 2 are very similar, but the gain in loop 3 is consistently lower when the discrete model is used. This points to an error in either the discrete or continuous model state space model given by Fisher and Seborg (1976). The results in table 5.6 of course agree with the compensator/controllers FD0320 and FD0330 (shown in equations 5.5 and 5.6) designed by Kuon (1975) using a discrete evaporator model.

Comparison of tables 5.4 and 5.6 leads to the conclusion, that the continuous TFM $G(s)G_h(s)$ can safely be used in place of the bilinear transformed discrete TFM $G(w)$ when designing a discrete control system for a continuous plant, even though the approximations of equation 4.7 are invalid. The use of the continuous TFM $G(s)G_h(s)$ has the advantage, although not explored in the above example, that the effect of different sample times can easily be investigated without time consuming transformations.

The simulated closed loop responses of the evaporator with the compensator/controller of equation 5.4 to step changes in setpoint of +10% in product concentration, y_1 , and +20% in first effect hold-up, y_2 , are plotted in figures 5.12 and 5.13 respectively. The discrete evaporator fifth order state space model was used in these simulations. It can be seen, that the objective of minimizing effects of level changes on product concentration has been achieved. These results compare favourably with those from other multivariable proportional controllers designed for the evaporator, Fisher and Seborg (1976).

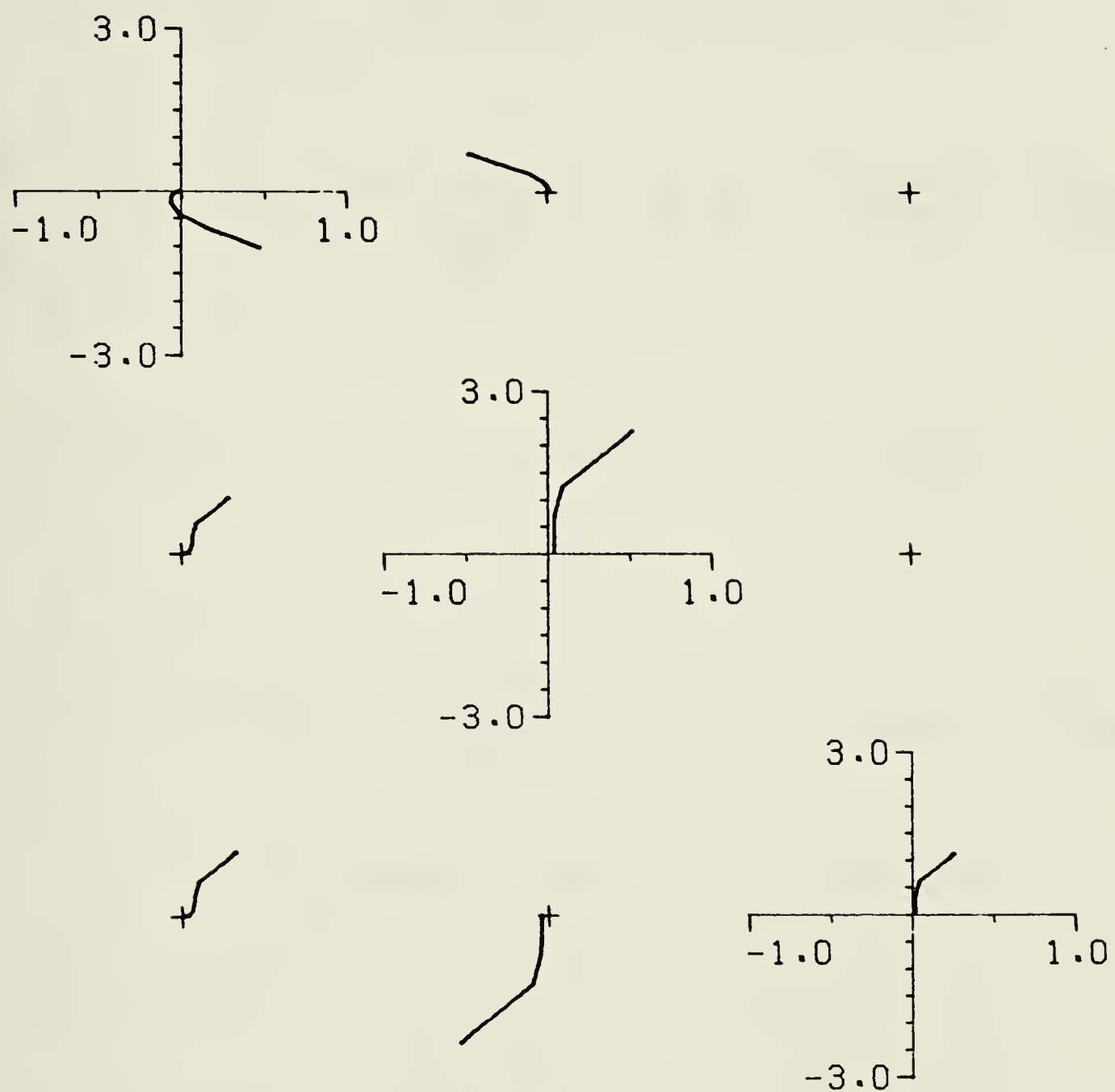


Figure 5.11 DNA of bilinear transformed discrete evaporator model $G(w)$.
Discrete frequency range $0.01 < v < 2.80$ rad/min.

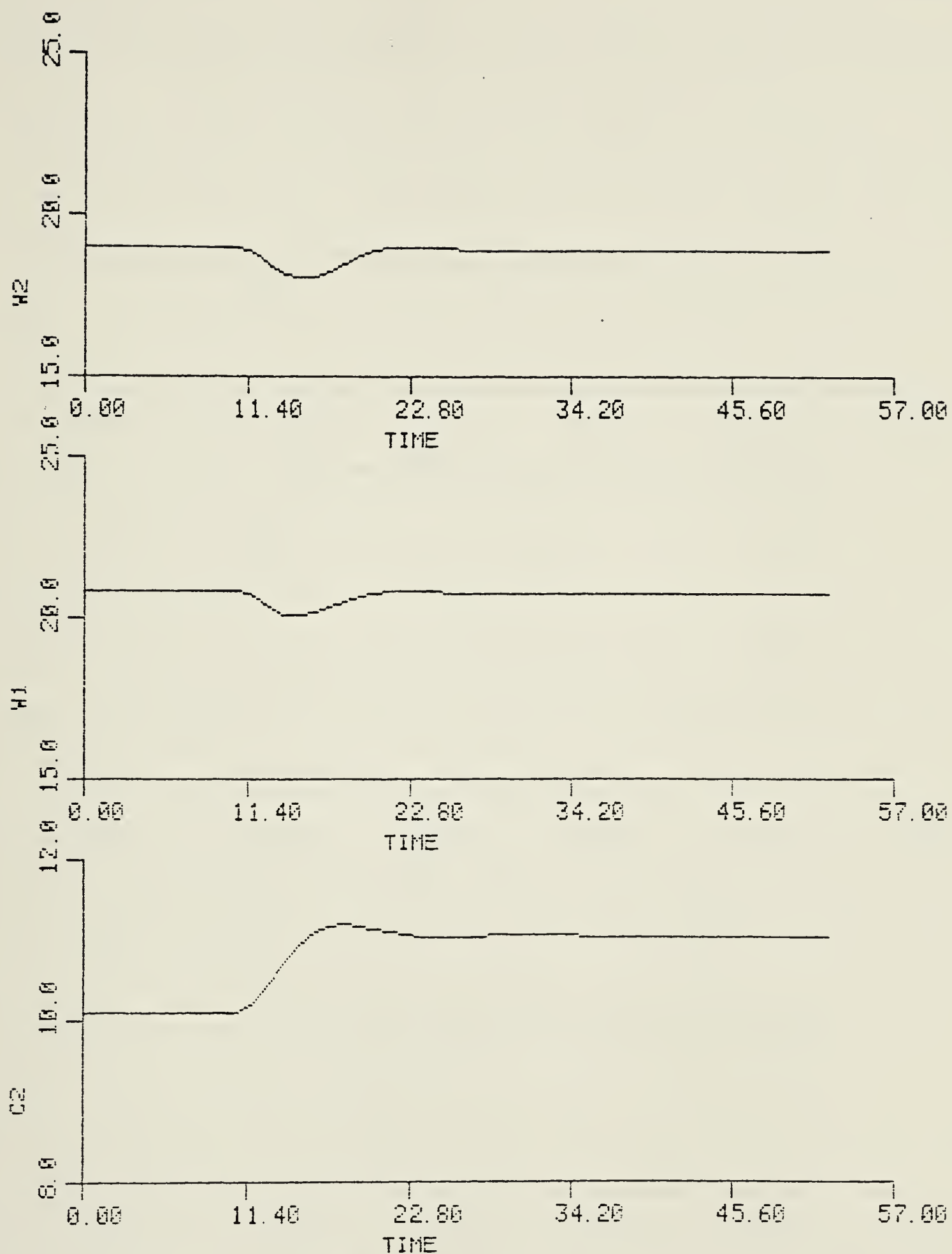


Figure 5.12 Simulated response of evaporator to a +10% change in product concentration. The fifth order discrete state space model and the compensator/controller of 5.3 were used.

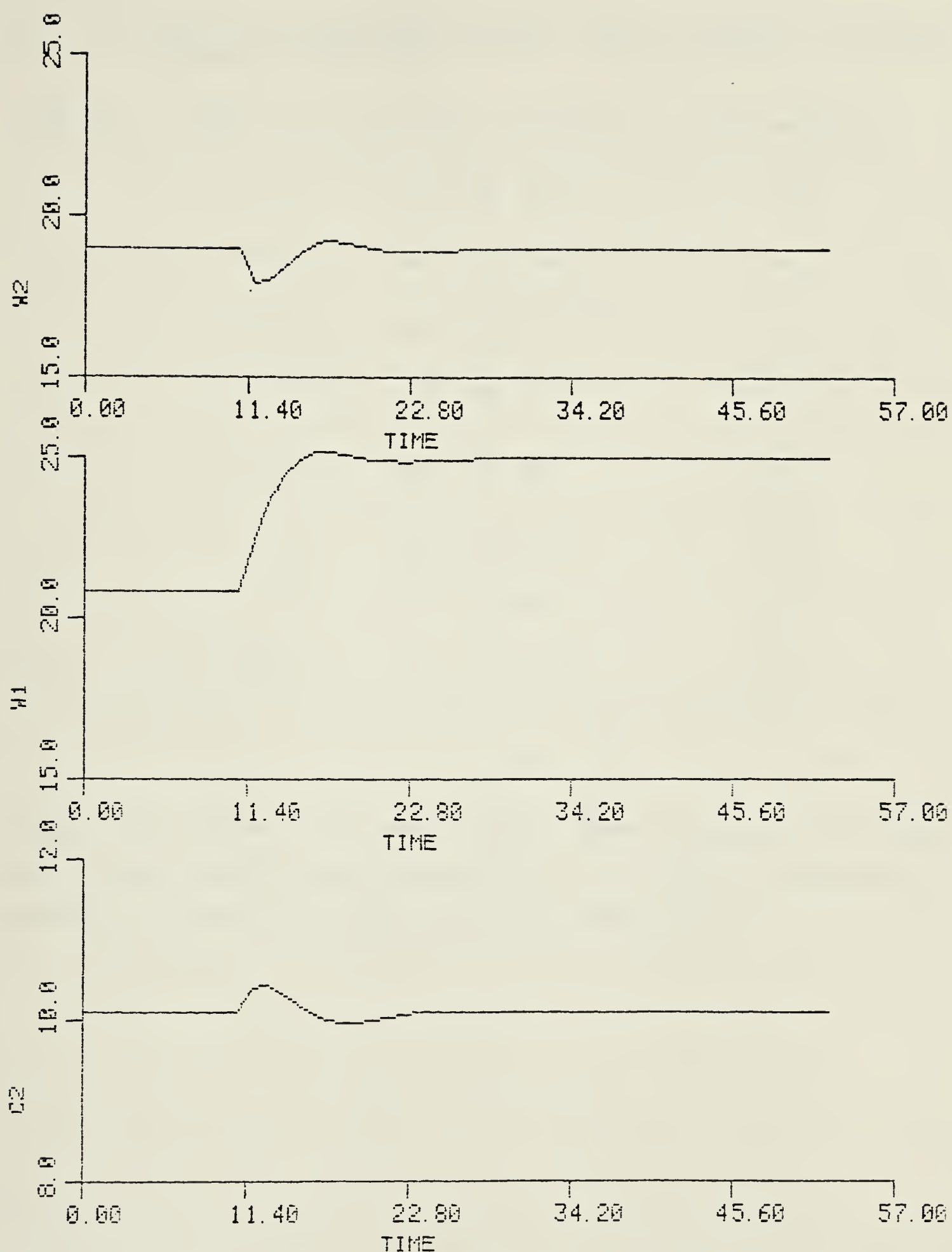


Figure 5.13 Simulated response of evaporator to a +20% change in first effect hold-up. The fifth order discrete state space model and the compensator/controller of equation 5.3 were used.

Table 5.6 Summary of proportional controller constant calculation for discrete evaporator model $G(w)K_1$.

Calc. no.	gain margins			proportional constants			F(s)	dominant ?
1	2	2	2	11.2	12.2	25.1		yes
2	2	3	3	9.9	7.8	16.6		yes
3	2	3	4	9.9	7.8	12.4		yes
4	2	4	4	11.1	3.6	12.4		no
5	2	5	5	11.8	2.5	9.9		no
6	3	4	4	5.9	4.5	12.4		yes
7	3	5	5	6.1	3.2	9.9		yes
8	2.5	4	4	7.5	4.1	12.4		yes

including those designed using other frequency domain techniques, Kuon (1975). The rise time, overshoot and settling time of the simulation responses are qualitatively in agreement with the values given in table 5.5.

5.3 Chemical reactor.

A model of an open loop unstable chemical reactor has been used in testing control system design techniques by Belletutti (1972), MacFarlane and Kouvaritakis (1977), and Hung and Anderson (1979). The different authors give slightly different continuous TFM models of the reactor. However, all the models have two inputs, two outputs and two right half plane poles, which makes the reactor an open loop unstable system. In this design exercise the model used by Hung and Anderson (1979) and listed in table 5.7 will be employed. This model has the right half plane poles at 0.0974 and 1.77 respectively.

The return difference matrix $F(s) = I + G(s)$ is matrix dominant as shown in figure 5.14, where $N_{12}(s)$ is plotted as a function of frequency. $N_{12}(s)$ is less than one at all frequencies, but the diagonal elements of the DNA of $G(s)$ give only one anticlockwise encirclement of the critical point, as evident from figure 5.15. Table 5.7 and figure 5.15 also show, that the elements of the first column of $G(s)$ are two orders of magnitude smaller than the elements of the second column. Multiplying the first column of $G(s)$ by -100 gives the DNA displayed in figure 5.16. Now the diagonal elements give a total of two anticlockwise encirclements of the critical point, but the return difference matrix is no longer matrix dominant. Figure 5.16 suggests element (2,1) can be reduced by the column operation

$$\text{column 1} = \text{column 1} - 1.6 * \text{column 2} \quad (5.7)$$

The return difference matrix $F(s) = I + G(s)K$ with

$$K_1 = \begin{bmatrix} -100.0 & 0.0 \\ -1.6 & 1.0 \end{bmatrix} \quad (5.8)$$

is matrix dominant, see figure 5.17, and the diagonal elements of the DNA $G(s)K_1$ gives two anticlockwise encirclements of the critical point. Hence, the system $G(s)K_1$ is closed loop asymptotically stable according to theorem 3.2. $G(s)K_1$ is matrix dominant, but not diagonally dominant, cf. figure 5.18, but it can be made diagonally dominant by transfer of dominance as described in section 3.5. The DNA of $G(s)K_1$ after a diagonal similarity transformation

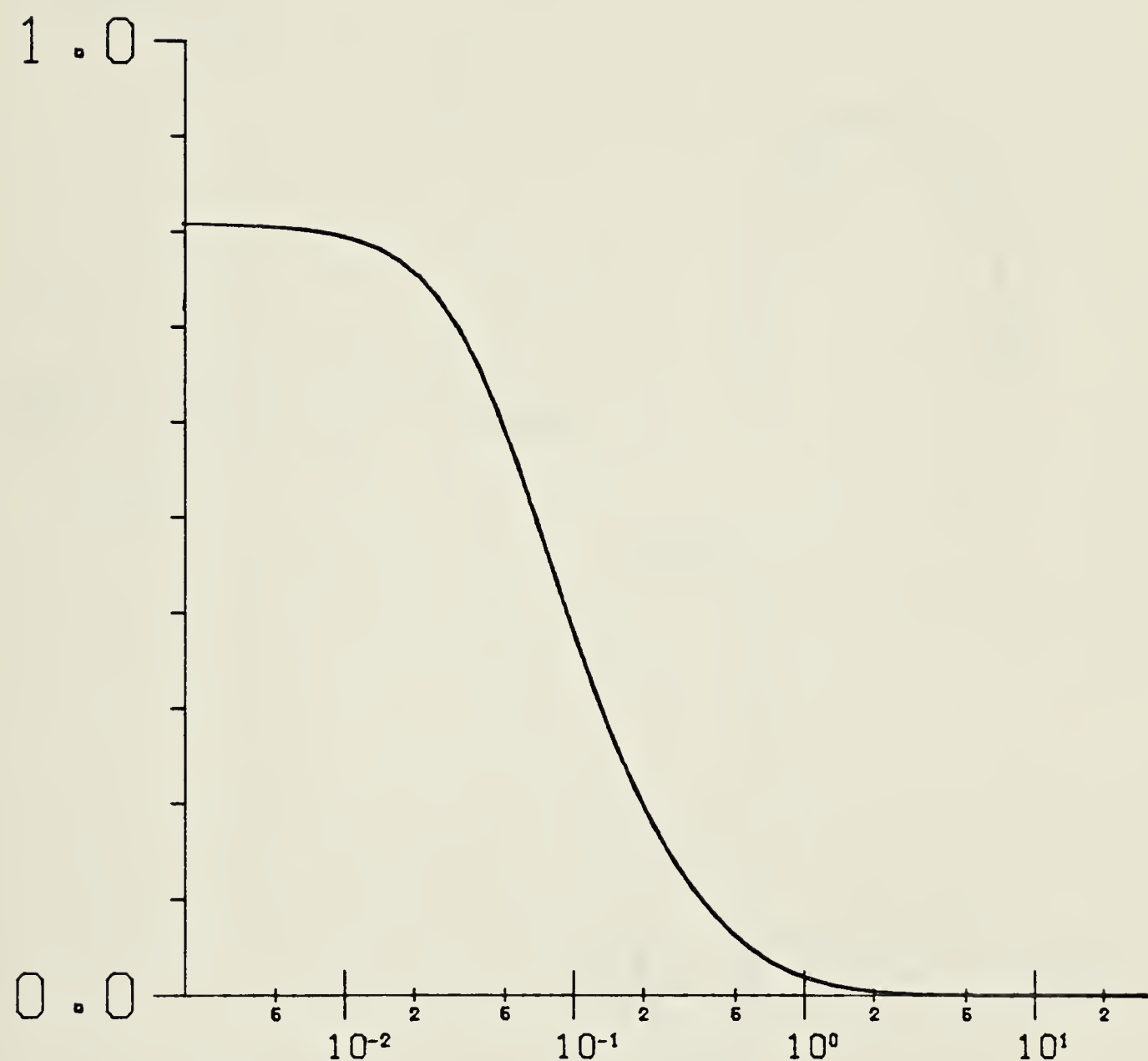


Figure 5.14 Matrix dominance test of $F(s) = I + G(s)$ with the chemical reactor TFM $G(s)$ from table 5.7.

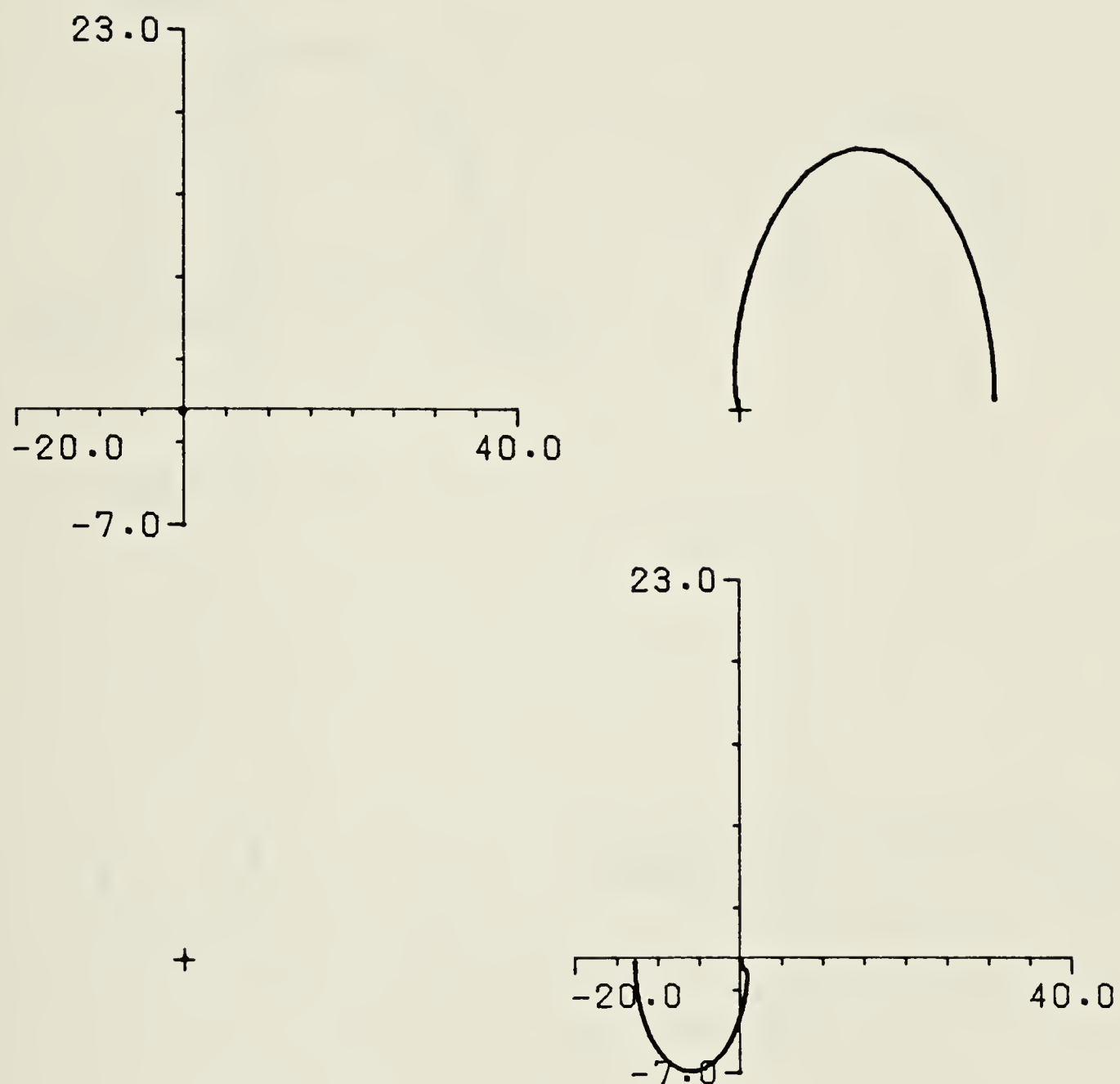


Figure 5.15 DNA of chemical reactor TFM $G(s)$ from table 5.7. Frequency range $0.002 < \omega < 30.5$ rad/1000s.

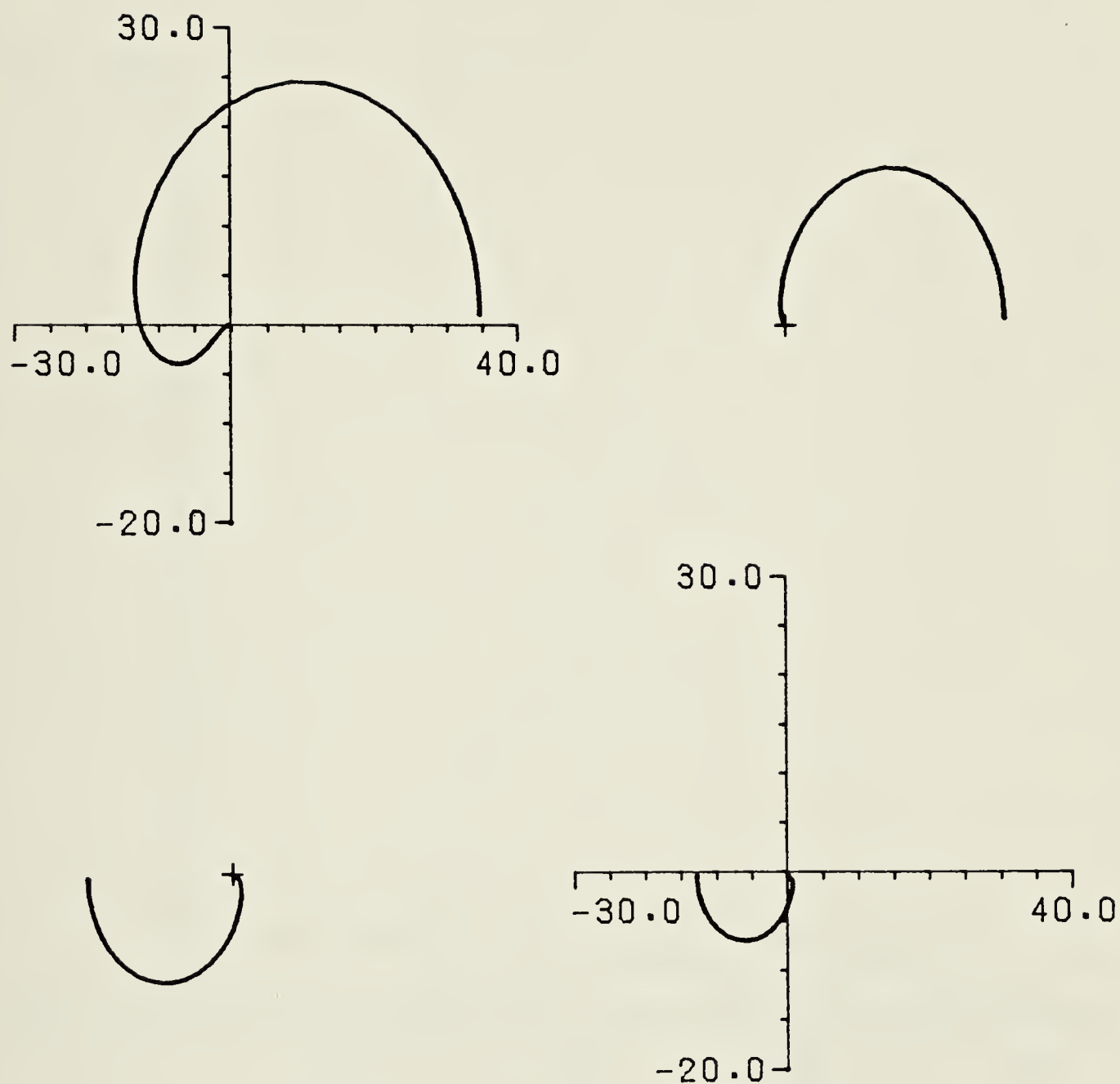


Figure 5.16 DNA of chemical reactor TFM $G(s)$ from table 5.7 after multiplication of column one by -100 . Frequency range $0.002 < \omega < 30.5$ rad/1000s.

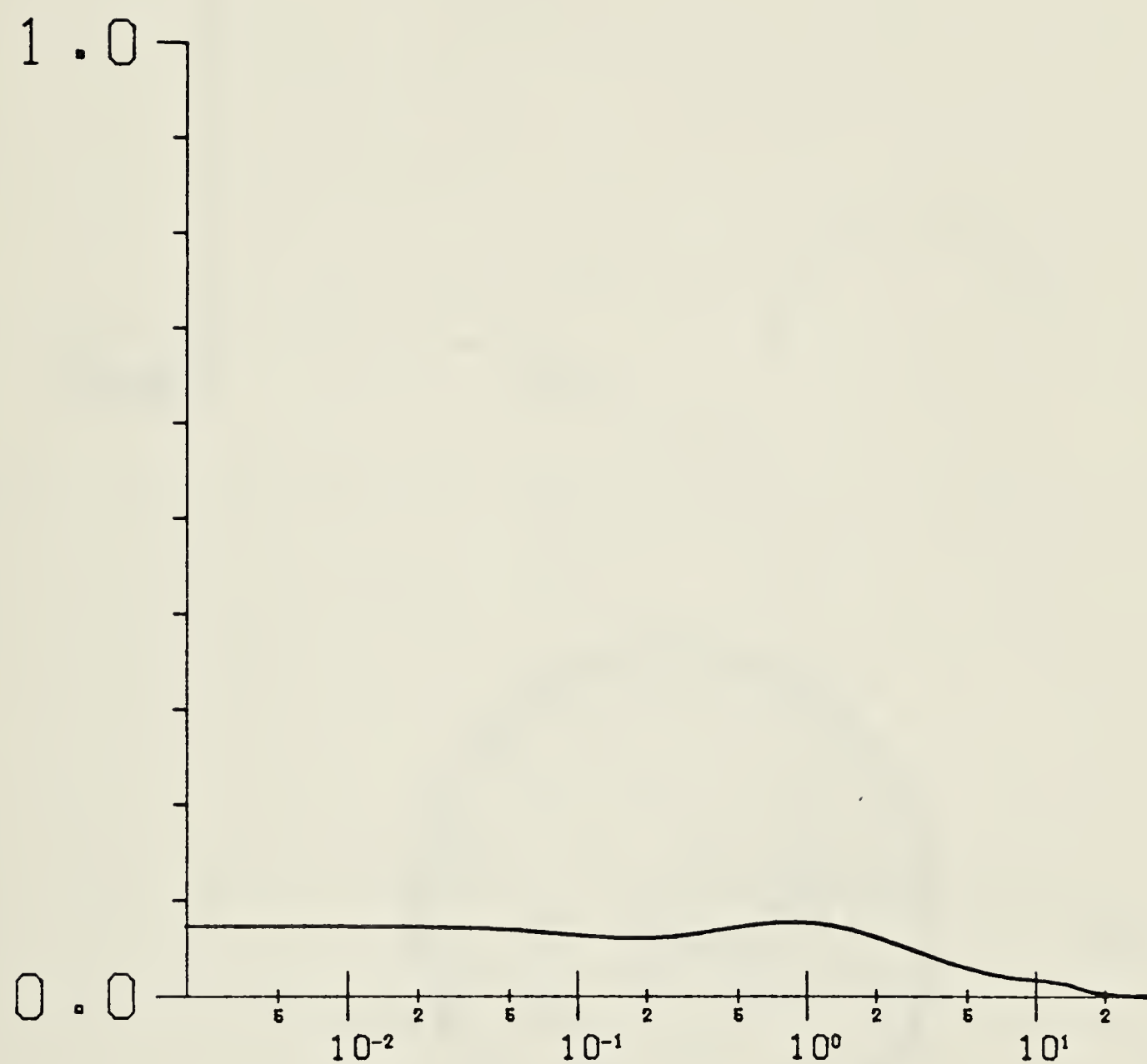


Figure 5.17 Matrix dominance test of $F(s) = I + G(s)K_1$, with the chemical reactor TFM $G(s)$ from table 5.7 and the compensator K_1 from equation 5.8.

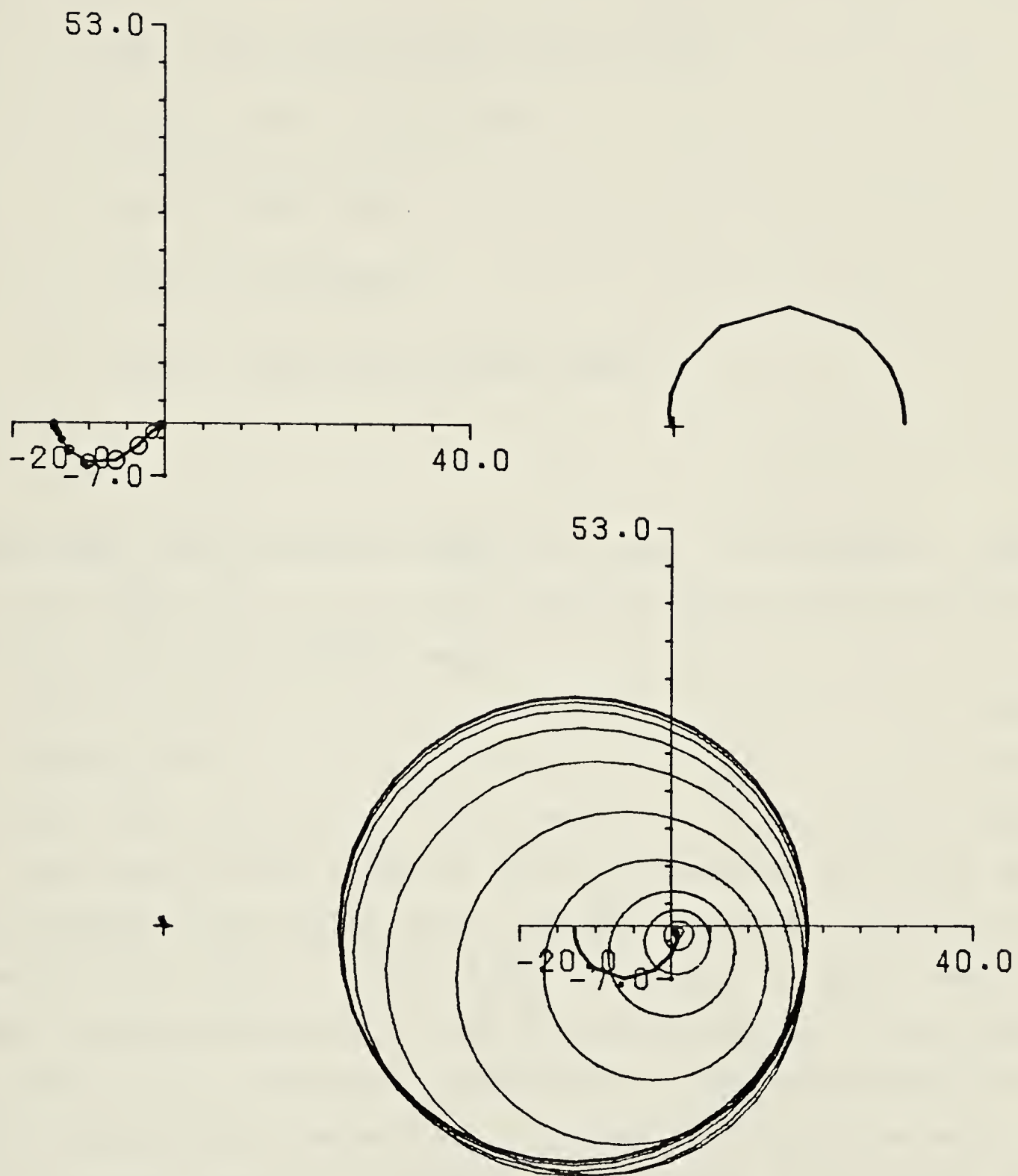


Figure 5.18 DNA of compensated chemical reactor TFM model with Gershgorin circles, based on column sums, superimposed on the diagonal elements. Frequency range $0.002 < \omega < 30.5$ rad/1000s.

Table 5.7 TFM model of chemical reactor as given by Hung and Anderson (1979). The model $G(s)$ has the form $G(s) = N(s)/d(s)$, where $d(s)$ is the characteristic polynomial, and $N(s)$ is a polynomial matrix.

$$d(s) = 7.55 - 79.43s + 18.47s^2 + 11.87s^3 + 1.0s^4$$

$$n_{11}(s) = -2.63 - 11.11s - 2.11s^2$$

$$n_{12}(s) = 233.5 + 29.2s$$

$$n_{21}(s) = 1.515 + 0.943s$$

$$n_{22}(s) = -96.5 - 58.25s + 43.83s^2 + 5.68s^3$$

calculated with column weighting factors of 3 and 1 is presented in figure 5.19. From figure 5.19 it can be seen, that the system will be stable with proportional gains in the following ranges

$$0.06 < k_1 < \infty \quad (5.9)$$

$$0.58 < k_2 < \infty \quad (5.10)$$

The Nyquist exact loci with $k_1 = 0.15$ and $k_2 = 0.15$ are shown in figure 5.20. These gains give gain margins of 23 and 3 respectively. As can be seen the corresponding phase margins are 60 and 90 respectively. The gain k_2 is outside the range given in inequality 5.10, but the return difference matrix is dominant, as shown in figure 5.21, and the Nyquist exact loci of figure 5.20 give a total of two counterclockwise encirclements of the critical point, so the system is asymptotically stable according to theorem 4.1. Through examination of plots of $|k_i h_i(s)| / |1 + k_i h_i(s)|$ for different $K_2 = \text{diag}\{k, k\}$ it was found, that improved control was obtained with higher gains. It was also observed, that the bandwidth was proportional to the gain. This is in agreement with the controllers designed by Bellettrutti (1972), by MacFarlane and Kouvaritakis (1977), and by Hung and Anderson (1979). The limitations on the proportional gains will in practice be dependent on the error in the linear model of the reactor. Plots of $|k_i h_i(s)| / |1 + k_i h_i(s)|$ for $k_1 = k_2 = 1.0$ are shown in figure 5.22, from which rise time, overshoot and settling time can be calculated using equations 4.12 to

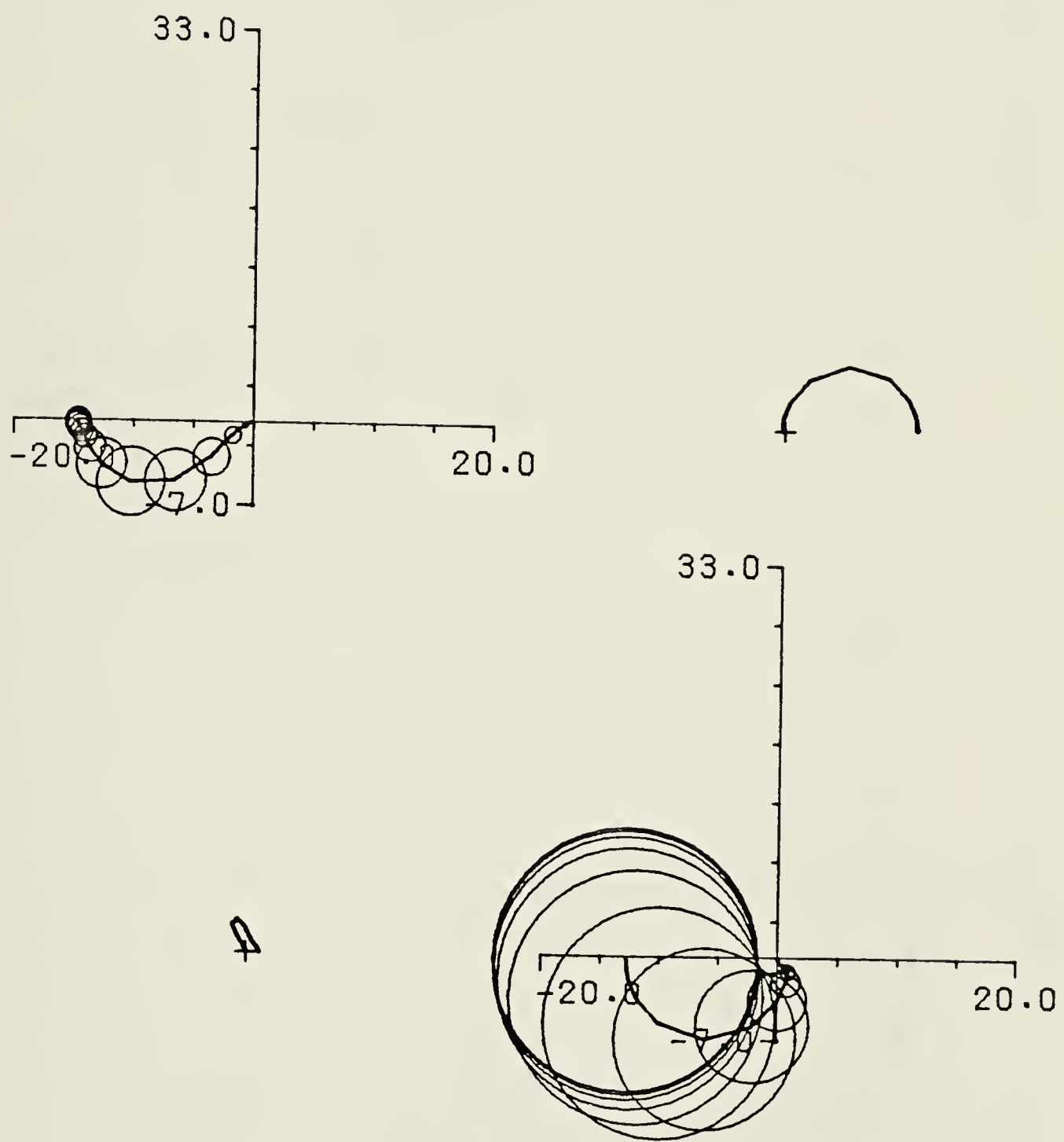


Figure 5.19 DNA of similarity transformed compensated chemical reactor TFM model with Gershgorin circles, based on column sums, superimposed on the diagonal elements. Frequency range $0.002 < \omega < 30.5$ rad/1000s.

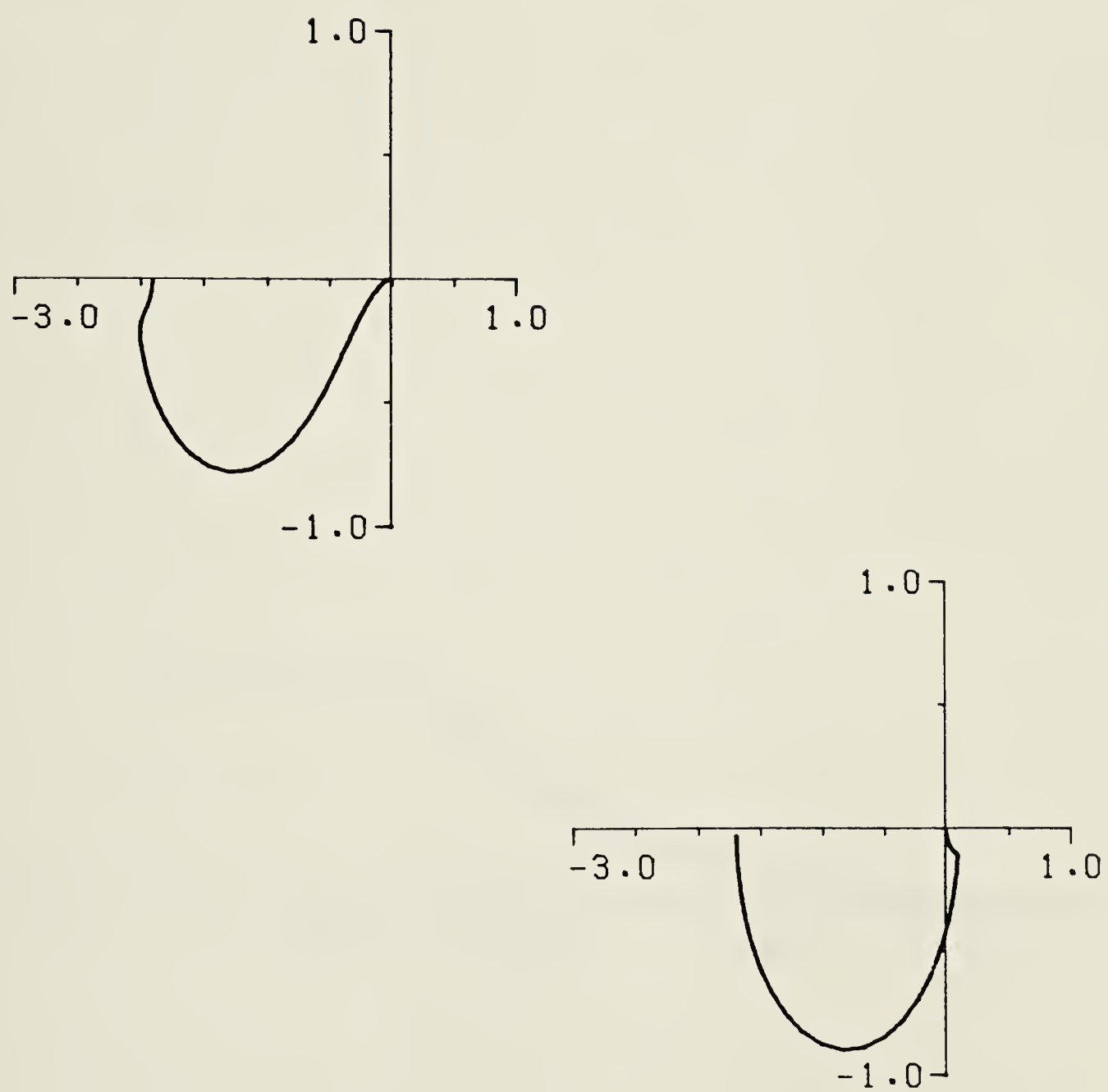


Figure 5.20 Nyquist exact loci of compensated chemical reactor model with $k_1 = 0.15$ and $k_2 = 0.15$. Frequency range $0.002 < \omega < 30.5$ rad/1000s.

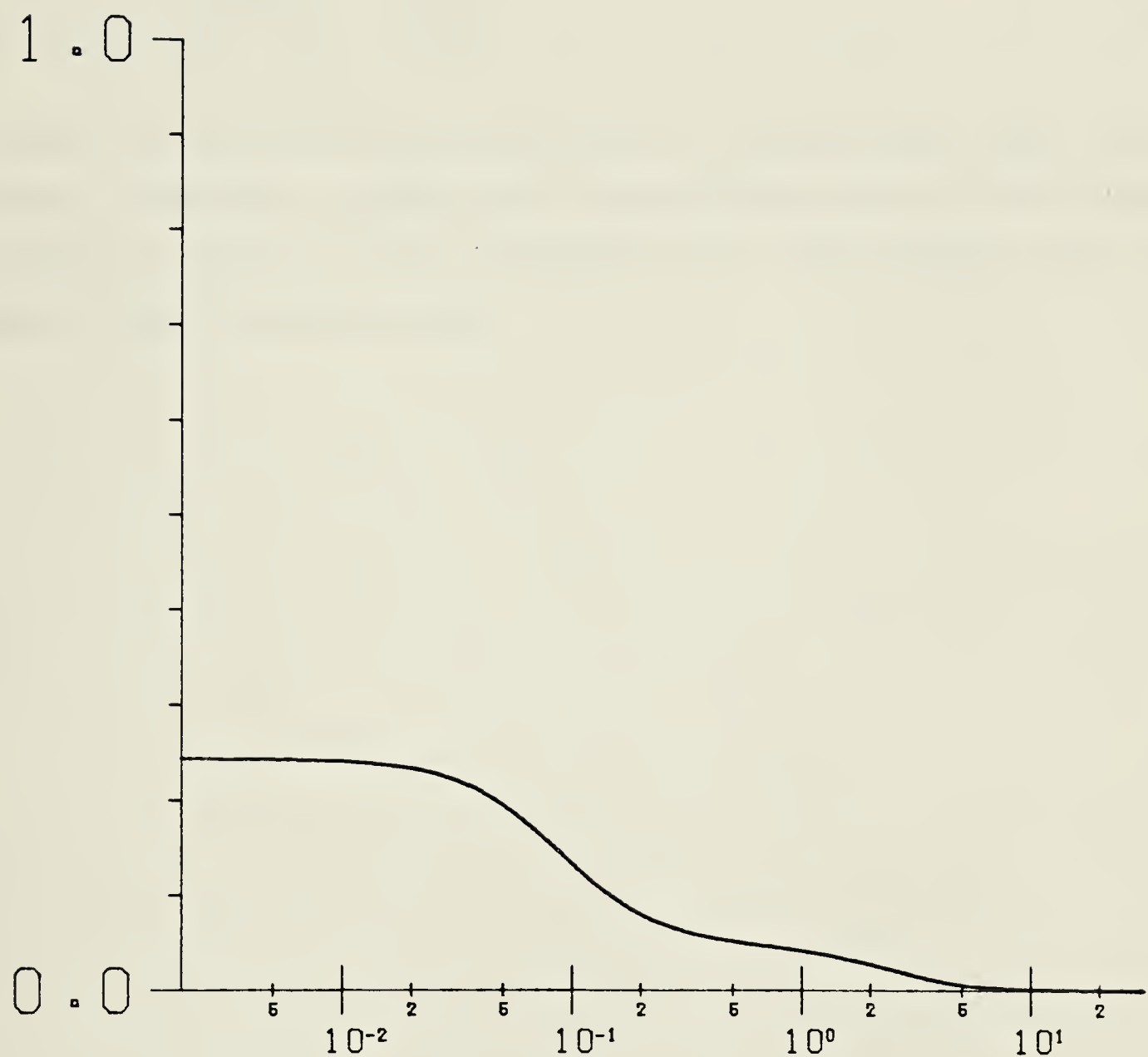


Figure 5.21 Matrix dominance test of $F(s) = I + G(s)K_1 K_2$ with the chemical reactor TFM model from table 5.7, the compensator K_1 from equation 5.8 and $K_2 = \text{diag}\{0.15, 0.15\}$.

4.14. The first loop has a rise time of 2 min., 65% overshoot, and a settling time of 20 min., while the rise time of the second loop is 59 min. The high overshoot could be reduced by introducing integral action into the compensator/controller. The final proportional compensator/controller is

$$K_1 K_2 = \begin{bmatrix} -100.0 & 0.0 \\ -1.6 & 1.0 \end{bmatrix} \quad (5.11)$$

It should be noted, that the low gain limits of the gain gain space with the constant compensator in equation 5.11 are somewhat lower, than those reported by Belletrutti (1972) using the characteristic locus desing technique and a high integrity diagonal controller matrix.

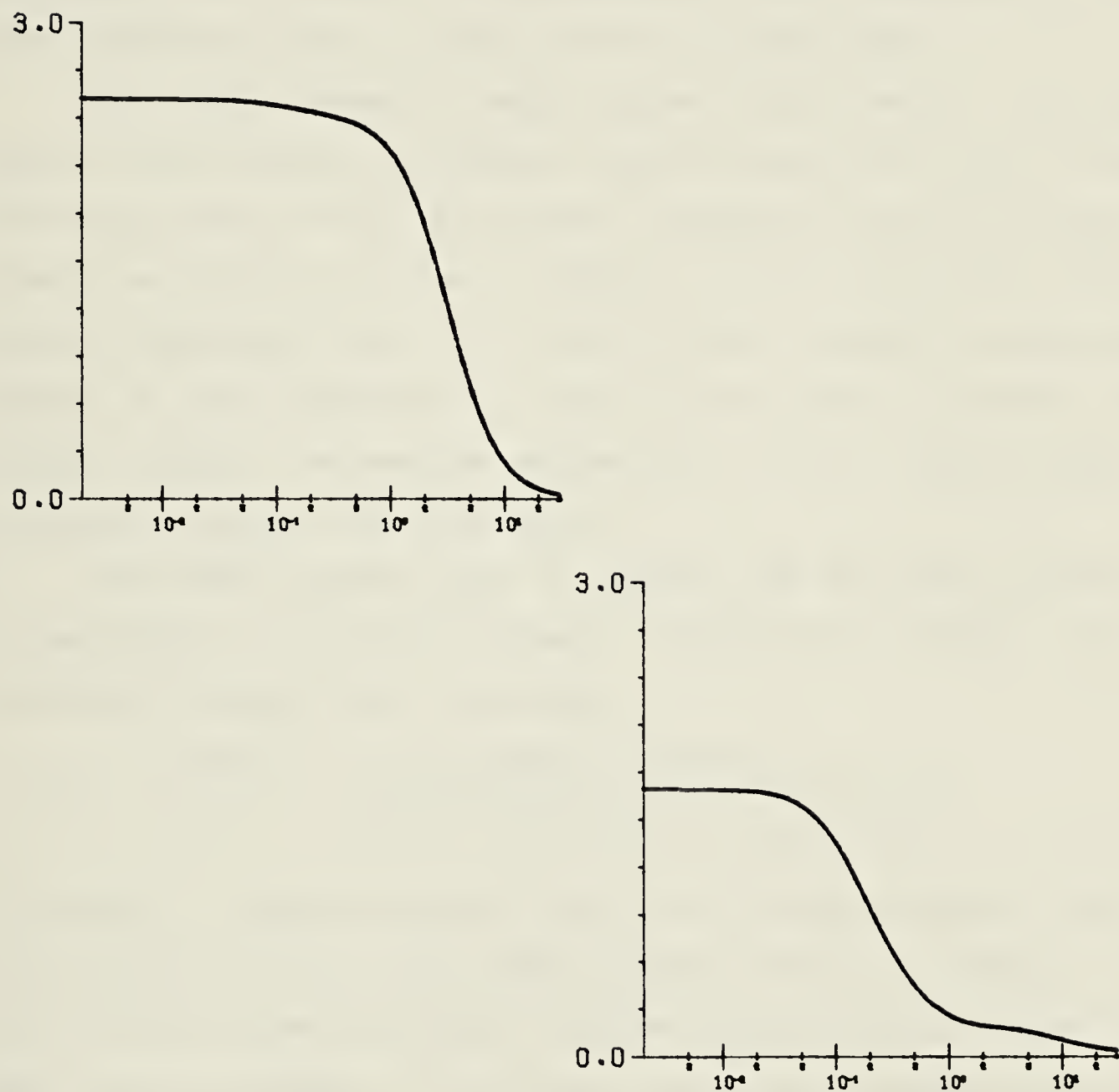


Figure 5.22 Plots of $|k_i h_i(s)| / |1 + k_i h_i(s)|$ for compensated chemical reactor model with $k_1 = k_2 = 1.0$. Frequency range $0.002 < \omega < 30.5$ rad/1000s.

5.4 Distillation column.

The binary pilot scale distillation column in the Department of Chemical Engineering at the University of Alberta has also been the subject of numerous control application studies, e.g. Berry (1973) and Bilec (1979).

Berry (1973) obtained a simple transfer function model of the distillation column by pulse testing. This transfer function model $G(s)$ is given in table 5.8. The model outputs are top and bottom composition, and the inputs are reflux flowrate and flowrate of steam to reboiler. As can be seen from figure 5.23 the return difference matrix $F(s) = I + G(s)$ is matrix dominant. It is not diagonally dominant at low frequencies, but $G(s)$ is both matrix and column diagonally dominant. However, this example illustrates how the NEL design procedure can be applied to systems with time delays.

The transfer functions $h_i(s)$ for systems with time delays become ratios of polynomials in s with non-constant coefficients. For example, $h_2(s)$ is for the distillation column model in table 5.8:

$$h_2(s) = \frac{-19.4e^{-3s}}{14.4s+1} - \frac{-k_1 * 18.9 * 6.6e^{-10s} (16.7s+1)}{(21.0s+1)(10.9s+1)(16.7s+1+k_1 * 12.8e^{-1s})} \quad (5.12)$$

The stability of transfer functions of this form has been studied by Lee (1976), who used basic direct Nyquist stability analysis. Hence, the stability of system with time delays can be analyzed using the Nyquist exact loci (Note: the time delays are easily handled by the computer aided design package, since the TFM manipulations of the NEL design procedure are implemented, not algebraically, but numerically).

Since $G(s)$ is column diagonally dominant initial gain estimates for the simultaneous calculation of the two proportional gains are best selected using Gershgorin circles on the diagonal elements $g_{11}(s)$ and $g_{22}(s)$ of the DNA of $G(s)$. The DNA of $G(s)K_1$, with Gershgorin circles superimposed on the diagonal elements is shown in figure 5.24 with the precompensator

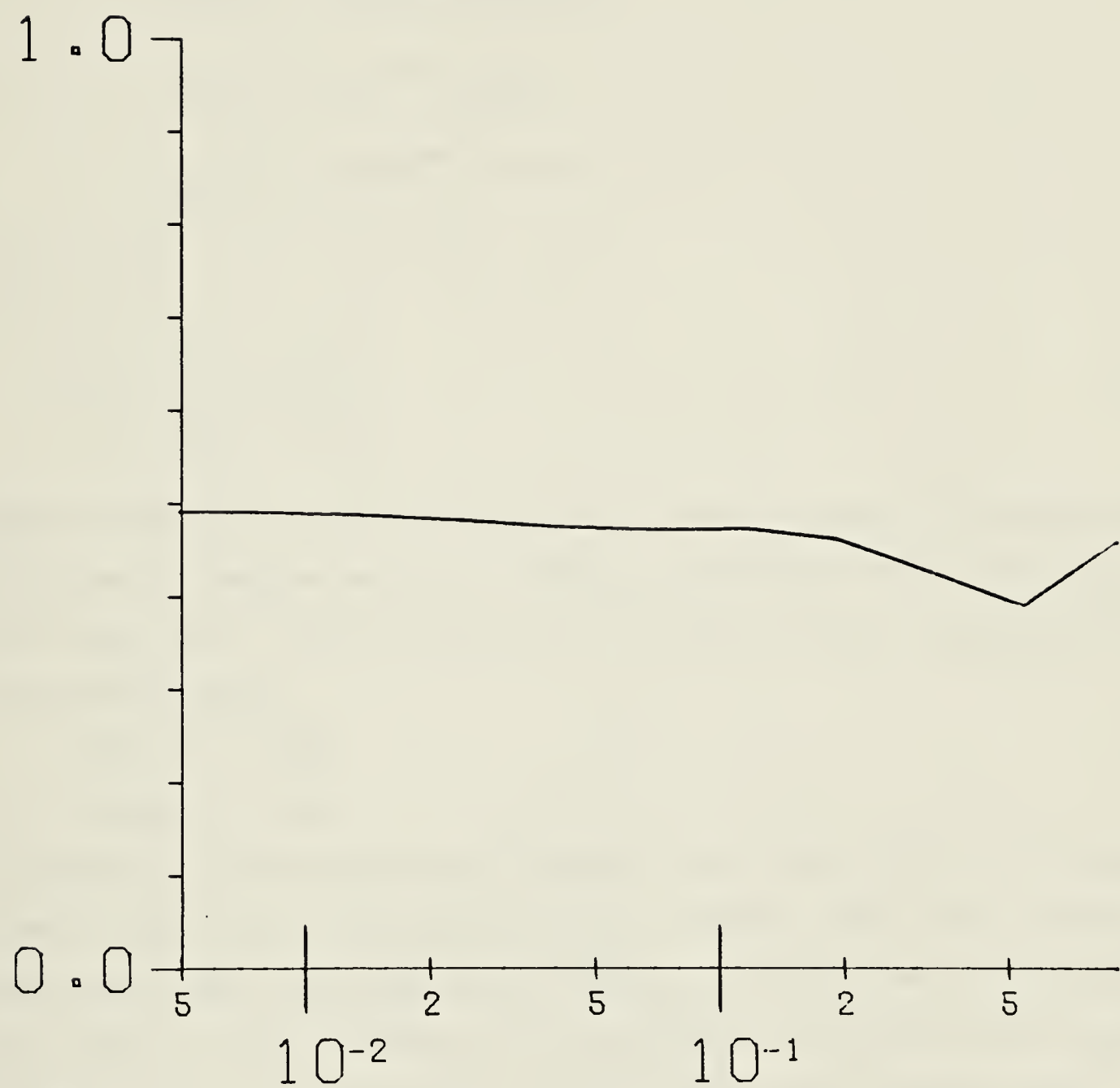


Figure 5.23 Matrix dominance test of $F(s) = I + G(s)$ with the distillation column TFM $G(s)$ from table 5.8.

Table 5.8 TFM model of binary pilot scale distillation column as given by Berry (1973).

$$g_{11}(s) = 12.8e^{-1s}/(16.7s+1)$$

$$g_{12}(s) = -18.9e^{-3s}/(21.0s+1)$$

$$g_{21}(s) = 6.6e^{-7s}/(10.9s+1)$$

$$g_{22}(s) = -19.4e^{-3s}/(14.4s+1)$$

$$K_1 = \begin{bmatrix} 1.0 & 0.0 \\ 0.0 & -1.0 \end{bmatrix} \quad (5.13)$$

Since the distillation column TFM $G(s)$ has no poles or zeros in the closed right half plane, the diagonal elements of $G(s)K_1 K_2$ should give zero encirclements of the critical point $(-1,0)$. This occurs if k_1 and k_2 of $K_2 = \text{diag}\{k_1, k_2\}$ lie in the following ranges

$$0.0 \leq k_1 < 0.89 \quad (5.14)$$

$$0.0 \leq k_2 < 0.25 \quad (5.15)$$

The upper limits were determined from the band swept out by the Gershgorin circles in figure 5.24. Proportional controller constants were then calculated for several gain margin specifications and initial gains of 0.45 and 0.12 respectively. The results of these calculations are summarized in table 5.9. Only calculations number 2 and 3 of table 5.9 do not give large dual resonance peaks in the plots of $|k_1 h_1(s)|/|1+k_1 h_1(s)|$ versus frequency as seen in figures 5.25 and 5.26. The proportional gains of these two calculations are comparable to those used by Wood and Berry (1973) in experimental test on the distillation column. It is not possible to use equations 4.12 to 4.14 due to the nature of the plots in figures 5.25 and 5.26. A large amount of interaction exist in the system, as the size of the coefficients of the sensitivity matrix A from calculation number 2 shows:

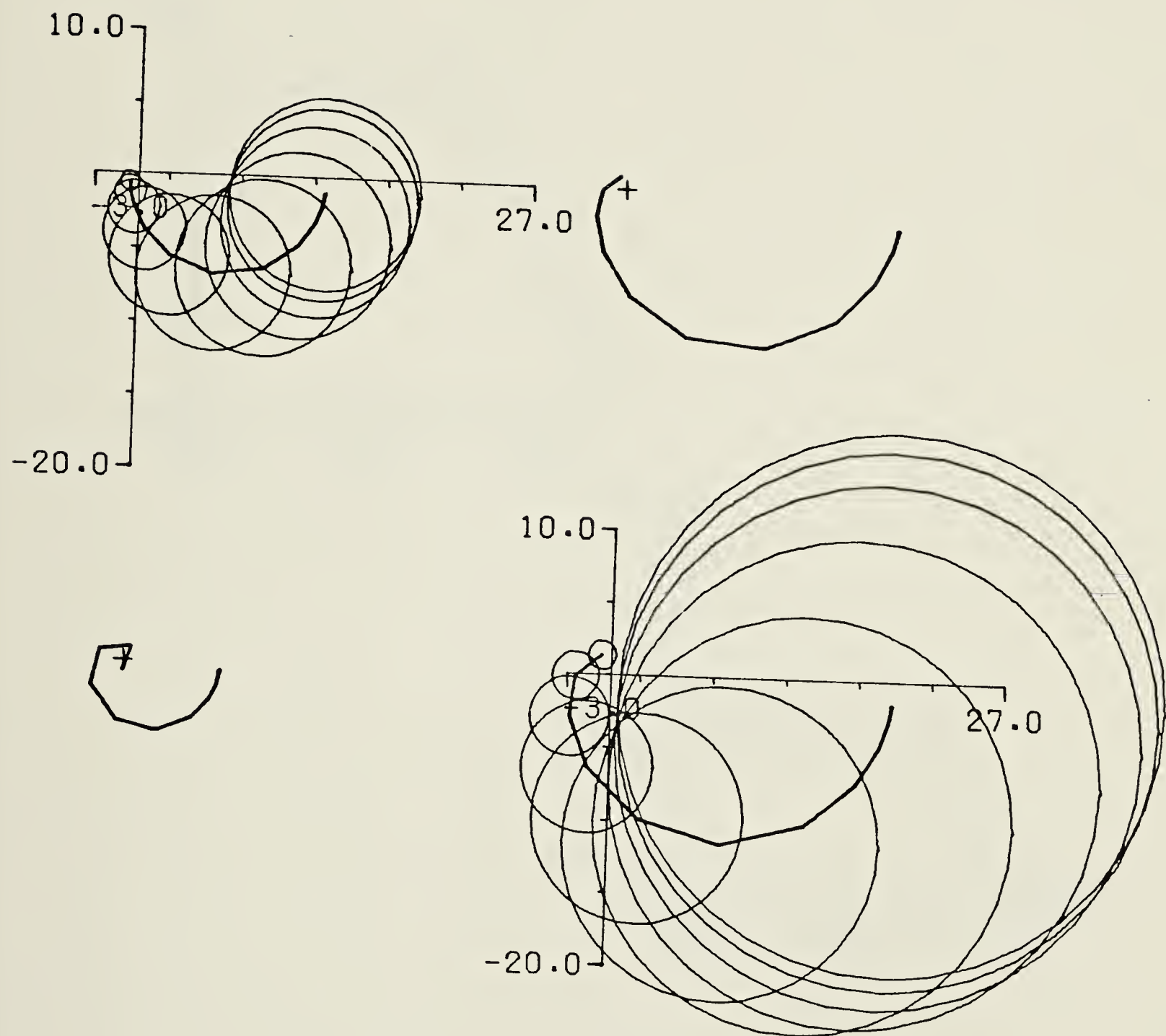


Figure 5.24 DNA of compensated distillation column TFM model with Gershgorin circles, based on column sums, superimposed on the diagonal elements. Frequency range 0.005 – 1.0 rad/s.

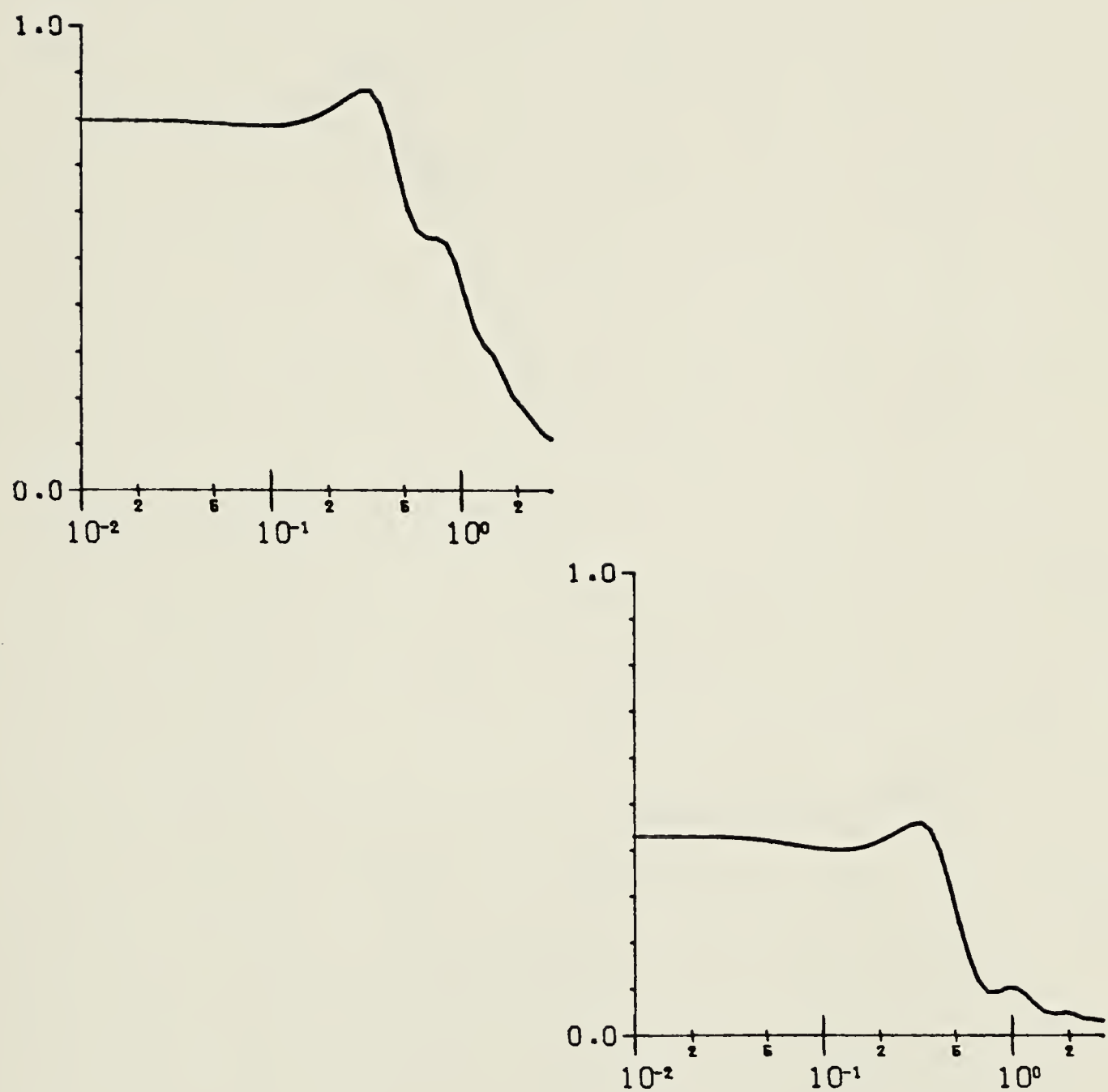


Figure 5.25 Plots of $|k_i h_i(s)| / |1 + k_i h_i(s)|$ versus frequency for compensated distillation column model with proportional gain from calculation number 2 of table 5.9.

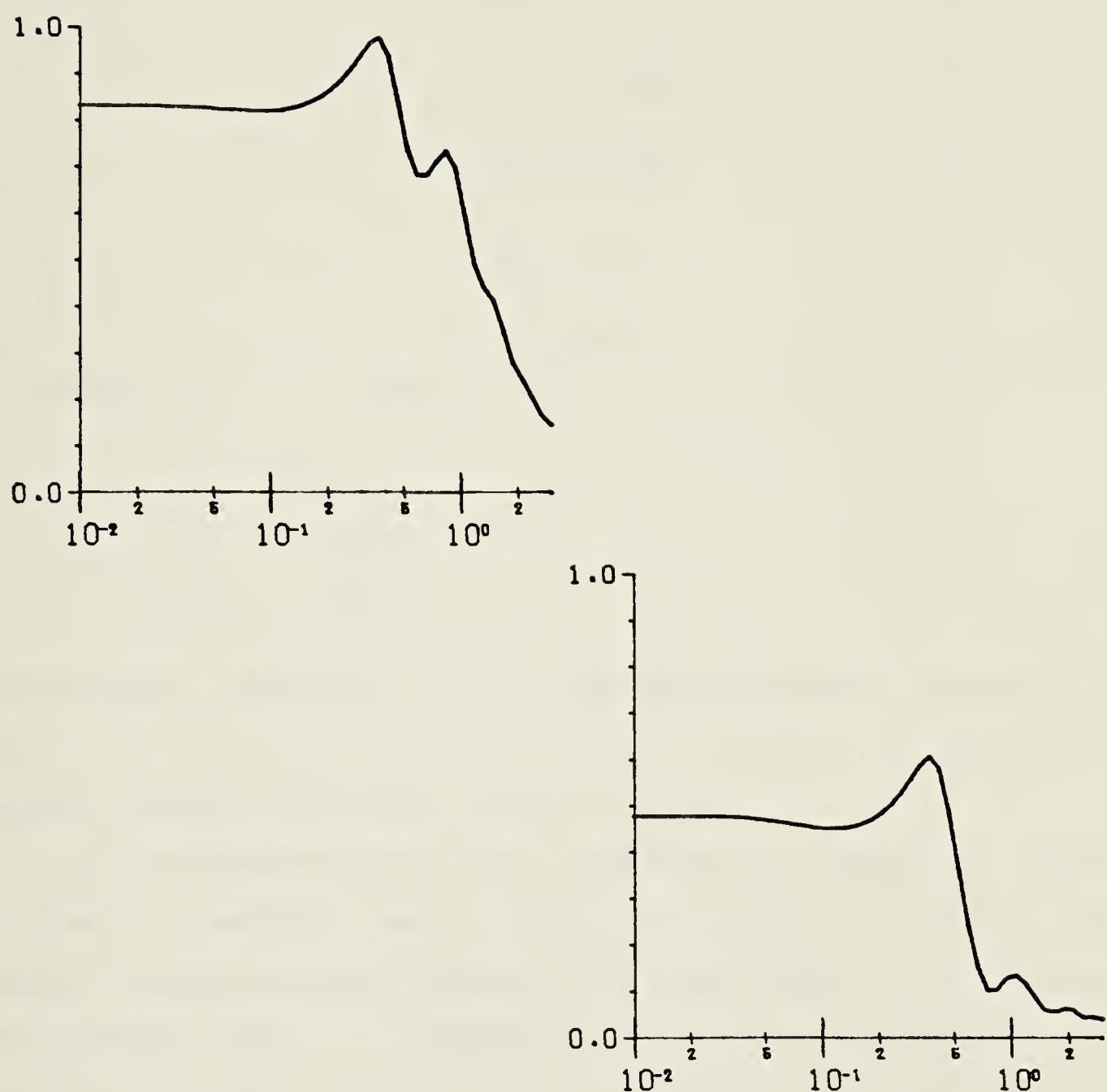


Figure 5.26 Plots of $|k_i h_i(s)| / |1 + k_i h_i(s)|$ versus frequency for compensated distillation column model with proportional gain from calculation number 3 of table 5.9.

Table 5.9 Summary of proportional controller constant calculation for compensated distillation column model $G(s)K_1$.

Calc. no.	gain margins proportional constants				F(s) dominant ?
1	2	2	0.89	0.12	yes
2	3	4	0.56	0.085	yes
3	4	4	0.43	0.068	yes
4	3	2	0.53	0.13	yes
5	4	2	0.40	0.14	yes

$$A = \begin{bmatrix} 0.72 & 0.25 \\ 0.20 & 4.51 \end{bmatrix} \quad (5.16)$$

The proportional controllers will not give tight composition control. If tight control of both compositions are required a dynamic compensator, which essentially decouples the system, must be designed.

The proportional gains of all calculations fall within the ranges of inequalities 5.14 and 5.15, and it is hence not necessary to test for stability using the Nyquist exact loci. However, the Nyquist exact loci with the gains from calculation number 2 of table 5.9 are shown in figure 5.27. It can be seen, that the Nyquist exact loci give no encirclements of the critical point, so the system is asymptotically stable according to theorem 4.1.

An attempt to use the algorithm outlined in section 4.4 to calculate the constants of two proportional plus integral controllers failed. This is probably happening because the crossover frequency is not used in estimating the integral gains. The algorithms of section 4.4 for two constant controller calculation should be modified to estimate integral and derivative gains based on crossover frequency, and then calculate proportional gains to give desired stability margins. Such a modification would eliminate the use of complex derivatives and the

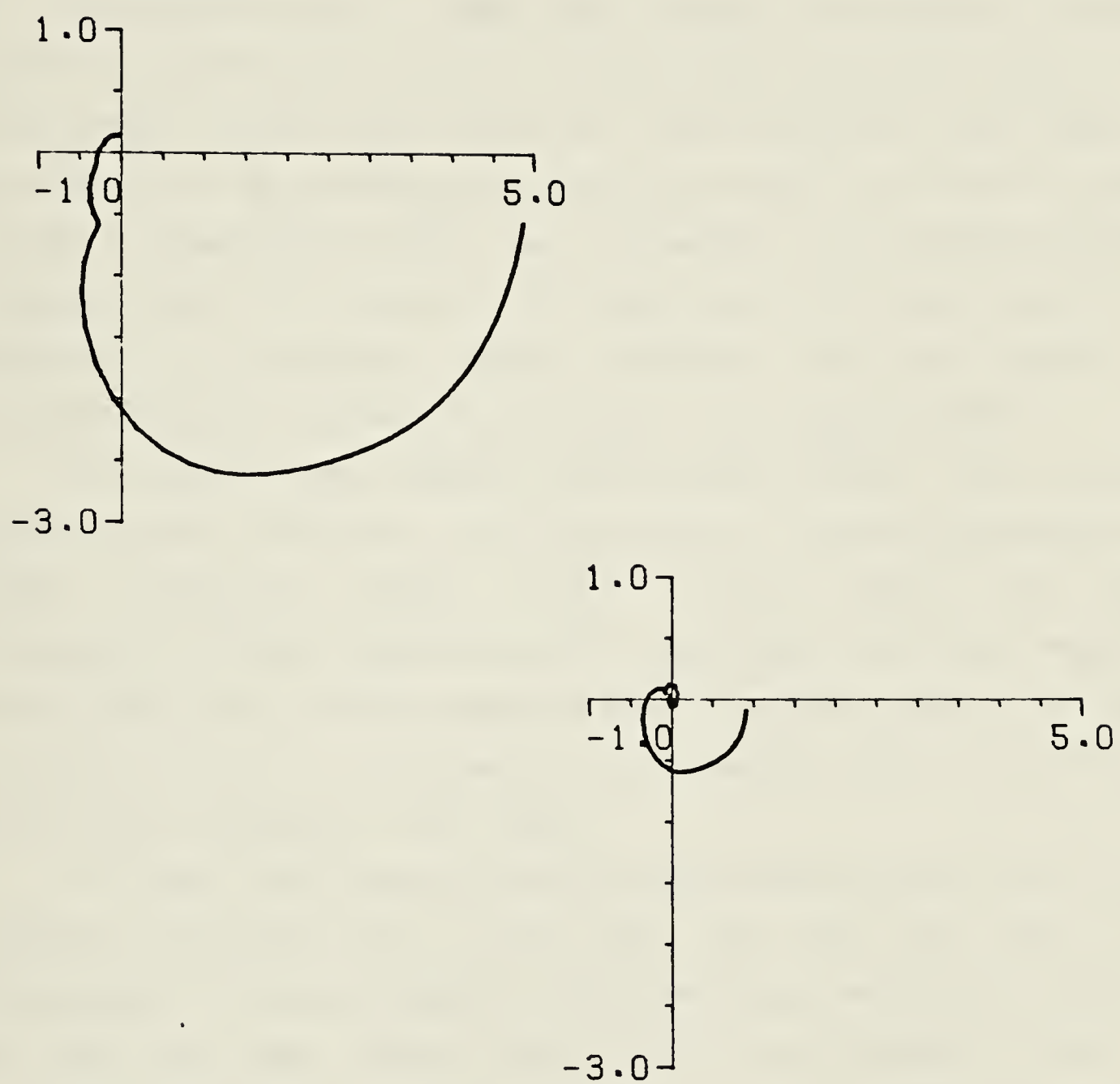


Figure 5.27 Nyquist exact loci for compensated distillation column TFM model with proportional gain from calculation number 2 of table 5.9. Frequency range $0.005 < \omega < 1.0$ rad/min.

mappings of equations 4.20 and 4.22.

5.5 Conclusions.

The Nyquist exact loci (NEL) design technique was applied to design of constant compensator/controllers for a double effect evaporator model, an open loop unstable chemical reactor model, and a binary distillation column model with time delays. The NEL procedure was found to be easy to use, and the resultant constant compensator/controllers were comparable to compensator/controllers designed using other techniques. The Nyquist exact loci were found to be informative in comparing design alternatives, and the absence of Gershgorin/Ostrowski circles made the displays more comprehensible.

The double effect evaporator design example showed, that a continuous transfer function model with a zero order hold is a good approximation to a bilinear transformed discrete transfer function model. The constant compensator/controller designed using NEL was simpler, than those designed by Kuon (1975), due to the less restrictive matrix dominance condition for stability. Simulations showed the compensator/controller designed using NEL performed as well as those designed by Kuon (1975).

The open loop unstable chemical reactor example showed, that a simple constant compensator gave a larger stable gain space, than found by the characteristic loci design procedure. This example also showed the estimate of the stable gain space obtained from the DNA with Gershgorin circles after transfer of dominance is conservative, and it can be enlarged using the NEL design technique.

The binary distillation column example showed, that the NEL design procedure can be applied to systems containing time delays with no difficulty. The proportional gain obtained using the NEL technique were comparable to those used in experimental test on the distillation column by Wood and Berry (1973). This example also showed, that the algorithms for calculating proportional plus integral and proportional plus derivative controllers described in section 4.4 need to be modified to consider the crossover frequency in the estimation of

integral and derivative constants.

6. Conclusions and recommendations.

6.1 Contributions of this work.

The main contributions of this work are:

- i. Analysis of interaction in multivariable control systems with the introduction of a classification of transmittances into: direct, parallel, interaction and disturbance transmittances.
- ii. Critical review of published measures of 'interaction' with a clarification of the difference between interaction and parallel transmittance.
- iii. Definition of matrix dominance as a less restrictive condition for the application of the multivariable Nyquist array stability theorems.
- iv. Development of a graphical test for matrix dominance, which also gives guidance in the design of a compensator for a system, which is not matrix dominant.
- v. Development of a systematic and flexible procedure for transfer of dominance in transfer function matrices of any size.
- vi. Development of the Nyquist exact loci (NEL) design techniques as a direct multivariable parallel to classical SISO control system design.
- vii. Application of the NEL design technique to three different systems, and comparison of the resultant multivariable controller with control systems designed using other methods.

Although not a major contribution this work has also involved the specification and partly implementation of a suite of interactive computer programs for using the NEL, DNA and INA design procedures. The specification of the package is contained in Jensen (1980). The programs were used in this work, and extensively tested during a multivariable control system design exercise in the course Ch.E. 644. Students with no previous exposure to the University of Alberta computing facilities used the programs without difficulty after only a short introduction to the package.

6.2 Further research.

Some recommendations for future research in this area include:

The following three recommendations reflects the trend in multivariable frequency domain design to design compensators to reduce interaction and/or satisfy an abstract condition, like diagonal dominance, and only indirectly consider time domain specifications such as rise time, overshoot and settling time.

- i. Development of algorithms for simultaneous calculation of controller constants in several single loop controllers subject to specified stability margins and to the condition, that the return difference matrix is matrix dominant. A linear programming approach combining the transfer of dominance algorithm of section 3.5 and the simultaneous gain calculation of section 4.4 should definitely be explored.
- ii. Further work should be done in the parallelism between the transfer function $h_i(s)$ and the SISO transfer function $g(s)$, for example the use of derivatives of the Nyquist exact loci as an indicator of interaction propagation should be analyzed further. Any relationship between these derivatives and the closed loop sensitivities should be investigated.
- iii. Development of an algorithm for simultaneous design of several lead - lag elements to give desired shape of the h_i loci.

Other recommendations in the general area of frequency domain control system design include:

- i. Development of a design procedure for the design of multivariable feedforward controllers for nonlinear plants with large parameter variations. The approach taken by Horowitz (1979,1980) to the design of feedback controllers for such systems should be considered for extension.
- ii. Analysis of connections between the transfer functions $h(s)$ and

stability criteria for nonlinear systems should be done, cf. Blight and McClamroch (1977).

- iii. Development of a graphical representation which will provide sufficient conditions for the Popov criterion to hold in the multiloop case for matrix dominant systems. This is an extension to work recently reported by Mees and Atherton (1980).

7. Nomenclature.

7.1 Technical abbreviations.

ADGA	Average Dynamic Gain Array.
CL	Characteristic Loci.
DNA	Direct Nyquist Array.
INA	Inverse Nyquist Array.
NEL	Nyquist Exact Loci.
RDGA	Relative Dynamic Gain Array.
RGA	Relative Gain Array.
SISO	Single-input, single-output.
TFM	Transfer Function Matrix.

7.2 Nomenclature for chapter 1.

e	vector of error signals.
g	transfer function of single-input, single-output system.
G_L	plant load transfer function matrix.
G_p	plant transfer function matrix.
h_i	transfer function between the i'th input and the i'th output when the i'th loop is open and all other loops are closed.
H	feedback transfer function matrix.
I	identity matrix.
K	compensator transfer function matrix.
K	diagonal controller transfer function matrix.
m	vector of manipulated variables.
Q	compensated plant transfer function matrix, $Q = G_p K_1$.
r	vector of reference input variables.
u	vector of compensated plant input variables.
y	vector of plant output variables.
y	vector of measured plant output variables.
η	vector of plant load or disturbance variables.

7.3 Nomenclature for chapter 2.

A	state matrix of state space model.
b; _i	the i'th column of the state space model input matrix B.
B	input matrix of state space model.
B _i	input matrix of state space model without the i'th column.
c; _i	the i'th row of state space model output matrix C.
c _{ij}	cofactor of element (i,j) of the return difference matrix.
C	output matrix of state space model.
C _i	output matrix of state space model without the i'th row.
D(t)	matrix of average dynamic gains calculated by integrating step responses over a time interval t = t ₂ - t ₁ .
F = {f _{ij} }	return difference transfer function matrix.
G _L = {g ^L _{ji} }	plant load transfer function matrix.
G = {g _{ij} }	plant transfer function matrix.
h; _i	transfer function between the i'th input and the i'th output when the i'th loop is open and all other loops are closed.
I _i	interaction coefficient as defined by Suchanti and Fournier for the i'th loop.
(IE); _i	the error integral of the i'th output for a unit step change in the i'th input with loop i closed and all other loops open.
(IĒ); _i	the error integral of the i'th output for unit step changes in all inputs with all loops closed.
H={h _{ij} }	feedback transfer function matrix.
K ₁ ={k _{ij} }	compensator transfer function matrix.
K ₂ =diag{k _{ij} }	controller transfer function matrix.
L; _i	parallel transmittance between the i'th input and the i'th output when the i'th loop is open and all other loops are closed.
M={μ _{ij} }	steady state relative gain array.
M(s)={μ _{ij} (s)}	relative dynamic gain array.
M(t)={μ _{ij} (t)}	average dynamic gain array.
M _{ij} =I+B _j (C _i B _j) ⁻¹ C _i	matrix used in definition of relative transient response functions.

$Q = \{q_{ij}\}$	compensated plant transfer function matrix.
$\hat{Q} = \{\hat{q}_{ij}\}$	inverse compensated plant transfer function matrix.
Q'_j	minor of $Q(s)K_2(s)$ formed by deleting all rows except row i and all columns except column j.
$r = \{r_i\}$	vector of reference input variables.
$R = \{r_{ij}\}$	closed loop transfer function matrix.
$R_L = \{r_{Lij}\}$	closed loop load transfer function matrix.
$R' = \{r'_{Lij}\}$	transfer function matrix for system with all but one feedback loop closed.
$R'_L = \{r'_{Lij}\}$	load transfer function matrix for system with all but one feedback loop closed.
$S = \text{diag}\{s_i\}$	feedback TFM with $s_i=0$ for $i=j$, and $s_i=1$ for $i \neq j$.
$u = \{u_i\}$	vector of compensated plant inputs.
$u(k)$	vector of inputs to discrete state space model.
$y = \{y_i\}$	vector of plant output variables.
$y(k)$	vector of outputs from discrete state space model.
$x(k)$	vector of states of discrete state space model.
κ	interaction coefficient as defined by Rijnsdorp (1965).
κ_i	extended interaction coefficient for the i'th input-output pair of a $m \times m$ multivariable system.
$\xi = \{\xi_i\}$	vector of load or disturbance variables.
Φ_{ij}	the relative transient response function between the j'th input and the i'th output.
ϕ_{ij}	the ratio of the cofactor of element (i,j) to the cofactor of element (i,i) of the return difference matrix.
ψ_{ij}	the ratio of the cofactor of element (i,j) to the cofactor of element (i,i) of the compensated plant transfer function matrix.
ω	the continuous frequency.

7.4 Nomenclature for chapter 3.

$A = \{a_{ij}\}$	real matrix with positive diagonal elements and nonpositive offdiagonal elements.
A	coefficients of constraint equations of general linear programming problem.
$B = \{b_{ij}\}$	companion matrix of a complex matrix, $b_{ii} = q_{ii} $ and $b_{ij} = -iq_{ij}$ for $i \neq j$.
$C = \{c_{ij}\}$	real matrix with diagonal elements zero, and offdiagonal elements nonnegative.
d_i^r	element of diagonal similarity transformation matrix, which will make the system row diagonal dominant.
$D = \text{diag}\{d_i\}$	diagonal similarity transformation matrix.
F	return difference matrix.
$g(x)$	function of decision variables in general linear programming problem.
G	plant transfer function matrix.
h_i	transfer function between the i 'th input and the i 'th output when the i 'th loop is open and all other loops are closed.
J	function to be maximized in transfer of dominance or general linear programming problem.
$N = \{n_{ij}\}$	polynomial transfer function matrix.
N_{ij}^c	real numbers, which are indicators of column matrix dominance.
N_{ij}^r	real numbers, which are indicators of row matrix dominance.
P_i	sum of off-diagonal elements of row i of a matrix.
$Q = \{q_{ij}\}$	complex matrix.
R_i	sum of off-diagonal elements of column i of a matrix.
x_i	vector of decision variables in general linear programming problem.
$W = \text{diag}\{w_i\}$	diagonal matrix with positive diagonal elements.
β_i	weighting factor for i 'th row or i 'th column in transfer of

dominance.

Γ_i function obtained by mapping of the Nyquist D -contour by q_{ii} .

Θ^r normalized minimal Gershgorin radius as calculated by Kantor and Andres method.

ω continuous frequency.

7.5 Nomenclature for chapter 4.

$A = \{a_{ij}\}$ matrix of derivatives of the Nyquist exact loci with respect to the controller gains.

$b = \{b_i\}$ vector of the distances the Nyquist exact loci are from their desired locations.

$G(s), G(z), \text{ or } G(w)$ plant transfer function matrix.

$G_h(s)$ continuous transfer function of a zero order hold.

h_i transfer function between the i 'th input and the i 'th output of a multivariable system in which the i 'th loop is open and all other loops are closed.

k_{D_i} derivative gain in the i 'th loop.

k_{I_i} integral gain in the i 'th loop.

k_{P_i} proportional gain in the i 'th loop.

K_1 compensator transfer function matrix.

$K_2 = \text{diag}\{k_i\}$ controller transfer function matrix.

M $|k_i h_i| / |1 + k_i h_i|$ at the resonance frequency.

n_{h_i} number of clockwise encirclements of the critical point $(-1, 0)$ by the Nyquist exact loci of $k_i h_i$.

p_o number of poles of the open loop transfer function matrix in the closed right half plane.

$Q = \{q_{ij}\}$ compensated plant transfer function matrix.

R_B band around the Nyquist loci of q_{ii} within which the loci of the transfer function h_i lies.

t_r rise time.

t_{s1}	settling time to within 1% of the final value.
T	sampling time.
v	discrete frequency.
$x=\{x_i\}$	vector of controller gain increments.
α	relaxation factor used in updating the controller gains.
γ	overshoot.
∇_{h_i}	function obtained by the mapping of the Nyquist D -contour by h_i .
ω	continuous frequency.
ω_b	frequency at which $ k_i h_i / 1+k_i h_i = 0.707$, the bandwidth.
ω_x	frequency at which $ k_i h_i / 1+k_i h_i = 0.5$.
Φ_{ij}	cofactor of element (i,j) of the return difference matrix divided by the cofactor of element (i,i) of the return difference matrix.

7.6 Nomenclature for chapter 5.

d	characteristic polynomial of transfer function matrix.
F	return difference matrix.
FD0320	constant compensator/controller designed by Kuon (1975) to give a gain margin of 5.
FD0330	constant compensator/controller designed by Kuon to give gain margins of 3.3.
$G=\{g_{ij}\}$	plant transfer function matrix.
h_i	transfer function between the i 'th input and the i 'th output of a multivariable system in which the i 'th loop is open and all other loops are closed.
K_1	constant compensator matrix.
$K_2=\text{diag}\{k_i\}$	proportional controller gains.
$N=\{n_{ij}\}$	polynomial part of a transfer function matrix with a common denominator of all elements.
N_{ij}^c	real numbers, which are indicators of column matrix

dominance.

N_{ij}^r real numbers, which are indicators of row matrix dominance.

8. References

- Ahson,S.I.,and Nicholson,N., 'Improvement of turbo-alternator response using the inverse Nyquist array method', 1976, Int. J. Control, **23**, 657-672.
- Araki,M.,and Nwokah,O.I., 'Bounds for closed-loop transfer functions of multivariable systems', 1975, IEEE Trans. on Automatic Control, AC-20, 666-670.
- Belletrutti,J.J., 'Theory and design of multivariable feedback systems', 1972, Ph.D.-Thesis, University of Manchester Institute of Science and Technology, Manchester, England.
- Blight,J.D.,and McClamroch,N.H., 'Graphical stability criteria for nonlinear multiloop systems', 1977, Automatica, **13**, 189-192.
- Bristol,E.H., 'On a new measure of interaction for multivariable process control', 1966, IEEE Trans. on Automatic Control, AC-11, 133-134.
- Bristol,E.H., 'A philosophy for single loop controllers in a multiloop world', 1968, 8th ISA Symp. on Instrumentation in the Chemical and Petroleum Industries, St.Louis, Missouri, 19-29.
- Bristol,E.H., 'RGA 1977: Dynamic effects of interaction', 1977, 16th IEEE Conf. on Decision and Control, New Orleans, Louisiana, 1096-1100.
- Bristol,E.H., 'Recent results on interaction in multivariable process control', 1978, 71st A.I.Ch.E. Annual Meeting, Miami, Florida.
- Bristol,E.H., 'Multivariable control: The analysis of interaction', 1979, private communication.
- Clement,C., 'Fixed bed reactor control and dynamics', 1980, Ph.D.-Thesis, Technical University of Denmark, Lyngby, Denmark.
- Davison,E.J., 'A nonminimum phase index and its application to interacting multivariable control systems', 1969, Automatica, **5**, 791-799.
- Davison,E.J.,and Man,F.T., 'Interaction index for multivariable control systems', 1970, Proc. IEE, **117**, 459-462.
- Fiedler,M.,and Ptak,V., 'On matrices with non-positive off-diagonal elements and positive principal minors', 1962, Czech. Math. J., **12**, 382-400.
- Fiedler,M.,and Ptak,V., 'Some results on matrices of class K and their application

- to the convergence rate of iteration procedures', 1966, Czech. Math. J., **16**, 260-273.
- Fiedler,M.,and Ptak,V., 'Diagonally dominant matrices', 1967, Czech. Math. J., **17**, 420-433.
- Fisher,D.G.,and Seborg,D.E., 'Multivariable computer control - a case study', 1976, North-Holland/American Elsevier, New York.
- Foss,A.S., 'Critique of chemical process control theory', 1973, A.I.Ch.E. Journal, **19**, 209-214.
- Franklin,G.F.,and Powell,J.D., 'Digital control of dynamic systems', 1980, Addison-Wesley Publishing Company, Reading, Massachusetts.
- Gagnepain,J.-P.,and Seborg,D.E., 'An analysis of process interactions with applications to multiloop control system design', 1979, 72nd A.I.Ch.E. Annual Meeting, San Francisco, California.
- Hung,N.T.,and Anderson,B.D.O., 'Triangularization technique for the design of multivariable control systems', 1979, 17th IEEE Conf. on Decision and Control, San Diego, California.
- Horowitz,I.M., 'Synthesis of feedback systems', 1963, Academic Press, New York, New York.
- Horowitz,I.M.,and Shaked,U., 'Superiority of transfer function over state-variable methods in linear time-invariant feedback system design', 1975, IEEE Trans. on Automatic Control, AC-20, 84-97.
- Horowitz,I., 'Quantitative synthesis of uncertain multiple input-output feedback system', 1979, Int. J. Control., **30**, 81-106.
- Horowitz,I., Golubev,B.,and Kopelman,T., 'Flight control design based on nonlinear model with incertain parameters', 1980, IEEE Trans. on Automatic Control, to be published.
- Jaaksoo,O., 'Interaction analysis in multivariable control system design', 1979, 2nd IFAC/IFIP Symp.on Software for Computer Control, Prague, Czechoslovakia, A-XXV-1 - A-XXV-5.
- Jensen,N., 'Requirements contract and external requirements specification for MULCON', 1980, Research Report 801201, Dept. of Chem. Eng., Univ. of Alberta, Edmonton, Alberta, Canada.

- Johnson,C.R., 'Hadamard products of matrices', 1974, Linear and Multilinear Algebra, **1**, 295-307.
- Kantor,J.C.,and Andres,R.P., 'A note on the extension of Rosenbrock's Nyquist array techniques to a larger class of transfer function matrices', 1979, Int J. Control, **30**, 387-393.
- Kominek,K.W.,and Smith,C.L., 'Analysis of system interaction', 1979, 86th A.I.Ch.E. National Meeting, Houston, Texas.
- Kuon,J.F., 'Multivariable frequency-domain design techniques', 1975, Ph.D.-Thesis, University of Alberta, Edmonton, Canada.
- Lee,E.B., 'Stability of linear multivariable feedback systems with time lags', 1976, in 'Control theory and topics in functional analysis: lectures presented at an international course at Trieste from 11. Sept. to 29. Nov. 1974', Vienna, IAEA.
- Lee,W.,and Weekman,V.W., 'Advanced control practice in the chemical process industry: A view from industry', 1976, A.I.Ch.E. Journal, **22**, 27-38.
- Leininger,G.G., 'The multivariable Nyquist array: The concept of dominance sharing', 1978, in Sain,M.K.,et al (Editors), 'Alternatives for linear multivariable control', National Engineering Consortium, Chicago, Illinois.
- Leininger,G.G., 'Diagonal dominance for multivariable Nyquist array methods using function minimization', 1979a, Automatica, **15**, 339-345.
- Leininger,G.G., 'New dominance characteristics for the multivariable Nyquist array method', 1979b, Int. J. Control, **30**, 459-475.
- MacFarlane,A.G.J., 'Notes on the vector frequency response approach to the analysis and design of multivariable feedback systems', 1972, UMIST, Manchester, England.
- MacFarlane,A.G.J.,and Bellettrutti,J.J., 'The characteristic locus design method', 1973, Automatica, **9**, 575-588.
- MacFarlane,A.G.J.,and Kouvaritakis,B., 'A design technique for linear multivariable feedback systems', 1977, Int. J. Control, **25**, 837-874.
- MacFarlane,A.G.J. (editor), 'Frequency-response methods in control systems', 1979, IEEE Press, New York.
- Mayne,D.Q., 'The design of linear multivariable systems', 1972, 5th IFAC World

- Congress, Paris, France.
- Mayne,D.Q., 'The design of linear multivariable systems', 1973, Automatica, **9**, 201-207.
- Mayne,D.Q., 'The effect of feedback on linear multivariable systems', 1974, Automatica, **10**, 405-412.
- Mee,D.H., 'Specification and criteria for multivariable control system design', 1976, Joint Automatic Control Conference, Purdue, Indiana, 627-633.
- Mees,A.I.,and Atherton,D.P., 'The Popov criterion for multiple-loop feedback systems', 1980, IEEE Trans. on Automatic Control, **AC-25**, 924-928.
- Niederlinski,A., 'A heuristic approach to the design of linear multivariable interacting control systems', 1971, Automatica, **7**, 691-701.
- Nisenfeld,A.E., 'Applying control computers to an integrated plant', 1973, Chem. Eng. Progr., **69**(9), 45-48.
- Nwokah,O.D.I., 'The convergence and local minimality of bounds for transfer functions', 1979, Int. J. Control, **30**, 195-202.
- Nwokah,O.D.I., 'A note on the stability of multivariable systems', 1980a, Int. J. Control, **31**, 587-592.
- Nwokah,O.D.I., 'A recurrent issue on the extended Nyquist array', 1980b, Int. J. Control, **31**, 609-614.
- Ostrowski,A., 'Über die Determinanten mit überwiegender Hauptdiagonale', 1937, Commentarii Mathematici Helvetici, **10**, 69-96.
- Ostrowski,A., 'Determinanten mit überwiegender Hauptdiagonale und die absolute Konvergenz von linearen Iterationsprozessen', 1956, Commentarii Mathematici Helvetici, **30**, 175-210.
- Rijnsdorp,J.E., 'Interaction in two-variable control systems for distillation columns - Part I', 1965, Automatica, **3**, 15-28.
- Rosenbrock,H.H., 'Design of multivariable control systems using the inverse Nyquist array', 1969, Proc. IEE, **116**, 1929-1936.
- Rosenbrock,H.H., 'The stability of multivariable systems', 1972, IEEE Trans. on Automatic Control, **AC-17**, 105-107.
- Rosenbrock,H.H. 'Computer aided control system design', 1974, Academic Press, London.

- Stainthorp,F.P., 'A simple method of arriving at control structures for multivariable systems', 1972, Measurement and Control, **5**, 284-287.
- Suchanti,N.C.,and Fournier,C.D., 'A new algorithm for pairing manipulated and controlled variables', 1973, 14th ISA Symp. on Instrumentation in the Chemical and Petroleum Industries, St.Louis, Missouri, 67-72.
- Taiwo,O., 'Improvement of turbo-alternator response by the method of inequalities', 1976, Int. J. Control, **27**, 305-311.
- Tung,L.S.,and Edgar,T.F., 'Dynamic interaction analysis and its application to distillation column control', 1977, 16th IEEE Conf. on Decision and Control, New Orleans, Louisiana, 1107-1112.
- Tung,L.S.,and Edgar,T.F., 'Analysis of control - output interactions in dynamic systems', 1978, 71st A.I.Ch.E. Annual Meeting, Miami, Florida.
- Witcher,M.F.,and McAvoy,T.F., 'Interacting control systems: steady state and dynamic measurement of interaction', 1977, ISA Trans., **16**(3), 35-41.
- Wood,R.K.,and Berry,M.W., 'Terminal composition control of a binary distillation column', 1973, Chem. Eng. Sci., **28**, 1707-1717.

9. Appendices

9.1 Appendix A. Derivation of $h_i(s)$.

In this appendix expressions for the transfer function $h_i(s)$ between the i 'th input and the i 'th output when the i 'th loop is open and all other loops are closed are derived.

Consider the multivariable system represented by the block diagram in figure 9.1. $Q(s)K_2(s)$ is the open loop transfer function matrix and S is a diagonal feedback matrix, defined by $S = \text{diag}\{s_k\}$, $k = 1, \dots, m$ with $s_i = 0$ and $s_k = 1$, $k \neq i$, i.e. the i 'th feedback loop is open. The closed loop transfer function for this system is

$$H'(s) = (I + Q(s)K_2(s)S)^{-1} Q(s)K_2(s) = \frac{1}{\det(I + Q(s)K_2(s)S)} \{c'_{ij}(s)\}^T Q(s)K_2(s) \quad (9.1)$$

where $\det(\cdot)$ denotes the determinant, and $c'_{ij}(s)$ is the (i,j) 'th cofactor of $I + Q(s)K_2(s)S$. The sought transfer function $h_i(s)$ is the (i,i) 'th element of $H'(s)$, hence

$$h_i(s) = h'_{ii}(s) = \frac{1}{\det(I + Q(s)K_2(s)S)} \sum_{j=1}^m c'_{ji}(s) q_{ji}(s) \quad (9.2)$$

The matrices $I + Q(s)K_2(s)S$ and $I + Q(s)K_2(s)$ only differ in the i 'th column. This means all cofactors of the i 'th column of $I + Q(s)K_2(s)S$ are the same as the cofactors of the i 'th column of $I + Q(s)K_2(s)$. Denoting the cofactors of $I + Q(s)K_2(s)$ by $c_{ij}(s)$ (no prime), then

$$\sum_{j=1}^m c_{ji}(s) q_{ji}(s) = \sum_{j=1}^m c'_{ji}(s) q_{ji}(s) \quad (9.3)$$

Furthermore, Laplace expansion of the determinant of $I + Q(s)K_2(s)S$ along the i 'th column gives

$$\det(I + Q(s)K_2(s)S) = c_{ii}(s) = c'_{ii}(s) \quad (9.4)$$

since only the i 'th element of the i 'th column of $I + Q(s)K_2(s)S$ is different from zero. This element is one. Hence the expression for $h_i(s)$ becomes

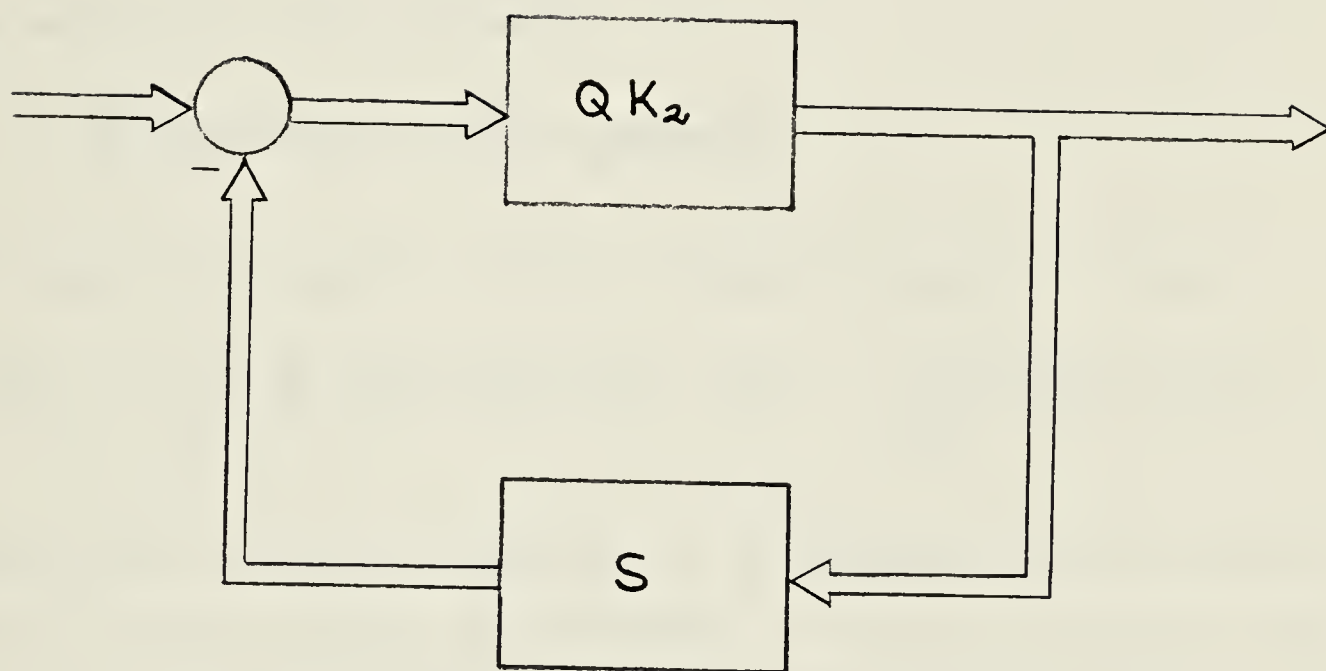


Figure 9.1 Blockdiagram of multivariable system with open loop transfer function matrix $Q(s)K(s)$, and feedback matrix $S = \text{diag}\{s_k\}$, $s_i=0$, $s_k=1$, $k \neq i$, i.e. all loops except the i 'th loop are closed.

$$h_i(s) = \frac{1}{c_{ii}(s)} \sum_{j=1}^m c_{ji}(s) q_{ji}(s) = q_{ii}(s) + \sum_{\substack{j=1 \\ j \neq i}}^m \phi_{ji}(s) q_{ji}(s) \quad (9.5)$$

The above expression gives $h_i(s)$ in terms of column sums. An equivalent expression can be established in terms of row sums. Laplace expansion of the determinant of $I+Q(s)K_2(s)$ along the i 'th column and along the i 'th row gives

$$\det(I+Q(s)K_2(s)) = c_{ii}(s) + \sum_{j=1}^m c_{ji}(s) k_i(s) q_{ji}(s) = c_{ii}(s) + \sum_{j=1}^m c_{ij}(s) k_j(s) q_{ij}(s) \quad (9.6)$$

The substitution of the relationship

$$\sum_{j=1}^m c_{ji}(s) k_i(s) q_{ji}(s) = \sum_{j=1}^m c_{ij}(s) k_j(s) q_{ij}(s) \quad (9.7)$$

into equation 9.5 gives the following alternative expression for $h_i(s)$:

$$h_i(s) = \frac{1}{c_{ii}(s)} \sum_{j=1}^m c_{ij}(s) k_j(s) q_{ij}(s) / k_i(s) = q_{ii}(s) + \sum_{\substack{j=1 \\ j \neq i}}^m \phi_{ij}(s) k_j(s) q_{ij}(s) / k_i(s) \quad (9.8)$$

Equations 9.5 and 9.8 are equivalent to the inductively derived equations (5.18) of Kuon (1975). However, the normalization of the return difference matrix used by Kuon is unnecessary, and in equation (5.18e) the transpose sign should be removed.

Note also, the above $h_i(s)$ is different from the $h_i(s)$ introduced by Rosenbrock (1972). Rosenbrock used $h_i(s)$ as the transfer function between the i 'th input and the i 'th output with loops $1, \dots, i-1$ closed and loops i, \dots, m open.

9.2 Appendix B. Cofactor equivalence.

In this appendix it is shown, that the ratio of cofactors of the return difference matrix $F(s)$ approach the corresponding ratio of cofactors of the compensated plant transfer function matrix $Q(s)$ in the limit of high feedback gains.

2×2 system: Consider the matrices $Q(s)$ and $F(s)$ for a 2×2 system

$$Q(s) = \begin{bmatrix} q_{11} & q_{12} \\ q_{21} & q_{22} \end{bmatrix} \quad F(s) = \begin{bmatrix} 1 + k_1 q_{11} & k_2 q_{12} \\ k_1 q_{21} & 1 + k_2 q_{22} \end{bmatrix} \quad (9.9)$$

with the following ratios of cofactors respectively

$$\Psi_{12} = -q_{21}/q_{22} \quad \Phi_{12} = -k_1 q_{21}/(1 + k_2 q_{22}) \quad (9.10)$$

$$\Psi_{21} = -q_{12}/q_{11} \quad \Phi_{21} = -k_2 q_{12}/(1 + k_1 q_{11}) \quad (9.11)$$

Hence, if $k = k_1 = k_2$, and $k \rightarrow \infty$ then

$$\lim \Phi_{12} = \Psi_{12} \quad \lim \Phi_{21} = \Psi_{21} \quad (9.12)$$

3×3 system: Consider the ratios of cofactors of element (1,2) of a 3×3 system. These are respectively

$$\Psi_{12} = \frac{q_{21}q_{33} - q_{23}q_{31}}{q_{22}q_{33} - q_{23}q_{32}} \quad (9.13)$$

and

$$\Phi_{12} = \frac{k_1 k_3 (q_{21}q_{33} - q_{23}q_{31}) + k_1 q_{21}}{k_2 k_3 (q_{22}q_{33} - q_{23}q_{32}) + 1 + k_2 q_{22} + k_3 q_{33}} \quad (9.14)$$

Hence, if $k = k_1 = k_2 = k_3$, and $k \rightarrow \infty$ then

$$\lim_{k \rightarrow \infty} \Phi_{12} = \Psi_{12} \quad (9.15)$$

and similarly for the other cofactor ratios.

$m \times m$ system: Let $K_2 = kl$, and $k \rightarrow \infty$ then in the ratio of cofactors of $I + kIQ$ only those elements with k^{m+1} as a common factor will not vanish in the limit, but those elements are exactly the ratio of cofactors of kIQ . However,

the ratio of cofactors of kIQ and Q are identical, since the minors of kI cancel out.

9.3 Appendix C. Proof of theorems 3.1 and 3.3.

In this appendix proofs are given of theorems 3.1 and 3.3 of chapter 3.

Proof of theorem 3.1: Let $A = \{a_{ij}\}$ be the companion matrix of Q , then according to the definition of matrix dominance A is an M-matrix, and according to theorem 4.3 of Fiedler and Ptak (1962), there exist a diagonal matrix $D = \text{diag}\{d_i\}$, with $d_i > 0$ for all i , such that AD is row diagonally dominant, i.e. for $i = 1, \dots, m$

$$|q_{ii}|d_i > \sum_{\substack{j=1 \\ j \neq i}}^m |q_{ij}|d_j \quad (9.16)$$

This implies that

$$|q_{ii}| > \sum_{\substack{j=1 \\ j \neq i}}^m |q_{ij}|(d_j/d_i) \quad (9.17)$$

The last inequality implies $D^{-1}QD$ is row diagonally dominant. This proves the theorem.

Proof of theorem 3.3: Diagonal dominance of $D^{-1}QD$ implies, that for $i = 1, \dots, m$

$$|q_{ii}| > \sum_{\substack{j=1 \\ j \neq i}}^m |q_{ji}|(d_i/d_j) \quad (9.18)$$

for column diagonal dominance, and

$$|q_{ii}| > \sum_{\substack{j=1 \\ j \neq i}}^m |q_{ij}|(d_j/d_i) \quad (9.19)$$

for row diagonal dominance. These are equivalent to respectively

$$|q_{ii}|(1/d_i) - \sum_{\substack{j=1 \\ j \neq i}}^m |q_{ji}|(1/d_j) > 0 \quad (9.20)$$

and

$$|q_{ii}|d_i - \sum_{\substack{j=1 \\ j \neq i}}^m |q_{ij}|d_j > 0 \quad (9.21)$$

Now let $x^t = \{d_1, \dots, d_i, \dots, d_m\}$ and $y^t = \{1/d_1, \dots, 1/d_i, \dots, 1/d_m\}$. Then inequalities 9.20 and 9.21 can be rewritten as:

$$A^T y > 0 \quad (9.22)$$

and

$$A x > 0 \quad (9.23)$$

where A is the companion matrix of Q . Since Q is row (column) diagonally dominant, then A^T (A) is an M-matrix (or a matrix of class K), and a solution y (x) to inequalities 9.22 and 9.23 always exist (theorem 4.3 of Fiedler and Ptak (1962)). The sought matrix D is then the matrix with the elements of y (x) as diagonal elements, and the duality theorem is proven.

9.4 Appendix D. Nyquist contours and encirclements.

In this appendix the modified Nyquist contours in the s-plane, z-plane and w-plane are described and the mapping of a pure integrator is described in the three planes.

The Nyquist contour in the s-plane, shown in figure 9.2 and consisting of the imaginary axis and a large semicircle in the right half plane, must be modified if the system has poles on the imaginary axis. The modified Nyquist contour in the s-plane consist of a large semicircle in the right half plane and the imaginary axis with small semicircles around the poles on the axis. The small semicircles can be drawn either to the right or to the left of the imaginary axis, thus giving rise to the two different modified Nyquist contours shown in figure 9.3. The contour in figure 9.3a with small semicircles to the right of the imaginary axis is known as the open right half plane Nyquist contour, D_1' , and the contour in figure 9.3b with small semicircles to the left of the imaginary axis is known as the closed right half plane Nyquist contour, D_2' . The modification of the Nyquist contour is necessary for the contour to remain closed and the mapping of the contour to remain conformal, when the mapping function has poles on the imaginary axis. Conformality of the mapping is necessary to allow counting of encirclements.

The contours in the z-plane, D_1' and D_2' , are shown in figure 9.4. By the transformation $z = e^{sT}$, where T is the sample time, the positive imaginary axis is mapped onto the upper semicircle, the negative imaginary axis is mapped onto the lower semicircle, and the large right half plane semicircle is mapped onto a large circle in the z-plane. The contours are closed by a cut from $(-1,0)$ to $(-\infty,0)$ along the negative real axis. Mathematically the large semicircle in the s-plane and the cut and the large circle in the z-plane represents the point at infinity.

The Nyquist contours in the w-plane, D_1'' and D_2'' , are shown in figure 9.5. These contours represent the mapping of D_1' and D_2' by the bilinear transformation $z = (1+w)/(1-w)$. The unit circle is mapped onto the imaginary axis,

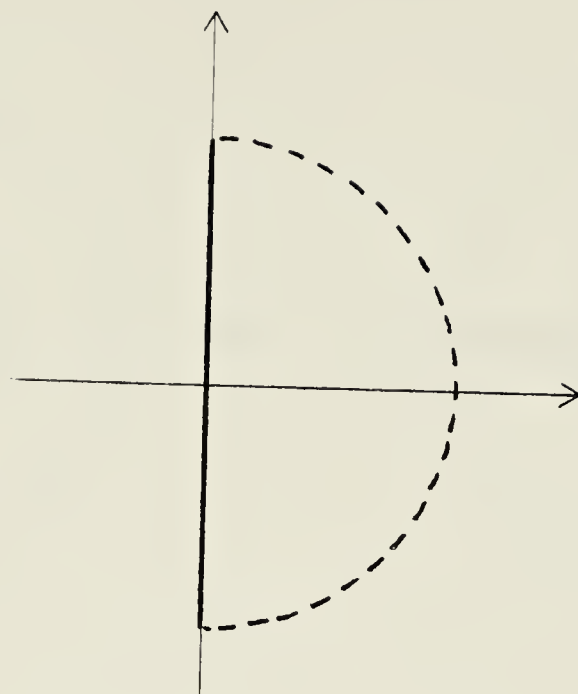


Figure 9.2 Nyquist D -contour in the s -plane

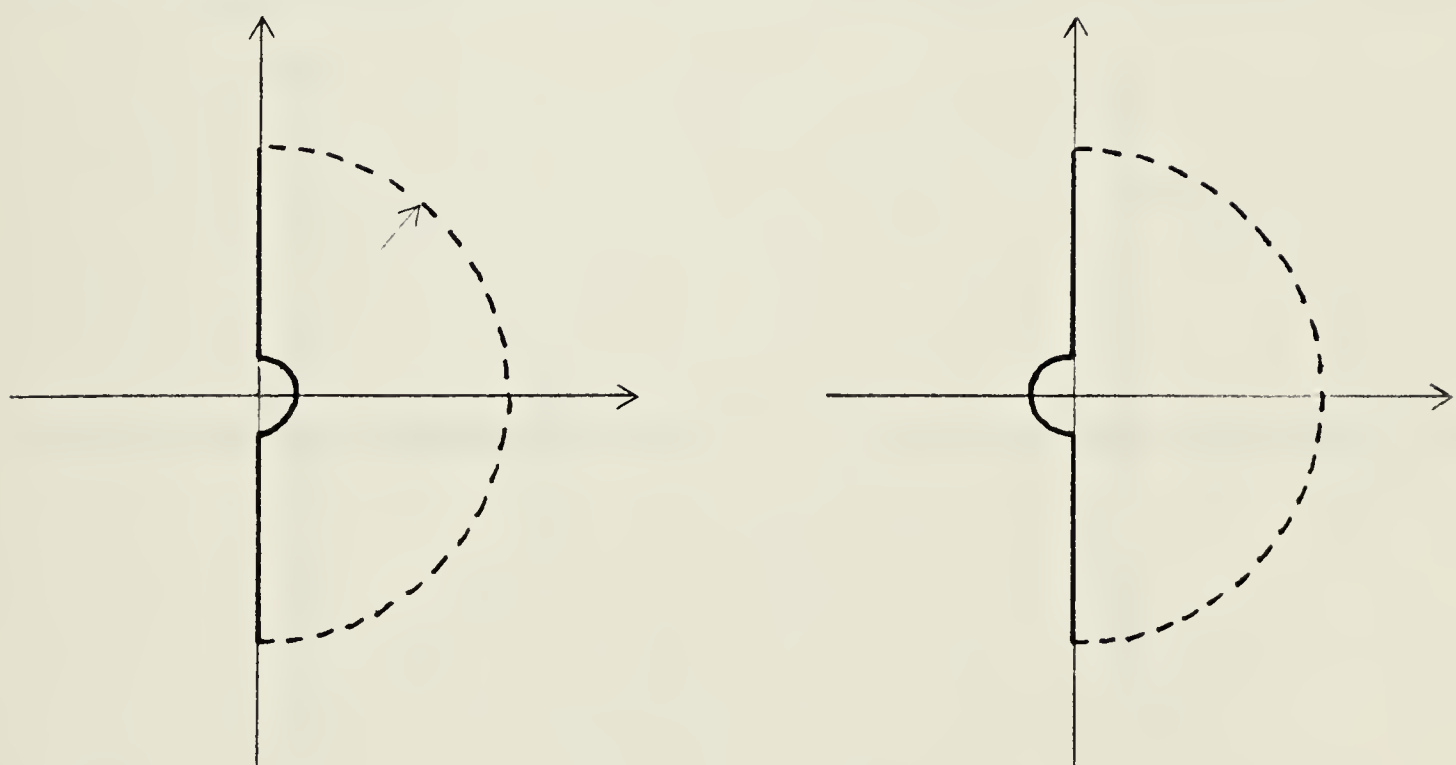


Figure 9.3 Modified Nyquist contour in the s -plane. a) D_1 -contour, and b) D_2 -contour.

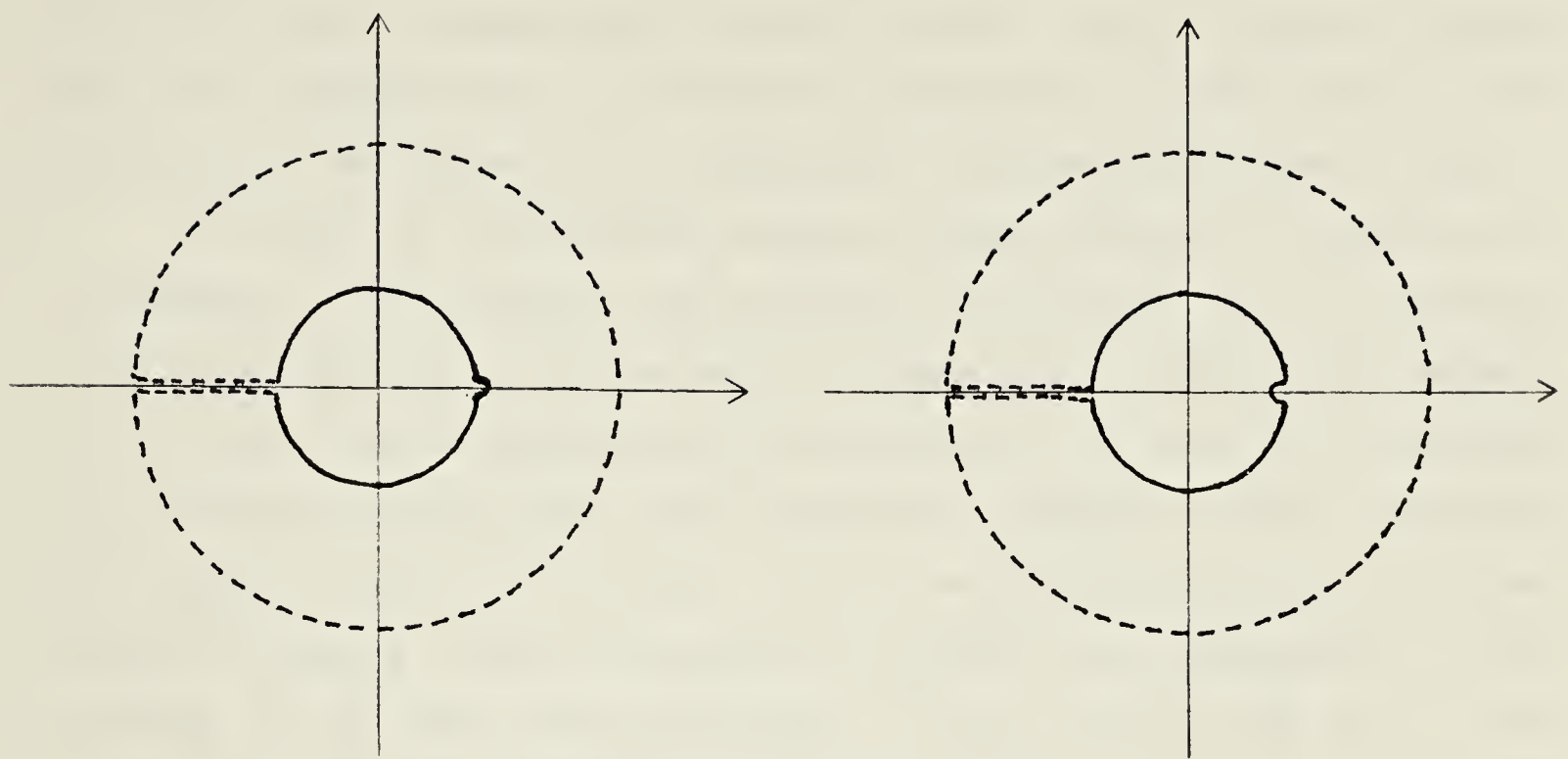


Figure 9.4 Modified Nyquist contours in the z -plane. a) D_1' -contour, and b) D_2' -contour.

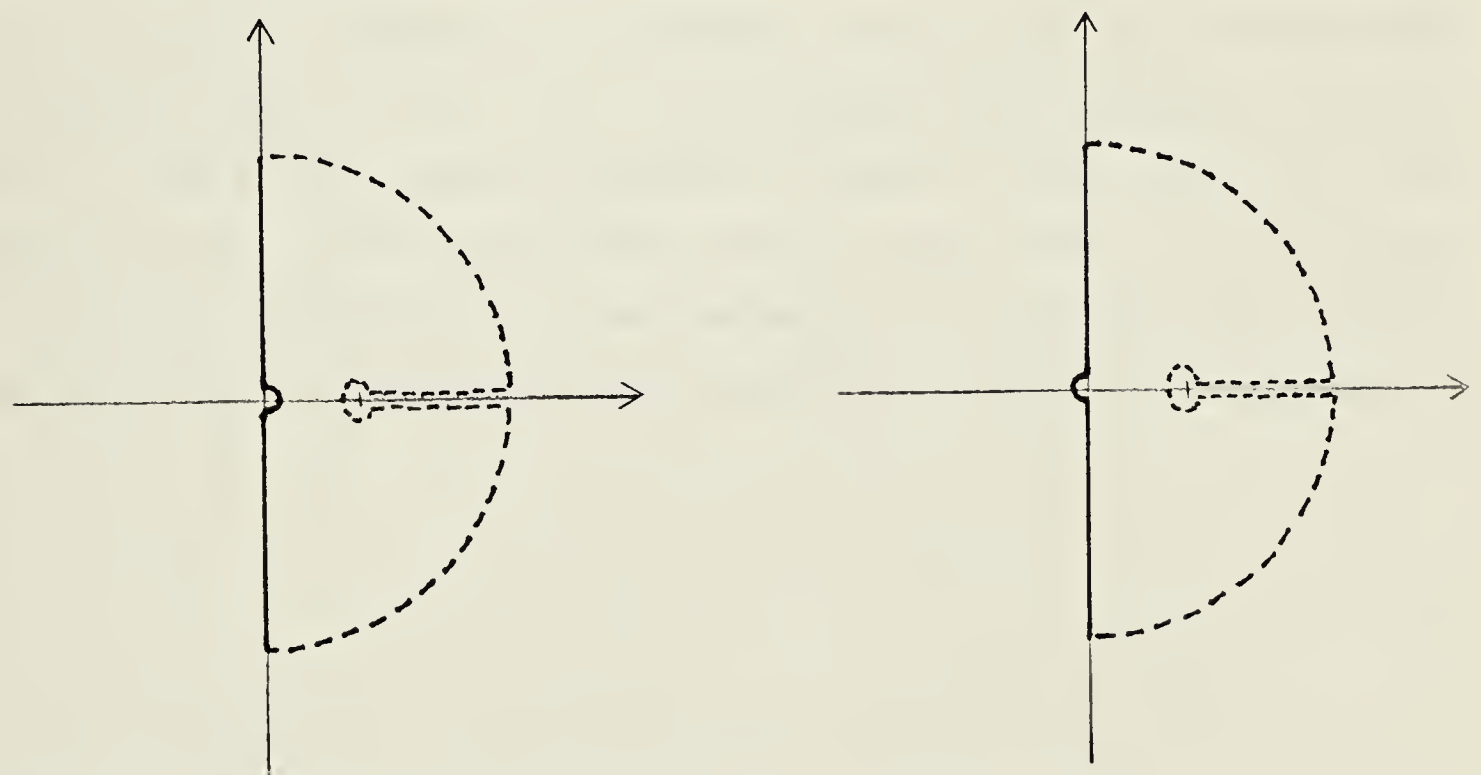


Figure 9.5 Modified Nyquist contours in the w -plane. a) D_1'' -contour, and b) D_2'' -contour.

the $(-1,0)$ point is mapped onto the point at infinity, the cut along the negative real axis is mapped onto a cut along the positive real axis from $(\infty, 0)$ to $(1, 0)$. The contours are closed by two quartercircles representing the point at infinity.

The use of the different modified Nyquist contours is illustrated by considering a pure integrator. The mappings of D_1 and D_2 by the continuous transfer function $G(s) = 1/s$ are shown in figure 9.6. As expected the mapping of D_1 gives zero encirclements and the mapping of D_2 gives one encirclement of the origin and the point $(-1,0)$. The discrete integrator, or the z-transform of $G_h(s)G(s) = (1-e^{sT})/s^2$, is $G(z) = T/(z-1)$. The mappings of D'_1 and D'_2 are shown in figure 9.7. Again the mapping of D'_1 gives zero encirclements and the mapping of D'_2 gives one encirclement of the origin and the point $(-1,0)$. However, this result hinges on the careful mapping of the cut along the negative real axis. Often $G(z)$ is subjected to a bilinear transformation $z = (1+w)/(1-w)$ before mapping of the Nyquist contour. With this transformation $G(z)$ becomes $G(w) = -T/2 + T/2w$. The mappings of D''_1 and D''_2 by $G(w)$ are shown in figure 9.8. These are identical to those in figure 9.6, due to the mapping of the cut along the positive real axis. This shows, it is crucial for the correct encirclement result to be obtained, that the contours D'_1 or D'_2 be used, and not D_1 or D_2 , when bilinear transformed systems are considered.

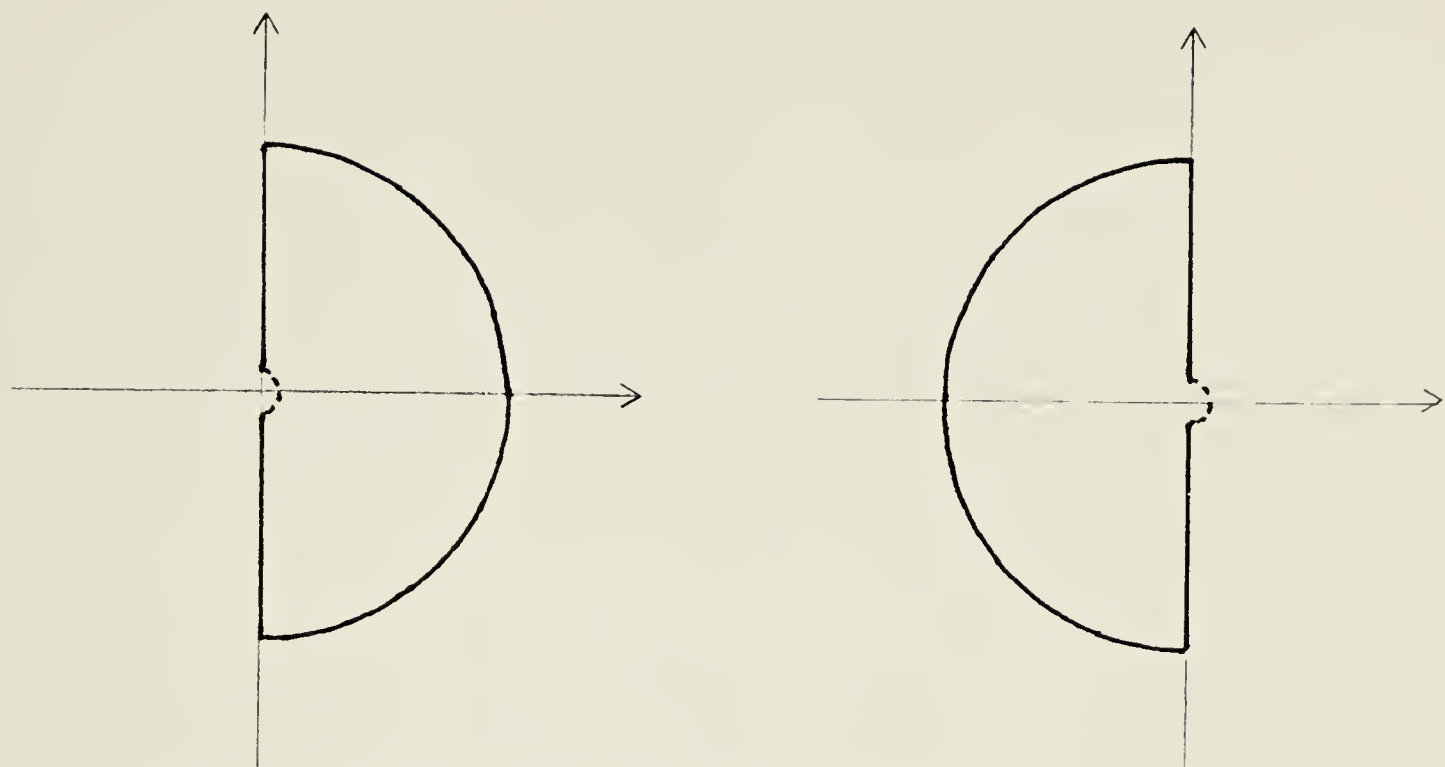


Figure 9.6 Mappings of D_1 and D_2 by $G(s) = 1/s$.

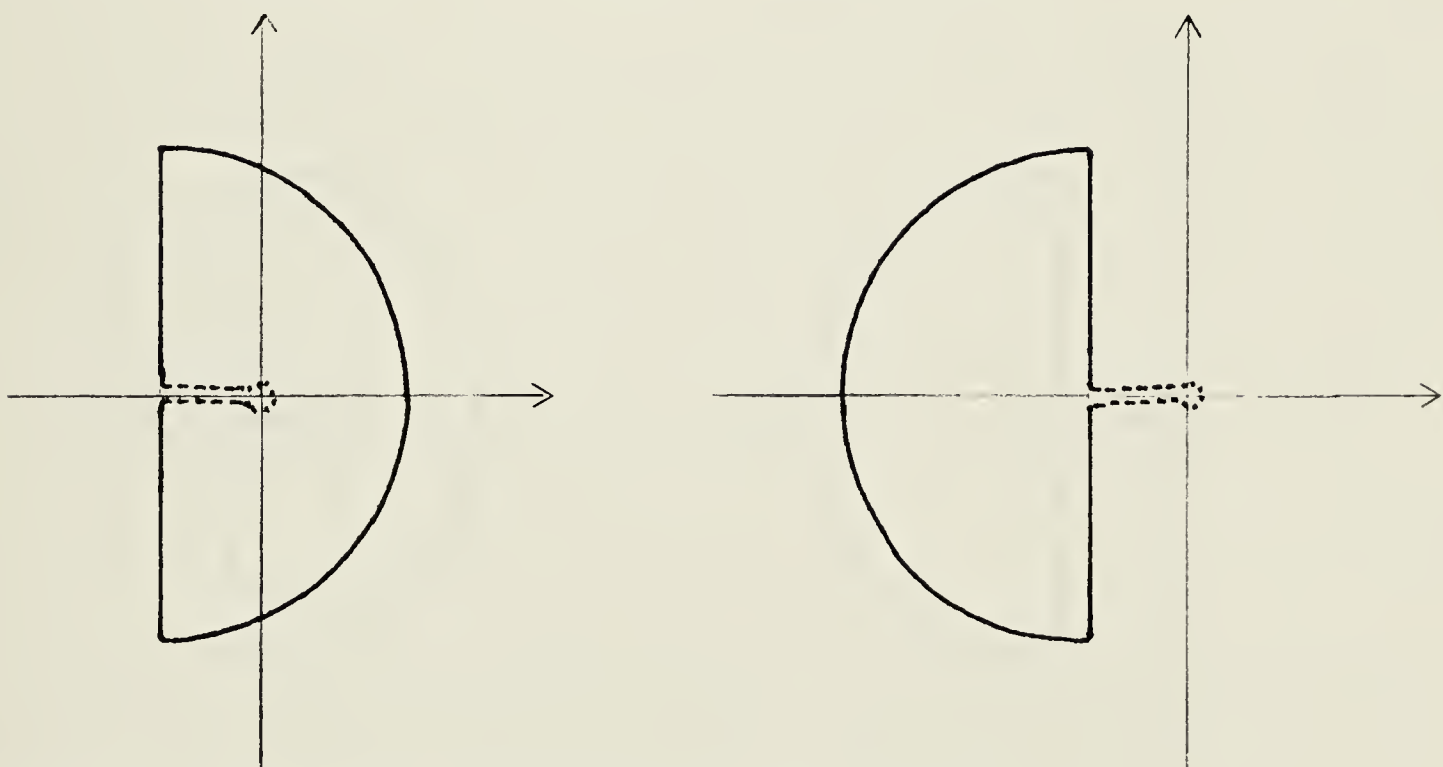


Figure 9.7 Mappings of D_1' and D_2' by $G(z) = T/(z-1)$.

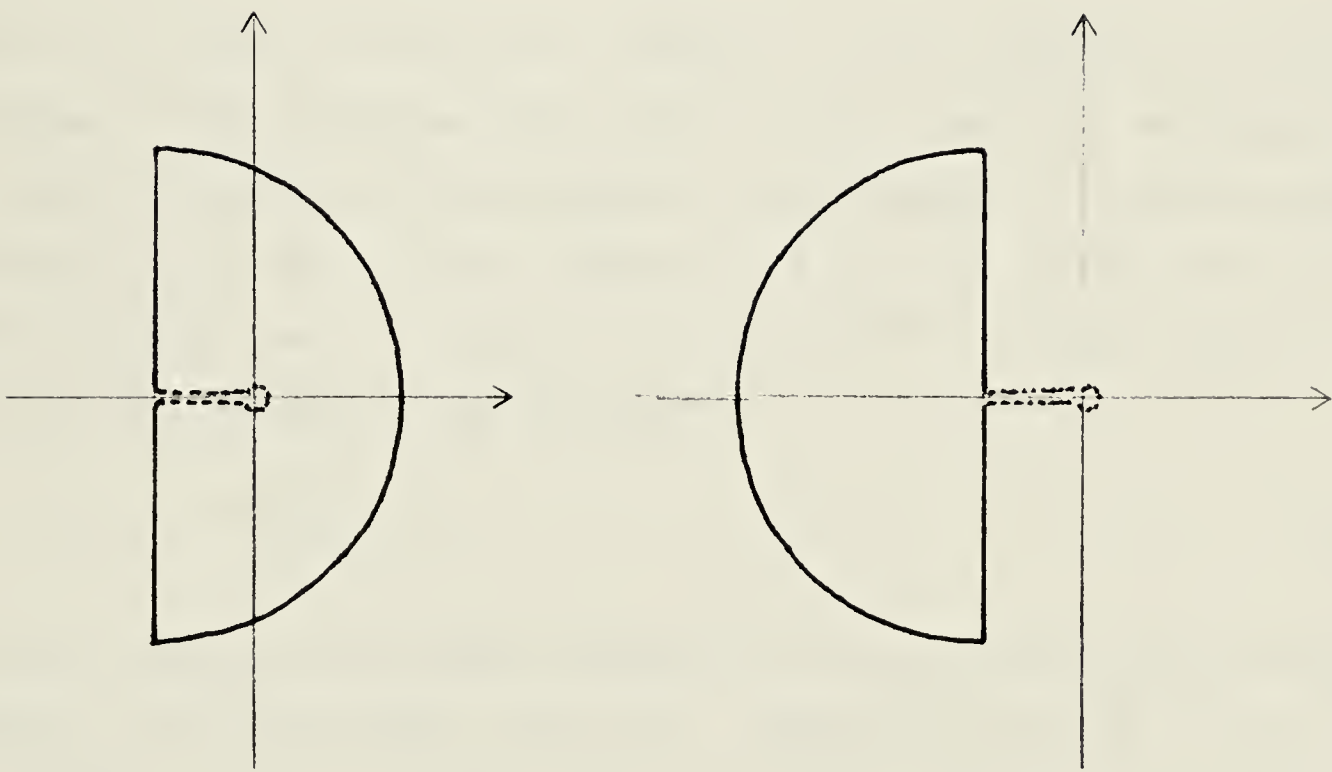


Figure 9.8 Mappings of D_1' and D_2'' by $G(w) = -T/2 + T/2w$.

9.5 Appendix E. Proof of theorem 4.1.

In this appendix a proof is given of theorem 4.1 of chapter 4.

Proof of theorem 4.1: Let $c_{ij}(s)$ be the cofactor of element (i,j) of the return difference matrix $F(s)$. From equation 9.5 of appendix A

$$1+k_i(s)h_i(s) = \frac{|F(s)|}{c_{ii}(s)} \quad (9.24)$$

hence

$$\prod_{i=1}^m (1+k_i(s)h_i(s)) = \left[\frac{|F(s)|^{m-1}}{\prod_{i=1}^m c_{ii}(s)} |F(s)| \right] |F(s)| \quad (9.25)$$

Since $F(s)$ is matrix dominant, by theorem 3.1 the mapping of the Nyquist D -contour by the determinant $|F(s)|$ gives the same number of encirclements of the origin as the sum of encirclements in the mapping of D by the diagonal elements $f_{ii}(s)$ of $F(s)$. Let the mapping of D by $f(s)$ encircle the origin n_{ii} times clockwise, then the mapping of D by $|F(s)|^{m-1}$ will give rise to n_{T1} clockwise encirclements of the origin, with

$$n_{T1} = (m-1) \sum_{i=1}^m n_{ii} \quad (9.26)$$

Since the minors of the diagonal elements of the matrix $F(s)$ and the diagonally dominant matrix $D(s)^{-1}F(s)D(s)$ (with $D(s) = \text{diag}\{d_i(s)\}$, $d_i(s) > 0$) are the same, the mapping of D by $c_{jj}(s)$ gives the following number of clockwise encirclements of the origin

$$m_j = \sum_{\substack{i=1 \\ i \neq j}}^m n_{ii} \quad (9.27)$$

So the mapping of D by $\prod_{i=1}^m c_{ii}(s)$ will give the following number of encirclements:

$$n_{T2} = \sum_{j=1}^m \sum_{\substack{i=1 \\ i \neq j}}^m n_{ii} = (m-1) \sum_{i=1}^m n_{ii}. \quad (9.28)$$

Therefore $n_{T1} = n_{T2}$, and by the principle of the argument the net number of encirclements by the quantity in the square bracket in equation 9.25 is zero. Hence the number of encirclements of the critical point $(-1,0)$ by the mapping of D by $k_i(s)h_i(s)$, $i = 1, \dots, m$ is equal to the number of encirclements of the origin by the mapping of D by $|F(s)|$, provided $F(s)$ is matrix dominant. This proves the theorem.

B30308